Distributed Computational Methods for Energy Management in Smart Grids

Submitted in partial fulfillment of the requirements for
the degree of
Doctor of Philosophy
in
Electrical and Computer Engineering

Javad Mohammadi

B.Sc., Electrical and Computer Engineering, Shahid Bahonar University of Kerman
M.Sc., Electrical and Computer Engineering, University of Tehran
M.Sc., Electrical and Computer Engineering, Carnegie Mellon University

Carnegie Mellon University
Pittsburgh, PA

September, 2016

Copyright © 2016 Javad Mohammadi

Keywords: Consensus+innovations, Distributed Processing, Optimality Conditions, Optimal Dispatch, Optimal Power Flow, Security Constrained Optimal Power Flow, Plug-in Electric Vehicles, Cooperative Charging, Receding Horizon

To my parents and my brothers (Ali and Mohammad)

Abstract

It is expected that the grid of the future differs from the current system by the increased integration of distributed generation, distributed storage, demand response, power electronics, and communications and sensing technologies. The consequence is that the physical structure of the system becomes significantly more distributed. The existing centralized control structure is not suitable any more to operate such a highly distributed system. This thesis is dedicated to providing a promising solution to a class of energy management problems in power systems with a high penetration of distributed resources. This class includes optimal dispatch problems such as optimal power flow, security constrained optimal dispatch, optimal power flow control and coordinated plug-in electric vehicles charging. Our fully distributed algorithm not only handles the computational complexity of the problem, but also provides a more practical solution for these problems in the emerging smart grid environment. This distributed framework is based on iteratively solving in a distributed fashion the first order optimality conditions associated with the optimization formulations. A multi-agent viewpoint of the power system is adopted, in which at each iteration, every network agent updates a few local variables through simple computations, and exchanges information with neighboring agents. Our proposed distributed solution is based on the *consensus+innovations* framework, in which the *consensus* term enforces agreement among agents while the *innovations* updates ensure that local constraints are satisfied.

Acknowledgments

The contributions and support of the following people were essential in the research that is presented in this thesis. To my parents, who dedicated their life to my progress, for endless love and support. To my brothers, Ali and Mohammad, for all good memories and being supportive. To my advisors, Prof. Gabriela Hug and Prof. Soummya Kar, for their valuable guidance and encouragement throughout my PhD. For being devoted to my future and for their honesty. To my thesis committee members Prof. José Moura, Prof. Ian Hiskens, and Prof. Florian Döfler, for their insight and expert opinions.

Thank you to the National Science Foundation, and the Department of Energy for making this research possible.

To Jon, for being there for me when I needed help. To Kyri, for being an amazing friend. To JY, for all the the scientific conversations. To Milos, for all the good time we spend together in the office. To Soheil, for encouraging words, and the time we spend in gym. To Pouria, for the road trips and being a good host. To Martin, for being my lunch buddy. To Amin, Hadi, and Mohsen, for tea breaks. To Hossein and Maryam, for organizing hiking trips. To Majid, Mina, Mahnoush, Afsoon, Mostafa, Sareh, Fattaneh, Amin, and Salim for the volleyball games. To Amin, Navid, Amir, and Erfan, and Pedram for all the after work time we spend together.

Finally, to my friends and colleagues, Anit, Ana, Stefanos, Nicola, Walter, Joya, Giovanni, Rui, June, Becky, Rohan and Nikos. To the EESG group and Prof. Marija Ilić for fruitful and exciting discussions, talks, and events.

Contents

List of Figures

List of Tables

Chapter 1

Introduction

This focus of this thesis is the provision of a distributed framework for addressing the needs of future power grids. The emergence of advanced power electronic technologies, abundance of local intelligence and communication capabilities, and ever increasing adoption of scalable energy resources, e.g., distributed energy generation and energy storage devices, have been shaping the paradigm of the future power grid. The operation of such a grid relies on maintaining the harmony between operation of different controllable elements of the system. The raising number of controllable elements increases the number of control variables and the complexity of operation problems, hence, renders the conventional centralized control approaches incapable of coordinating all controllable devices. Motivated by this need, this thesis focuses on addressing coordination challenges of the future grid by leveraging the inherent distributed structure of the smart grid. To this end, we present a distributed coordination solution for a class of optimal dispatch problems. This section gives a background and motivation to solve these problems and presents a brief overview of our contributions. Finally an outline of the thesis concludes this section.

1.1 Background and Motivation

1.1.1 Transition to Smart Grid

In 2012, the electric energy demand in the US reached 3,800 billion kilowatt-hours and it is expected to keep growing over the next decades. The majority of this demand is currently supplied by dispatchable bulk power plants such as coal and nuclear plants, i.e., plants for which the power output can be controlled to anywhere between zero and the capacity of the plant. At every point in time, the electric power output of these plants is adjusted to cover the instantaneous electric power demand as there is only very limited storage in the system and load is considered to be mostly unadjustable. The future electric power grid, which is commonly referred to as smart grid, is expected to differ from the current system by the increased integration of the following technologies:

Distributed Generation: Power generation resources that include for example wind, solar, or fuel cells tend to be of smaller capacity and therefore also more distributed across the system. This goes as far as having a significant part of the generation connected at the distribution system level.

Distributed Storage: With the increase in non-dispatchable generation resources such as wind and solar generation, the overall variability and intermittency that needs to be handled by dispatchable generation increases. At least part of this variability can be balanced by locally added storage devices.

Demand Response: The concept of demand response relies on the fact that the time instance of the consumption of part of the load can be shifted without inconveniencing the customer. Incentives to achieve such shifting include real-time or time of use pricing or various types of demand response programs, where customers receive rebates for being flexible.

Power Electronics: Power electronics enables multiple of the above mentioned concepts

and technologies, e.g., converter technologies are needed to connect Photovoltaic sources or storage to the system. It is also the key enabler for adding flexibility to the transmission grid via Flexible AC Transmission Systems (FACTS) and High Voltage DC (HVDC) lines by which power can be routed actively throughout the grid.

Sensing and Communication Technology: The key component of a smart grid is the deployment and usage of distributed sensing and communication technology to collect high resolution data and exchange information with the intention of enabling intelligent decision making. The overlay of the physical system with an extensive communication network is what turns the power grid into a cyber-physical system.

The consequence of this transition from the operational perspective is that overall the flexibility in the grid increases; but this also means that more control decisions need to be made. This flexibility is vital not just for balancing the increased variability but also to be able to handle the uncertainty inherent to the non-dispatchable generation resources. A key question that needs to be answered is how the sensing and communication network can be used efficiently to ensure a reliable and safe operation of the electric power grid despite the increased challenges imposed on the supply side.

1.1.2 Current Operational Practices

The electric power system is a large scale system spanning multiple states, countries, and even continents. The responsibility for the control of such a system is therefore shared by multiple entities. This sharing of responsibility occurs on multiple dimensions: first of all, the system is divided into geographical areas within which all the assets belong to the same control area and are coordinated. Second, depending on if the system belonging to a specific area is vertically integrated or part of an electricity market. In the first case (vertically integrated), overseeing and controlling both generation and transmission is done by a single entity and the chosen dispatch of the available generators is based on their cost

effectiveness. In the latter case, the responsibility for operating the transmission grid and generation is assigned to different entities. Moreover, in this case, generators and load serving entities submit bids for production and consumption to a market. Decisions on who is producing how much are made by the market operator. In both cases, the task of optimally scheduling generation as well as other tasks within a control area are carried out using an Energy Management System (EMS). The coordination among neighboring control areas is generally done such that overall suboptimal solutions for generation dispatch result because the areas agree on a flow on their tie lines and schedule the supply of the remaining loads according to their dispatch procedure.

Moreover, the distribution side of the power system is experiencing a paradigm shift. The conventional distribution grid was designed to deliver power from upstream to downstream, and ultimately to the end users. Given the conventional grid's design and limited number of controllable elements, a centralized control structure was suitable to cope with the complexity of control and operation problems in a conventional environments. However, in recent years the number of distributed energy resources including distributed generation and intelligent and adjustable demand has increased significantly and ways need to be found to handle the increasing number of control variables.

In this thesis we present *consensus+innovations* based distributed approaches to solve functions that are part of the Energy Management System of a transmission grid or the Distribution Management System of a distribution network. These functions fulfill important tasks in the operation of the system to ensure reliable and cost-effective supply of the demand. In what follows, we will apply the *consensus+innovations* framework to obtain algorithmic procedures to address the optimal power flow (OPF), security constrained optimal power flow (SCOPF), power flow control (PFC) and plug-in electric vehicles coordinated charging (PEV-CC) problems that conform to the distributed multi-agent structure of the system. The specifics of these distributed algorithms vary depending on the ap-

plication/task, however, broadly speaking, these algorithms have a common structure in which the network agents iterate over problem-specific local variables that are updated from time-to-time using the information received from neighboring agents and local data.

1.2 Contribution

In this thesis, we study distributed energy management procedures with a view to address the major challenges encountered in conventional grid operations. In particular, we focus on a class of optimal power dispatch functions, including OPF, SCOPF, PFC and PEV-CC problems, and provide distributed algorithmic procedures to achieve these functionalities. We adopt a multi-agent formalism in which geographically distributed network entities are designated as agents with local sensing, communication, and computation abilities. The agent distinction is generic and varies from one application to the other. An agent may correspond to a single generator/load/storage entity or may represent a power system bus, thereby consisting of the collection of generator/load/storage entities connected to that bus. An agent may also refer to an area consisting of multiple buses.

To realize our distributed algorithms, we will assume that the network agents are equipped with appropriate computational capabilities and can communicate with each other according to a pre-defined possibly sparse inter-agent communication graph. We leverage the existing framework of *consensus+innovations* decision-making architecture, a family of distributed inference and optimization procedures for multi-agent networks (see for example [1]), to achieve proper inter-agent coordination required to solve the above-mentioned system tasks in an optimal distributed fashion. More specifically, given that different (possibly geographically distributed) entities/areas/components control or have access to different sets of variables and information in the power system, we will employ a multi-agent networked framework in which each network agent can directly control or access only a local subset of the state and control variables. Viewed in this multi-agent

context, the generic formulation of optimal dispatch problems can be interpreted as a collaborative distributed optimization problem in which the network agents collectively aim to minimize a global cost, i.e., a cost which possibly depends on all of the network variables and information, and under constraints which couple these variables.

In order to achieve inter-agent coordination to solve the relevant (global) optimization problems, we will assume that there exists a preassigned inter-agent communication network (possibly sparse and different from the power system physical inter-connection network) through which the agents can exchange information to coordinate their actions. The *consensus+innovations* architecture is well suited to such distributed networked scenarios and has been developed to solve important subclasses of collaborative decision-making problems of the form with modest computation/communication requirements at the agents.

The contributions of this dissertation are as follows:

- **Development of a fully distributed solution for optimal dispatch problems:** Our proposed approach is an iterative procedure that uses the optimality conditions of underlying optimal dispatch problem as *innovation-gradient* terms in the updates of local variables. Each bus is represented by an agent, and that agent is responsible for updating few local variables and sharing limited information with neighboring buses/agents. Therefore, the iterative update procedure is completely distributed. In fact, our approach reduces the optimization problem to solving a coupled system of linear equations with geometric constraints in a fully distributed manner through an iterative process.
- **Modification of the proposed fully distributed algorithm to allow for different levels of distributedness:** The fully distributed approach requires buses (agents) to exchange variable updates after every iteration, which might be prohibitive for an actual implementation. We further propose a more realistic version

of our proposed algorithm which does not require every bus to exchange information with all of its neighboring buses after every single iteration. Our modified algorithm groups buses into areas where the exchange between buses within the areas may take place every iteration while communication with buses in another area might take place only every x-th iteration. This structure further allows for assigning an agent to each area to perform the intra-area computations at a central location within the area which makes the intra-area communications redundant.

- **Extension of the fully distributed algorithm to improve the convergence by altering communication topology:** Our proposed solution only uses information from physically connected neighboring buses to perform local updates and solve optimal dispatch problems such as OPF, SCOPF and PFC problems. Consequently, the convergence speed of the algorithm measured as number of required iterations is highly dependent on the diameter of the network, i.e., the furthest distance between any two buses in the system, because as the diameter increases the number of iterations it takes for information to travel from one end of the system to the other increases as well. We propose an extended version of our original algorithm which allows for sharing additional information between buses without physical connections across the system, hence, can speed up the convergence of the algorithm. A key aspect is the constrained selection of these additional communication links and the effective integration of this information in the update of the local variables.

- **Development of a fully distributed receding horizon framework to optimize cooperative charging of a fleet of plug-in electric vehicles taking into account charging scenarios:** We propose a fully distributed solution for PEVs Cooperative Charging (PEV-CC) problem. The PEV-CC minimizes the charging costs for a PEV fleet whilst considering limitations of PEVs and charging infrastructure. The PEV-CC is a multi-time step problem and a receding horizon is employed

to integrate feedback into the decision-making process. Driving uncertainties are accounted for by considering multiple driving scenarios for individual PEVs. Our distributed iterative procedure achieves a distributed solution for the first order optimality conditions of the underlying optimization problem through local computations and limited communication. The algorithm is designed to reach an agreement on a price signal among PEVs over the course of iterations, while local PEV constraints are enforced at each iteration. Therefore, each iteration yields a feasible solution for the PEV-CC problem.

1.3 Thesis Outline

The chapters that comprise this thesis are outlined as follows:

- **Chapter 2** presents an overview of the proposed distributed methods using a generic problem formulation.
- **Chapter 3** focuses on finding a distributed solution for the optimal power flow problem. At first, this chapter gives an overview of the existing centralized and distributed approaches to solve the OPF problem and then discusses in details the applicability of our proposed *innovations* based approach to solve this problem. While numerous test cases are used to examine the performance of our method, this chapter also analytically justifies the optimally of the achieved solution.
- **Chapter 4** presents a *innovations* based distributed approach to solve the security constrained optimal power flow problem. To this end, this chapter compares the proposed technique with the state of the art methods and validates the performance of our solution both through simulation results and analytical discussions.
- **Chapter 5** solves the power flow control problem, i.e., optimal power flow problem in the case that lines are equipped with power flow control devices, in a distributed

manner. This chapter includes the formulation of distributed updates for the proposed *innovations* based solution as well as case studies and analytical arguments concerning the optimality of the proposed solution.

- **Chapter 6** offers a new perspective for application of our proposed distributed *consensus+innovations* approach to solve problems in the distribution grid. Specifically, this chapter focuses on solving the plug-in electric vehicles coordinated charging problem. Given the multi-time step nature of this problem, this chapter formulates a receding horizon iterative update scheme which provides a feasible solution for the original optimization problem at each iteration. Moreover, this chapter provides a proof of concept by conducting simulation results and presenting convergence analysis of the proposed approach.
- **Chapter 7** concludes this thesis and discusses future research directions.

Chapter 2

Methods

In this thesis, we present a distributed solution for a class of optimal dispatch problems. The methods developed in this thesis are based on the *consensus+innovations* update structure. Some chapters include formulations based upon *innovations*-based updates, e.g., chapters 3, 4 and 5, while chapter 6 utilizes the *consensus+innovations* structure to solve the underlying optimization problem in a distributed manner. To avoid redundancy, the general formulation of the developed methods are discussed here. Later, each chapter of this thesis discusses a specific application of our proposed method in great detail.

2.1 Problem Formulation

The general compact mathematical formulation for the aforementioned class of optimal dispatch problems is given by

$$\min_{x} \ \mathfrak{F}(x) \tag{2.1}$$

$$\text{s.t. } \mathfrak{G}(x) = 0 \tag{2.2}$$

$$\mathfrak{H}(x) \leq 0, \tag{2.3}$$

where, $\mathfrak{F}$ is the objective function, and x refers to the vector of variables. Also, $\mathfrak{G}$ and $\mathfrak{H}$ represent equality constraints, e.g., load balance equations in the optimal power flow problem, and inequality constraints, e.g., line flow constraints in the OPF problem, respectively. Our proposed method is based on solving the first order optimality conditions of the underlying optimization problem (2.1)-(2.3). Our technique reduces the original optimization problem to solving a (constrained) system of equations, i.e., the first order optimality conditions. To this end, in the following section, we derive the optimality conditions for the aforementioned compact formulation.

2.2 Optimality Conditions

The Lagrange function for the above optimization problem is given by

$$L = \mathfrak{F}(x) + \lambda \mathfrak{G}(x) + \mu \mathfrak{H}(x), \tag{2.4}$$

where λ's and μ's correspond to Lagrange multipliers associate with equality and inequality constraints, respectively. The first order optimality conditions are given by

$$\begin{aligned}
\frac{\partial L}{\partial x} =& \frac{\partial \mathfrak{F}(x)}{\partial x} + \lambda \frac{\partial \mathfrak{G}(x)}{\partial x} + \mu \frac{\partial \mathfrak{H}(x)}{\partial x} &= 0 &\quad (2.5)\\
\frac{\partial L}{\partial \lambda} =& \mathfrak{G}(x) &= 0 &\quad (2.6)\\
\frac{\partial L}{\partial \mu} =& \mathfrak{H}(x) &\leq 0 &\quad (2.7)\\
& \mu &\geq 0 &\quad (2.8)\\
& \mu\, \mathfrak{H}(x) &= 0. &\quad (2.9)
\end{aligned}$$

In order to find a solution for (2.1)-(2.3), the above system of constrained equations needs to be solved. If the original optimization problem, defined by (2.1)-(2.3), is convex and also satisfies the strong duality conditions, any solution that fulfills all of the above first order

optimality conditions is the optimal solution of the problem. If the underlying optimization problem is non-convex but satisfies the constraint qualification, any solution that satisfies all of the above optimality conditions constitutes a local optimal solution of the original problem.

2.3 Solution approach

In this section, we present our proposed distributed solution to solve the discussed first order optimality conditions (2.5)-(2.9). Our distributed approach leverages the fact that first order optimality conditions in the considered problems are inherently distributed, meaning that, each of these equations merely involve local information. In the following subsection, we present an *innovations*-based approach to find a distributed solution for (2.5)-(2.9). Moreover, depending on the nature of the primal optimization problem, the optimality conditions may include a common global variable. In this case, instead of dealing with a global variable directly we create local copies of this variable and solve the first order optimality conditions in a distributed manner while enforcing consensus among all local copies. This approach is referred to as the *consensus+innovations* based method and it is presented in the later subsection.

2.3.1 Innovations based Approach

This subsection is devoted to a brief review of the generic *innovations*-based procedure for finding distributed solutions to cooperative decision-making processes. The *innovations*-based setup requires each agent (decision maker) to carry out local information processing and information exchange with neighboring agents in order to optimize a global decision-making task. This setup assumes that each agent has access to merely local information and the communication graph is at least as dense as the physical/constraint graph.

The set of first order optimality conditions lends itself to be solved by a cooperative decision-making process among V agents. In the proposed iterative process, each agent $v \in \{1, \cdots, V\}$ is responsible for updating the variables associated with itself, and exchanging information with neighboring agents. The updates are formulated based on the following general form,

$$x_v(k+1) = \mathbb{P}_v \left[x_v(k) + \Phi_v \mathfrak{C}_v(x_w(k)) \right] \quad w \in \Omega_v, \tag{2.10}$$

where k denotes the iteration counter, and $x_v(k)$ includes the variables associated with agent v at iteration k. Moreover, Ω_v is the set of neighboring agents for agent v. In (2.10) , the function $\mathfrak{C}_v(\cdot)$ represents the first order optimality constraints related to agent v. Also, Φ_v is the vector of tuning parameters. Moreover, $\mathbb{P}_v$ is the projection operator which projects x_v onto its determined feasible space. In chapters 3, 4, and 5, we discuss applications of the discussed *innovations*-based method to solve various optimal dispatch problems (including OPF, SCOPF, PFC problems) in great details.

2.3.2 Consensus+Innovations based Approach

Following up on the *innovation*-based approach, here, we utilize a *consensus+innovations* technique to solve the distributed restricted agreement problem, i.e., enforcing an agreement between V agents on a common variable $\boldsymbol{\Upsilon}$ such that the following global restriction is satisfied. A generic restricted agreement problem is presented as

$$\sum_{v=1}^{V} \mathfrak{D}_v(\boldsymbol{\Upsilon}) = Z, \tag{2.11}$$

where, $\mathfrak{D}_v(\cdot)$ is a certain real-valued function. Moreover, $\boldsymbol{\Upsilon}$ should satisfy local constraints of an individual agent v, e.g., upper and lower bounds restricting values of function $\mathfrak{D}_v(\cdot)$.

The underlying assumption restricts each agent v's data access to its own information

and its predefined neighboring agents (Ω_v). Under broad assumptions on $\mathfrak{D}_v(\cdot)$, i.e., regularity conditions such as Lipschitz continuity and monotonicity, and connectedness of the communication graph, an iterative *consensus+innovations* type procedure can be designed and deployed to find a distributed solution for the aforementioned restricted agreement-type problem (for more details see [2]).

The iterative process of the *consensus+innovations* algorithm requires each agent to preserve and update a local copy of $\boldsymbol{\Upsilon}$ at each iteration k, denoted by $\boldsymbol{\Upsilon}_v(k)$. The update rule for the local copy of the common variable follows the following format,

$$\boldsymbol{\Upsilon}_v(k+1) = \boldsymbol{\Upsilon}_v(k) - \beta_k \left(\sum_{w \in \Omega_v} (\boldsymbol{\Upsilon}_v(k) - \boldsymbol{\Upsilon}_w(k)) \right) - \alpha_k \left(\widehat{\mathbf{Z}}_v(k) - \widetilde{\mathfrak{D}}_v(k) \right), \tag{2.12}$$

where β_k and α_k are tuning parameters. Also, $\widehat{\mathbf{Z}}_v$ is agent v's estimation of the global commitment Z, which will be updated based on the newly received local information in each iteration (this will be discussed in extensive details in chapter 6). Finally, we can design a projected *consensus+innovations* variant that ensures that the updated local function lies in the predefined feasible region of $\mathfrak{D}_v(\cdot)$,

$$\widetilde{\mathfrak{D}}_v(k) = \mathbb{P}\left[\mathfrak{D}_v(\boldsymbol{\Upsilon}_v(k))\right].$$

Here $\mathbb{P}[\cdot]$ denotes the projection operator onto the feasible space imposed by local constraints.

Typical conditions that ensure convergence, i.e., $\boldsymbol{\Upsilon}_v(k) \to \boldsymbol{\Upsilon}$ as $k \to \infty$ for all v with $\boldsymbol{\Upsilon}$ satisfying (2.11) are (see [1]):

1. Sufficient regularity of the local functions $\mathfrak{D}_v(\cdot)$.
2. Connectivity of the inter-agent communication graph.
3. The following conditions on the weight parameters α and β:

- The weight parameters are positive.
- The sequences α_k and β_k are decaying, i.e., as $k \to \infty$, $\alpha_k \to 0$, $\beta_k \to 0$.
- The weights are persistent, i.e.,

$$\sum_{k \geq 0} \alpha_k = \sum_{k \geq 0} \beta_k = \infty.$$

- The innovation excitation (α_k) decays at a faster rate than the consensus tuning parameter (β_k), i.e., $\beta_k / \alpha_k \to \infty$ as $k \to \infty$.

Chapter 3

Distributed Optimal Power Flow

3.1 Introduction

3.1.1 Motivation and Related Work

The control responsibility of the electric power system is shared among many control entities, each responsible for a specific part of the system. While these control areas are coordinated to a certain degree, the coordination generally does not lead to system wide optimal performance, i.e., only suboptimal solutions are achieved. Within each control area, a highly centralized control structure is used to determine the settings of the controllable devices in that area usually taking the neighboring control areas into account as static power injections.

The recent interest in distributed methods to solve economic dispatch and optimal power flow problems stems mostly from the fact that the amount of distributed generation and intelligent and adjustable demand is expected to increase significantly, and ways need to be found to handle the increasing number of control variables even within a single control area. While this is also the main motivation for this chapter, the same methods can also be employed to achieve improved coordination among control areas thereby leading to optimal

overall system utilization.

Distributed approaches to solve the Optimal Power Flow (OPF) problem to determine the optimal generation settings taking into account grid constraints have mostly been based on decomposition theory such as Lagrangian Relaxation and Augmented Lagrangian Relaxation [3]. Examples for such applications in power systems include [4, 5, 6, 7].

Reference [8] proposed an auxiliary problem principle technique to find a distributed solution for OPF in a large scale power system. Also, [9] presented a Lagrangian Relaxation based technique to solve the multi area OPF by modeling each interconnecting line using fictitious buses. Exchanging price signals between areas is suggested as a coordination method to reach a decentralized solution for OPF in [10]. A more recent approach is presented in [11] where an alternating direction method of multipliers, an augmented Lagrangian relaxation method, is employed to solve a multi-step DC optimal power flow problem. In [12], an ADMM based method is presented which takes into account the possibility of partitioning the problem into region-based sub-problems to find a more efficient solution by reducing the number of sub-problems.

On the other hand, there has been a range of publications on the usage of consensus based approaches to solve the economic dispatch problem including [13, 14, 15, 16, 17]. Given the incremental cost rule, a consensus approach can be employed to seek an agreement for the marginal cost value. The additional constraint of total generation having to be equal to total load is taken into account differently in the various approaches. In [13], a leading role is assigned to one of the distributed agents whereas in [15, 16] local *innovation* gradients computed solely on the basis of local demand/supply information are used to enforce that constraint.

Moreover, distributed control methods can be classified as on-line or off-line solution approaches. While off-line solution approaches are focused on the operation of the network in near future, e.g., day ahead, on-line control approaches are mainly concerned with real

time operation of the network. Examples for on-line distributed methods include [18, 19, 20]. Reference [18] presented a decentralized solution for the tertiary frequency control problem, i.e., energy management, by optimizing droop control gains in primary frequency control. Also, [19] proposed a primal-dual gradient-based distributed approach to modify the conventional Automatic Generation Control (AGC) to improve its economic efficiency by incorporating economic objectives into AGC. Along this line, [20] proposed a distributed control algorithm for frequency control that asymptotically minimizes a quadratic cost of power generation.

In this chapter, we present an off-line approach which enables a distributed solution of the DC Optimal Power Flow problem. Hence, the objective is to minimize the generation cost to fully supply the load while ensuring that no line limits are violated. Our proposed approach, denoted by $\mathcal{I}-\mathcal{DOPF}$ (*Innovation* based Distributed Optimal Power Flow), is based on obtaining a solution to the first order optimality conditions of the corresponding optimization problem in a fully distributed fashion. In other words, the $\mathcal{I}-\mathcal{DOPF}$ algorithm is an application of the *Innovation*-based method that was presented in Sect. 2.3.1. The optimality conditions include constraints which constitute a coupling of the Lagrange multipliers associated with the power flow equations and line constraints at neighboring buses and lines. This is used to formulate a term in the updates of the local variables and multipliers which takes into account these couplings. In addition, the power flow equations at the buses are used to form another term which corresponds to an *innovation* term enforcing the demand/supply balance. The information that buses share with neighboring buses is limited to the updates of the bus angle and the local Lagrange multipliers, i.e., there is no need to share information about the generation settings or the cost parameters during the iterative process.

The $\mathcal{I}-\mathcal{DOPF}$ requires buses to exchange variable updates after every iteration, which might be prohibitive for an actual implementation. We further propose a more realistic

version of our proposed algorithm, denoted by $\mathcal{AI}-\mathcal{DOPF}$ (Asynchronous *Innovation* based Distributed Optimal Power Flow), which does not require every bus to exchange information with all of its neighbors after every single iteration. The $\mathcal{AI}-\mathcal{DOPF}$ groups buses into areas where the exchange between buses within the areas may take place every iteration while communication with buses in another area might take place only every x-th iteration.

The $\mathcal{I}-\mathcal{DOPF}$ approach is based on solving the first order optimality conditions of the considered problem by integrating these conditions as *innovation-gradient* terms into the update of the local variables. Information only from physically connected neighbors is taken into account in these local updates. Consequently, the convergence speed of the algorithm measured as number of required iterations is highly dependent on the diameter of the network, i.e., the furthest distance between any two buses in the system, because as the diameter increases the number of iterations it takes for information to travel from one end of the system to the other increases as well.

In this chapter, we also suggest to add additional communication between buses that are not physically connected to improve the speed at which information is spread throughout the network thereby increasing convergence speed. This approach is denoted by $\mathcal{EI}-\mathcal{DOPF}$ (Enhanced *Innovation* based Distributed Optimal Power Flow). The key questions that $\mathcal{EI}-\mathcal{DOPF}$ needs to address are which additional communication links should be incorporated, what information should be exchanged and how such information can be taken into account in an intelligent way in the local variable updates.

3.1.2 Notation

Parameters and Constants

P_{L_i}	Load at bus i
a_n, b_n, c_n	Cost function parameters of generator n
$\overline{P}_{G_n}$	Maximum generation of generator n
$\underline{P}_{G_n}$	Minimum generation of generator n
Ω_G	Set of all generators
Ω_B	Set of all buses
Ω_{G_i}	Set of all generators at bus i
Ω_L	Set of all lines in the grid
Ω_i	Set of all buses physically connected to bus i
Ω_{i^+}	Set of all buses that bus i communicates with in addition to its physical neighbors
X_{ij}	Reactance of line ij
$\overline{P}_{ij}$	Line flow limit of line ij
$\alpha, \beta, \gamma, \tau, \eta$	Tuning paramters
N_B	Number of buses

Variables

P_{G_n}	Power output of generator n
θ_i	Voltage angle at bus i
μ_n^+, μ_n^-	Lagrangian multipliers related to upper and lower generation limits of generator n
μ_{ij}	Lagrangian multiplier of the line flow constraint of line ij
λ_i	Lagrangian multiplier of the load balance equation of bus i

3.2 DC Optimal Power Flow

3.2.1 Problem Formulation

The goal in DC Optimal Power Flow is to determine the generation dispatch which minimizes the cost to supply a given load taking into account operational constraints such as line limits and generation capacities. The grid is modeled using a DC approximation, hence, it is assumed that angle differences across lines are small, voltage magnitudes are all equal to 1pu and resistances of the lines are negligible.

Modeling generation costs using a quadratic cost function, the mathematical problem formulation results in

$$\min_{P_G} \sum_{n\in\Omega_G} \left(a_n P_{G_n}^2 + b_n P_{G_n} + c_n\right) \tag{3.1}$$

$$\text{s.t.} \sum_{n\in\Omega_{G_i}} P_{G_n} - P_{L_i} = \sum_{j\in\Omega_i} \frac{\theta_i - \theta_j}{X_{ij}},\ \forall i \in \{1,\ldots,N_B\} \tag{3.2}$$

$$\theta_1 = 0 \tag{3.3}$$

$$\underline{P}_{G_n} \leq P_{G_n} \leq \overline{P}_{G_n},\quad \forall n \in \Omega_G \tag{3.4}$$

$$-\overline{P}_{ij} \leq \tfrac{\theta_i-\theta_j}{X_{ij}} \leq \overline{P}_{ij} \quad \forall ij \in \Omega_L. \tag{3.5}$$

Comparing with the compact problem formulation presented in Sect. 2.1, (3.1) and (3.2) corresponds to (2.1) and (2.2), respectively. Moreover, (3.4) and (3.5) are representations of the inequality constraint (2.3). Here, $i = 1$ is taken to be the slack bus.

3.2.2 Optimality Conditions

The Lagrange function for this optimization problem is given by

$$L = \sum_{n\in\Omega_G} \left(a_n P_{G_n}^2 + b_n P_{G_n} + c_n\right) + \sum_{n\in\Omega_G} \mu_n^+ \left(P_{G_n} - \overline{P}_{G_n}\right) + \sum_{n\in\Omega_G} \mu_n^- \left(-P_{G_n} + \underline{P}_{G_n}\right)$$

$$+\sum_{i=1}^{N_B}\lambda_i\left(-\sum_{n\in\Omega_{G_i}}P_{G_n}+P_{L_i}+\sum_{j\in\Omega_i}\frac{\theta_i-\theta_j}{X_{ij}}\right)$$
$$+\sum_{ij\in\Omega_L}\mu_{ij}\left(\frac{\theta_i-\theta_j}{X_{ij}}-\overline{P}_{ij}\right)+\sum_{ij\in\Omega_L}\mu_{ji}\left(-\frac{\theta_i-\theta_j}{X_{ij}}-\overline{P}_{ij}\right), \tag{3.6}$$

where λ's and μ's correspond to Lagrange multipliers. Following the derivation presented in Sect. 2.2, the first order optimality conditions are given by

$$\frac{\partial L}{\partial P_{G_n}} = 2a_nP_{G_n}+b_n-\lambda_n+\mu_n^+-\mu_n^- = 0 \tag{3.7}$$
$$\frac{\partial L}{\partial \theta_i} = \lambda_i\cdot\sum_{j\in\Omega_i}\frac{1}{X_{ij}}-\sum_{j\in\Omega_i}\lambda_j\frac{1}{X_{ij}}+\sum_{j\in\Omega_i}\left(\mu_{ij}^+-\mu_{ij}^-\right)\frac{1}{X_{ij}} = 0 \tag{3.8}$$
$$\frac{\partial L}{\partial \lambda_i} = -\sum_{n\in\Omega_{G_i}}P_{G_n}+P_{L_i}+\sum_{j\in\Omega_i}\frac{\theta_i-\theta_j}{X_{ij}} = 0 \tag{3.9}$$
$$\frac{\partial L}{\mu_n^+} = P_{G_n}-\overline{P}_{G_n} \leq 0 \tag{3.10}$$
$$\frac{\partial L}{\mu_n^-} = -P_{G_n}+\underline{P}_{G_n} \leq 0 \tag{3.11}$$
$$\frac{\partial L}{\partial \mu_{ij}} = \frac{\theta_i-\theta_j}{X_{ij}}-\overline{P}_{ij} \leq 0 \tag{3.12}$$
$$\frac{\partial L}{\partial \mu_{ji}} = -\frac{\theta_i-\theta_j}{X_{ij}}-\overline{P}_{ij} \leq 0, \tag{3.13}$$

for all $i\in\{1,\ldots,N_B\}$, $n\in\Omega_G$ and $ij\in\Omega_L$ plus the complementary slackness conditions for the inequality constraints and the positivity constraints on the μ's. The sign of λ is not restricted. Consequently, in order to find a solution to the DC-OPF problem, the above constrained equation system needs to be solved. Given that the choice of the slack bus does not have any influence on the result of the underlying optimization problem, $\theta_1=0$ is omitted from the Lagrangian function and first order optimality conditions. Since the discussed DC-OPF problem is convex and also satisfies the strong duality conditions, any solution that fulfills all of the discussed first order optimality conditions is the optimal

solution of the DC-OPF problem. Here, we assume that the primal optimization problem is strictly feasible.

3.3 Distributed Approach

This section presents the distributed updates for $\mathcal{I}-\mathcal{DOPF}$, $\mathcal{AI}-\mathcal{DOPF}$ and $\mathcal{EI}-\mathcal{DOPF}$ algorithms. These proposed iterative procedures solve the constrained system given in Sect. 3.2.2.

3.3.1 The $\mathcal{I}-\mathcal{DOPF}$ Algorithm

In $\mathcal{I}-\mathcal{DOPF}$ each bus exchanges information with all of its physically connected neighbors at each iteration. In the proposed approach, each bus i updates the variables $\lambda_i,\ \theta_i$ and $P_{G_n}, n \in \Omega_{G_i}$ which are directly associated with that bus and the μ_{ij}'s which are associated with the constraints on flows going out of bus i and into line ij. The format of local updates follows the general update format that is presented in Sect. 2.3.1. As will be seen, $\mu_n^+,\ \mu_n^-$ do not need to be known and therefore no update is needed.

The Lagrange multipliers λ_i are updated according to

$$\begin{aligned}
\lambda_i(k+1) &= \lambda_i(k) - \beta \cdot \left(\frac{\partial L}{\partial \theta_i}\right) + \alpha \cdot \left(\frac{\partial L}{\partial \lambda_i}\right) \\
&= \lambda_i(k) - \beta \cdot \left(\lambda_i(k) \sum_{j\in\Omega_i} \frac{1}{X_{ij}} - \sum_{j\in\Omega_i} \lambda_j(k) \frac{1}{X_{ij}} + \sum_{j\in\Omega_i} (\mu_{ij}(k) - \mu_{ji}(k)) \frac{1}{X_{ij}}\right) \\
&\quad -\alpha \cdot \left(\sum_{n\in\Omega_{G_i}} P_{G_n}(k) - P_{L_i} - \sum_{j\in\Omega_i} \frac{\theta_i(k) - \theta_j(k)}{X_{ij}}\right), \qquad (3.14)
\end{aligned}$$

where $\alpha, \beta > 0$ are tuning parameters and k denotes the iteration index. Hence, the first term corresponds to the optimality condition (3.8) which reflects the coupling between the Lagrange multipliers and the second term constitutes an *innovation* term based on the

power balance equations (3.9). The update makes intuitive sense, e.g., if the power balance (3.9) is not fulfilled because generation is too high, it leads to a reduction in λ_i which on the other hand, as shown next, leads to a decrease in the $P_{G_n}, n \in \Omega_{G_i}$. Furthermore, if no line constraints are binding the μ's are equal to zero and the part of the update in the first row leads to finding an agreement between the λ's at all buses.

Knowing the value of the Lagrange multiplier λ_i, the following update for the generators $P_{G_n}, n \in \Omega_{G_i}$ can be carried out:

$$P_{G_n}(k+1) = \mathbb{P}_n \left[P_{G_n}(k) - \frac{1}{2a_n} \cdot \frac{\partial L}{\partial P_{G_n}} \right] = \mathbb{P}_n \left[\frac{\lambda_i(k) - b_n}{2a_n} \right]. \tag{3.15}$$

Here $\mathbb{P}_n$ is the operator which projects the value determined by (3.15) into the feasible space defined by the upper and lower limits $\overline{P}_{G_n}$ and $\underline{P}_{G_n}$, i.e., if the value is greater than $\overline{P}_{G_n}$, $P_{G_n}(k+1)$ is set to that upper limit and similarly for the lower limits. This is equivalent to using the full equation (3.7) including the multipliers μ_n^+ and μ_n^- to update P_{G_n}. As these multipliers do not appear in any other constraint it is not necessary to provide an update for them. In that case, the P_{G_n} update includes projecting onto a specific upper and lower bound for each segment.

The bus angles are updated according to

$$\begin{aligned} \theta_i(k+1) &= \theta_i(k) - \gamma \left(\frac{\partial L}{\partial \lambda_i} \right) \\ &= \theta_i(k) - \gamma \left(- \sum_{n \in \Omega_{G_i}} P_{G_n}(k) + P_{L_i} + \sum_{j \in \Omega_i} \frac{\theta_i(k) - \theta_j(k)}{X_{ij}} \right), \end{aligned} \tag{3.16}$$

with $\gamma > 0$ being a tuning parameter. Hence, the power balance equation (3.9) is used for the update. It again makes intuitive sense because if the power balance is not fulfilled and the load plus what is flowing onto the lines is greater than the generation at that bus, the

angle is reduced which results in a reduction of the residual of that constraint.

The Lagrange multipliers $\mu_{ij},\ \mu_{ji}$ appear in the λ updates (3.14), and hence, values and updates for these multipliers are needed.

The update is given by

$$\mu_{ij}(k+1) = \mathbb{P}\left[\mu_{ij}(k) + \delta\left(\frac{\partial L}{\partial \mu_{ij}}\right)\right] = \mathbb{P}\left[\mu_{ij}(k) - \delta\left(\overline{P}_{ij} - \frac{\theta_i(k) - \theta_j(k)}{X_{ij}}\right)\right] \tag{3.17}$$

$$\mu_{ji}(k+1) = \mathbb{P}\left[\mu_{ji}(k) + \delta\left(\frac{\partial L}{\partial \mu_{ji}}\right)\right] = \mathbb{P}\left[\mu_{ji}(k) - \delta\left(\overline{P}_{ij} + \frac{\theta_i(k) - \theta_j(k)}{X_{ij}}\right)\right], \tag{3.18}$$

with $\delta > 0$ being a tuning parameter. Consequently, the inequalities (3.12) and (3.13) are used. The projection operator ($\mathbb{P}$) enforces the positivity constraint on the μ's by setting the $\mu_{ij}(k+1)$ and $\mu_{ji}(k+1)$ equal to zero if the update (3.17) and (3.18) yield negative values, respectively. Assuming that the current value for the line flow $P_{ij} = (\theta_i - \theta_j)/X_{ij}$ from bus i to bus j is positive but below its limit $\overline{P}_{ij}$ the update (3.17) yields a decreasing value for μ_{ij} with a minimum value of zero due to the projection into the feasible space $\mu_{ij} \geq 0$. If the flow is above the line limit, the value for μ_{ij} may increase or stay zero. The same discussion applies to μ_{ji}. Our presented updates in (3.14)-(3.18) requires each bus to merely exchange its λ and θ with neighboring buses. In other words, the $\mathcal{I} - \mathcal{DOPF}$'s procedure maintain information local and confidential.

It should be noted that all of these updates have purposely been defined only based on the variables from the previous iteration in order to allow for a parallel computation of all of the updates. If implemented in series, i.e., (3.16) uses the already updated generation values, the number of iteration until convergence decreases but computation time increases because all the computations at a specific bus have to be done after each other.

The pseudo code for the $\mathcal{I} - \mathcal{DOPF}$ is given in Table 3.1. Note that the stopping condition can be chosen according to some user-defined criterion, e.g., the changes in the

variables need to be lower than a pre-defined threshold, and the measurement of res and rel (see Sect. 3.5.2) is simply for the purpose of performance analysis.

Table 3.1: Pseudo code for the $\mathcal{I}-\mathcal{DOPF}$ algorithm

```
Initialize tuning parameters
Initialize variables λ, θ, μ, P_G
    While convergence criteria is not satisfied
      for i=1:number of buses
        Update λ_i using (3.14)
        Update P_{G_i} using (3.15)
        Update θ_i using (3.16)
        Update μ_ij and μ_ji using (3.17) and (3.18)
        Communicate λ_i and θ_i to neighboring buses
      end
      measure res and rel
    end
```

3.3.2 The $\mathcal{AI}-\mathcal{DOPF}$ Algorithm

Asynchronous Update

In the $\mathcal{AI}-\mathcal{DOPF}$'s procedure, some buses only exchange information after every x-th iteration, whereas $\mathcal{I}-\mathcal{DOPF}$ requires every bus to exchange information with all of its neighbors after every single iteration. Figure 3.1 visualizes the two different implementations. The asynchronous implementation may be used in a situation in which the goal is to coordinate multiple areas, each area, for instance being operated by a single central entity: the internal iterations for the buses within each area could be done at a central location within the area and the designated area centers exchange information with each other, referred to as outer iterations, after every few of these inner iterations. We introduce an

iteration counter k_i for each bus and iteration counter n_{ij} for the update of the information between buses i and j, assuming that n_{ij} only increases after every x-th increase of k_i and k_j. Hence, updates (3.14), (3.16), (3.17) and (3.18) are adjusted to

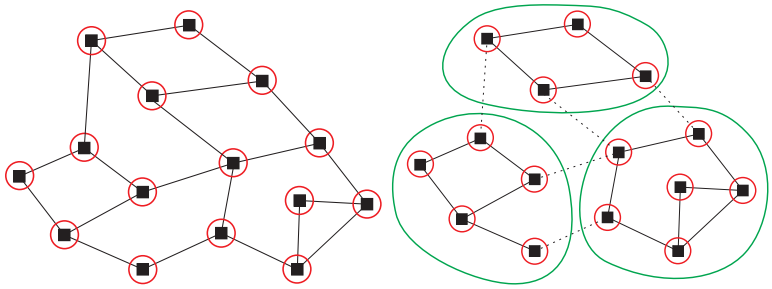

(a) (b)

Figure 3.1: (a) Synchronous update and (b) asynchronous update

$$\begin{aligned}\lambda_i(k_i+1) &= \lambda_i(k_i) - \beta \cdot \left(\lambda_i(k_i) \sum_{j\in\Omega_i} \frac{1}{X_{ij}} - \sum_{j\in\Omega_i} \lambda_j(n_{ij}) \frac{1}{X_{ij}} + \sum_{j\in\Omega_i} \left(\mu_{ij}(k_i) - \mu_{ji}(n_{ij})\right) \frac{1}{X_{ij}} \right) \\ &\quad -\alpha \cdot \left(\sum_{n\in\Omega_{G_i}} P_{G_n}(k_i) - P_{L_i} - \sum_{j\in\Omega_i} \frac{\theta_i(k_i) - \theta_j(n_{ij})}{X_{ij}} \right) \end{aligned} \tag{3.19}$$

$$\theta_i(k_i+1) = \theta_i(k_i) - \gamma \left(- \sum_{n\in\Omega_{G_i}} P_{G_n}(k_i) + P_{L_i} + \sum_{j\in\Omega_i} \frac{\theta_i(k_i) - \theta_j(n_{ij})}{X_{ij}} \right) \tag{3.20}$$

$$\mu_{ij}(k_i+1) = \mathbb{P}\left[\mu_{ij}(k_i) - \delta \left(\overline{P}_{ij} - \frac{\theta_i(k_i) - \theta_j(n_{ij})}{X_{ij}} \right) \right] \tag{3.21}$$

$$\mu_{ji}(k_i+1) = \mathbb{P}\left[\mu_{ji}(k_i) - \delta \left(\overline{P}_{ij} + \frac{\theta_i(k_i) - \theta_j(n_{ij})}{X_{ij}} \right) \right]. \tag{3.22}$$

Distributedness

Distributed algorithms may be implemented because they provide the ability to optimally coordinate entities which are unwilling to exchange significant amounts of information or because they allow for a parallelization of the computations thereby improving computational performance. Hence, even if the computations are carried out at a single centralized location, there is value in employing distributed methods.

In this regard, Fig. 3.2 gives an overview of two different levels of distributedness. The letter B is used to indicate the updates of the variables at a specific bus. Fig. 3.2(a) shows the fully distributed algorithm in which computations for all buses are carried out at physically distinct locations, e.g., at the bus itself. As for each update, information only from neighboring buses is needed, the communication network topology is the same as the physical electrical system.

In Fig. 3.2(b), a hybrid implementation of a distributed algorithm is shown. The updates for a set of buses within an area are carried out at a single location and communication takes place with neighboring areas to receive information about the values at the border buses over the iterations. Such an implementation may enable optimal coordination among the current control areas while achieving computational improvements within the control area itself.

The question of the level of asynchronism and the level of distributedness may go hand-in-hand but could also be considered separately. One can envision a completely distributed implementation as shown in Fig. 3.2(a) with either fully synchronized or with some asynchronous updates. For the hybrid implementation given in Fig. 3.2(b), while it is not necessary, it would be natural and probably most effective to implement synchronous updates within the area and asynchronous updates between the areas because the update within the area only requires exchanging information between geographically co-located processors.

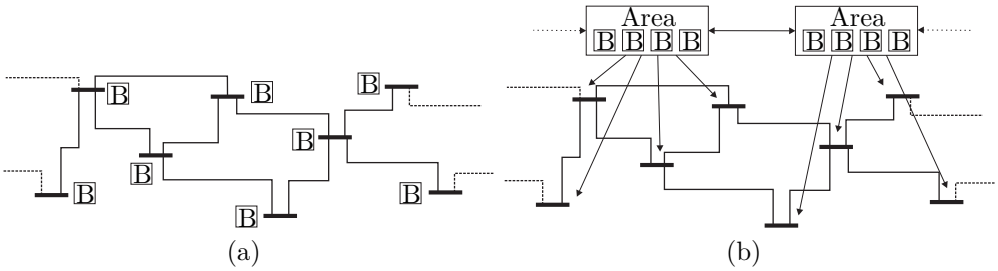

Figure 3.2: (a) Fully distributed and (b) Partially distributed implementation

3.3.3 The $\mathcal{EI} - \mathcal{DOPF}$ Algorithm

Inclusion of Additional Communication Links in Variable Update

In the $\mathcal{I} - \mathcal{DOPF}$ approach, the updates only depend on variables associated with that bus and neighboring buses. Specifically, (3.14) uses its own power balance function and the coupling of the Lagrangian multipliers to update the λ. By using the λ_j of its neighboring buses in its update of λ_i, bus i indirectly takes into account the power balance at bus j because bus j uses its own power balance equation in the update of λ_j. Consequently, the number of iterations that it takes for a bus to indirectly take into account the power imbalance at one of its non-immediate neighbors depends on the shortest path between those buses.

We suggest that direct communication of the power imbalance, i.e. the residual of the power balance equation, between buses with a notable distance and the integration of that imbalance in the update of the local λ_i's can potentially decrease the number of required iterations to trade information between different regions of the system. As a result, the convergence rate of the algorithm will improve. The following is a modified version of (3.14), which incorporates the information about the power imbalance at a distant bus:

$$\begin{aligned}\lambda_i(k+1) =& \lambda_i(k) - \beta \left(\lambda_i(k) \sum_{j \in \Omega_i} \frac{1}{X_{ij}} - \sum_{j \in \Omega_i} \lambda_j(k) \frac{1}{X_{ij}} + \sum_{j \in \Omega_i} (\mu_{ij}(k) - \mu_{ji}(k)) \frac{1}{X_{ij}} \right) \\ & - \tau \left(\sum_{h \in \Omega_{i+}} \Delta P_h(k) \right) - \alpha \left(\sum_{n \in \Omega_{G_i}} P_{G_n}(k) - P_{L_i} - \sum_{j \in \Omega_i} \frac{\theta_i(k) - \theta_j(k)}{X_{ij}} \right),\end{aligned} \tag{3.23}$$

where Ω_{i+} denotes the set of buses h that bus i communicates with in addition to its physical neighbors and ΔP_h represents the power imbalance of bus h.

Based on (3.23), bus i is aware of the power imbalance at bus h. Given that bus h incorporates the power imbalances at its neighboring buses with the delay of only one iteration, information from buses connected to bus h now also flow faster to bus i. Thus, intuitively, an additional communication link between buses i and h improves the flow of information in the system, and leads to faster convergence.

The updates for P_{G_i}, θ_i, μ_{ij}, and μ_{ji} are the same as the updates presented in (3.15)-(3.18). Note that the updates are still linearly independent combinations of the first order optimality conditions, thus the proper choice of values for the tuning parameters α, β, γ, δ and τ ensures that the updates are stable and the iterative procedure converges to the optimal solution of the DC Optimal Power Flow problem.

Choice of Communication Links

Given that adding communication links can be expensive, the choice of which buses should be connected by additional communication links is critical and influences the level of convergence rate improvement. In the following, we present some general guidelines which may be employed while selecting additional communication links. These criteria determine the merit of a specific bus to become part of an additional communication link.

Generation Capacity and Cost Parameters: Buses with a notable generation capacity and low generation cost are important players in preserving the supply/demand equality of the entire system. Since generators are responsible for supplying the demand of the system, the sooner large and low cost generators detect the supply/demand imbalance the fewer iterations are needed for them to respond and counterbalance the imbalance.

Demand: Major load buses have a notable influence on the supply/demand equality. Thus, the communication of the power imbalance at buses to which large consumers are

connected with other influential players such as low cost generators, can have a significant impact on the required number of iterations to solve the problem.

Distance: The distance between two buses, i.e. the shortest path between two buses, is another important criteria when choosing additional communication links. The higher the distance, the more effective (in general) the communication link in improving convergence speed.

Based on the above criteria, buses can be prioritized and communication links may be added accordingly.

3.4 Convergence Analysis

This section presents a formal proof that any limit point of the $\mathcal{I}-\mathcal{DOPF}$ is the optimal solution of the OPF problem. To this end, we introduce a sufficient condition for the convergence of the proposed algorithm. Furthermore, this section presents an approximate parameter tuning discussion. Finally, justifications of the approximate tuning parameter method concludes this section.

In order to derive the convergence properties for the $\mathcal{I}-\mathcal{DOPF}$ algorithm, we first introduce a compact form the distributed updates. The update rules for the all variables in $\mathcal{I}-\mathcal{DOPF}$ can be written in a dense form as

$$\begin{aligned} X(k+1) &= \widetilde{X}(k) - A\widetilde{X}(k) + C \\ \widetilde{X}(k+1) &= \mathbb{P}[X(k+1)], \end{aligned} \tag{3.24}$$

where X is the vector of the stacked variables $(\lambda_i, \theta_i, \mu_{ij}, P_{G_i})$ for all buses $i = \{1, \ldots, N_B\}$, $j \in \Omega_i$ and $\mathbb{P}$ is the projection operator which ensures that the Lagrange Multipliers for the line constraints stay positive and the generation outputs stay within the given bound. Hence, $\widetilde{X}$ is the vector of the stacked projected variables. Equation (3.26) presents (3.24) in

more detail. In (3.26), I and B are the identity and bus admittance matrices, respectively. Moreover, $B_y = H \cdot (\mathcal{I} \cdot diag\frac{1}{X_{ij}})^T$, where $\mathcal{I}$ is the incidence matrix, and $H = [I, -I]^T$.

$$X(k+1) = \left(I - \begin{bmatrix} -\alpha & \beta & 0 & 0 \\ \gamma & 0 & 0 & 0 \\ 0 & 0 & -\delta & 0 \\ 0 & 0 & 0 & \frac{1}{2a} \end{bmatrix} \right) \begin{bmatrix} \frac{\partial L}{\partial \lambda} \\ \frac{\partial L}{\partial \theta} \\ \frac{\partial L}{\partial \mu} \\ \frac{\partial L}{\partial P_G} \end{bmatrix} \tag{3.25}$$

$$X(k+1) = \left(I - \overbrace{\begin{bmatrix} \beta B & -\alpha B & \beta B_y^T & \alpha I \\ 0 & \gamma B & 0 & -\gamma I \\ 0 & -\delta B_y & 0 & 0 \\ -\frac{I}{2a} & 0 & 0 & I \end{bmatrix}}^{\text{A}} \right) \widetilde{X}(k) + \overbrace{\begin{bmatrix} \alpha P_L \\ -\gamma P_L \\ -\delta \overline{P}_{ij} \\ -\frac{b}{2a} \end{bmatrix}}^{\text{C}}. \tag{3.26}$$

3.4.1 Optimality of the Solution

In the following Theorem 1, we first show that a fixed point of the proposed iterative scheme necessarily satisfies the optimality conditions (3.7)–(3.13) of the OPF problem.

Theorem 1: Let X^* be a fixed point of the proposed algorithm defined by (3.24). Then, $X^\star$ satisfies all of the optimality conditions of the OPF problem (3.7)–(3.13).

Proof: To prove this theorem, we verify the claim that $X^\star$ fulfills all of the first order optimality conditions. Note that $X^\star$ is the vector of stacked variables $(\lambda_i^\star, \theta_i^\star, \mu_{ij}^\star, \mu_{ji}^\star, P_i^\star)$ for all buses $i = \{1, \ldots, N_B\}$.

Claim 1: $X^\star$ fulfills the optimality conditions which enforce the positivity of the Lagrangian multipliers associated with the line limits, i.e., $\mu_{ij}^\star \geq 0$.

Verification by contradiction: Let us assume on the contrary that in $X^\star$ one of the line limit multiplier variables, say $\mu_{ij}^\star$, is negative. Now, note that, evaluating (3.17) at $X^\star$

results in a non-negative value for μ_{ij} due to the projection of μ_{ij} into the set of positive reals. In other words, we have

$$\mu_{ij}^{\star} \neq \mathbb{P}\left[\mu_{ij}^{\star} - \delta \cdot \left(\overline{P}_{ij} - \frac{\theta_i^{\star} - \theta_j^{\star}}{X_{ij}}\right)\right],$$

which contradicts the fact that X^* is a fixed point of (3.17). A similar argument would establish that $\mu_{ji}^{\star} \geq 0$.

Claim 2: $X^{\star}$ satisfies the optimality conditions associated with the line limit constraints, (3.12)–(3.13).

Verification by contradiction: Let us assume that $X^{\star}$ does not fulfill (3.12) for all i and j, i.e., there exists (i, j) such that $\frac{\theta_i^{\star} - \theta_j^{\star}}{X_{ij}} > \overline{P}_{ij}$. This implies that the value of the innovation term in (3.17) is negative when evaluated at $X^{\star}$. Also, note that, based on the claim 1, $\mu_{ij}^{\star} \geq 0$. Therefore, evaluating (3.17) at $X^{\star}$ results in a value greater than $\mu_{ij}^{\star}$, i.e.,

$$\mu_{ij}^{\star} < \mathbb{P}\left[\mu_{ij}^{\star} - \delta \cdot \left(\overline{P}_{ij} - \frac{\theta_i^{\star} - \theta_j^{\star}}{X_{ij}}\right)\right],$$

which contradicts the fact that X^* is a fixed point of (3.17). Similar arguments can be used to prove that $X^{\star}$ fulfills (3.13).

Claim 3: $X^{\star}$ satisfies the optimality conditions associated with the complementary slackness condition, i.e., for all pairs (i, j),

$$\mu_{ij}^{\star} \cdot \left(\frac{\theta_i^{\star} - \theta_j^{\star}}{X_{ij}} - \overline{P}_{ij}\right) = 0.$$

Verification by contradiction: Let us assume on the contrary that X^* does not satisfy the above complementary slackness condition, i.e., there exists a pair (i, j) such that both $\mu_{ij}^{\star}$ and $\frac{\theta_i^{\star} - \theta_j^{\star}}{X_{ij}} - \overline{P}_{ij}$ are non-zero. Hence, according to the claims 1 and 2, we must have, $\mu_{ij}^{\star} > 0$ and $\frac{\theta_i^{\star} - \theta_j^{\star}}{X_{ij}} < \overline{P}_{ij}$, respectively. Now, note that evaluating (3.17) at $X^{\star}$, results in a value less than $\mu_{ij}^{\star}$, which clearly contradicts the fact that X^* is a fixed point of (3.17).

Claim 4: $X^{\star}$ satisfies the local load balance equation (3.9).

Verification by contradiction: Let us assume on the contrary that $X^\star$ does not fulfill (3.9), i.e., there exists i such that the value of the innovation term in (3.16) is non-zero when evaluated at $X^\star$. Clearly, this would lead to

$$\theta_i^\star \neq \theta_i^\star - \gamma \left(-\sum_{n \in \Omega_{G_i}} P_{G_n}^\star + P_{L_i} + \sum_{j \in \Omega_i} \frac{\theta_i^\star - \theta_j^\star}{X_{ij}} \right),$$

thus contradicting the fact that X^* is a fixed point of (3.16).

Claim 5: The coupling between the Lagrangian multipliers, given by (3.8), is maintained at $X^\star$.

Verification by contradiction: Let us assume on the contrary that $X^\star$ does not fulfill (3.8) for some i. Note that (3.14) includes two innovation terms: the innovation term associated with the Lagrangian multipliers' coupling and the innovation term which represents the local power balance equation. We already verified that the local power balance equation is zero at $X^\star$ (see claim 4). Thus, the contradiction hypothesis necessarily implies that the innovation term associated with the Lagrangian multipliers' coupling attains a non-zero value at $X^\star$. This, in turn, implies that the the value of (3.14) is not equal to $\lambda_i^\star$ when evaluated at $X^\star$, which clearly contradicts the fact that X^* is a fixed point of (3.14).

Claim 6: $X^\star$ satisfies the optimality conditions associated with the generation limits, (3.10)–(3.11).

Verification by contradiction: Let us assume on the contrary that there exists i such that $P_{G_i}^\star$ does not lie in $[\underline{P}_{G_i}, \overline{P}_{G_i}]$. Now, note that, plugging in $\lambda^\star$ in (3.15), would then result in a value different from $P_{G_i}^\star$, since the projection operator enforces the value of P_{G_i} to stay in the specified region, $[\underline{P}_{G_i}, \overline{P}_{G_i}]$. This, in turn, clearly contradicts the fact that X^* is a fixed point of (3.15).

We now discuss the consequences of Theorem 1. To this end, note that, since the proposed iterative scheme (3.24) involves continuous transformations of the iterates, it follows that, if (3.24) converges, the limit point is necessarily a fixed point of the iterative

mapping. Since, by Theorem 1, any fixed point of (3.24) solves the first order optimality conditions (3.7)–(3.13), we may conclude that, if (3.24) converges, it necessarily converges to a solution of the first order optimality conditions (3.7)–(3.13). This immediately leads to the following optimality of limit points of the proposed scheme.

Theorem 2: Suppose the OPF problem (3.1)–(3.5) has a feasible solution that lies in the interior of the associated constraint set, and, further, assume that the proposed algorithm defined by (3.24) converges to a point $X^{\star}$. Then X^{*} constitutes an optimal solution of the OPF problem (3.1)–(3.5).

Proof: By Theorem 1 and the above remarks, $X^{\star}$ fulfills the optimality conditions (3.7)–(3.13). Since the DC-OPF is a convex problem and, by assumption, is strictly feasible, it follows readily that the primal variables ($P^{\star}$,$\theta^{\star}$) in X^{*} constitutes an optimal solution to the OPF problem (3.1)–(3.5).

In summary, we note that Theorems 1 and 2 guarantee that any fixed point of the proposed algorithm constitutes an optimal solution to the OPF problem, and, hence, in particular, if the scheme achieves convergence, the limit point is necessarily an optimal solution of the OPF problem.

Finally, we note, that whether the scheme converges or not depends on several design factors, in particular, the tuning parameters α, β, γ and δ. Hence, a general sufficient condition for convergence is presented in the following subsection.

3.4.2 Sufficient Condition for Convergence

To this end, the following assumption on the matrix A as defined in (3.26) is imposed:
A.1: There exists an ℓ_p-norm such that the tuning parameters α, β, γ and δ can be designed to achieve $\|I - A\|_p < 1$.

Remark 1: Note that the projection operator $\mathbb{P}$ in our context involves component-wise projections, and, hence, is non-expansive with respect to ℓ_p-norms, i.e., the following holds

for any two iterates $X(k)$ and $X(v)$,

$$\|\mathbb{P}(X(k)) - \mathbb{P}(X(\nu))\|_p \leq \|X(k) - X(\nu)\|_p . \tag{3.27}$$

Remark 2: Based on *Remark 1*, the following equations hold,

$$\begin{aligned} &\left\|\widetilde{X}(k+1) - \widetilde{X}(k)\right\|_p \\ &= \left\|\mathbb{P}[(I-A)\widetilde{X}(k) + C] - \mathbb{P}[(I-A)\widetilde{X}(k-1) + C]\right\|_p \\ &\leq \left\|(I-A)\widetilde{X}(k) + C - (I-A)\widetilde{X}(k-1) - C\right\|_p \\ &\leq \|(I-A)\|_p \left\|\widetilde{X}(k) - \widetilde{X}(k-1)\right\|_p . \end{aligned} \tag{3.28}$$

Consequently, (3.28) leads to

$$\left\|\widetilde{X}(k+1) - \widetilde{X}(k)\right\|_p \leq \|I-A\|_p^k \left\|\widetilde{X}(1) - \widetilde{X}(0)\right\|_p . \tag{3.29}$$

Theorem 3: Let *A.1* hold, then the algorithm presented in (3.24) achieves convergence.

Proof: The distance between the values of $\widetilde{X}$ at two iterations k and ν is given by,

$$\begin{aligned} &\left\|\widetilde{X}(k) - \widetilde{X}(\nu)\right\|_p = \\ &\left\|\widetilde{X}(k) - \widetilde{X}(k-1) + \widetilde{X}(k-1) - \cdots + \widetilde{X}(\nu+1) - \widetilde{X}(\nu)\right\|_p \\ &\leq \left\|\widetilde{X}(k) - \widetilde{X}(k-1)\right\|_p + \cdots + \left\|\widetilde{X}(\nu+1) - \widetilde{X}(\nu)\right\|_p . \end{aligned} \tag{3.30}$$

Moreover, using (3.29) the following equation can be derived:

$$\begin{aligned} &\left\|\widetilde{X}(k) - \widetilde{X}(\nu)\right\|_p \\ &\leq \left\|\widetilde{X}(k) - \widetilde{X}(k-1)\right\|_p + \cdots + \left\|\widetilde{X}(\nu+1) - \widetilde{X}(\nu)\right\|_p \end{aligned} \tag{3.31}$$

$$\leq \left(\|I - A\|_p^k + \cdots + \|I - A\|_p^\nu \right) \left\| \widetilde{X}(1) - \widetilde{X}(0) \right\|_p .$$

Since *A.1* holds, we have

$$\lim_{\nu \to \infty} \|I - A\|_p^\nu = 0. \tag{3.32}$$

Hence, combining (3.31) and (3.32) further implies,

$$\forall\ \epsilon > 0,\ \exists\ N\ s.t.\ \ k, \nu > N\ \Rightarrow \left\| \widetilde{X}(k) - \widetilde{X}(\nu) \right\|_p \leq \epsilon. \tag{3.33}$$

Therefore the sequence of $\left\{ \widetilde{X}(i) \right\}_{i=0}^{\infty}$, which is introduced by (3.24), is a Cauchy sequence. Since a sequence of real vectors converges to a limit in $\mathbb{R}^n$ if and only if it is Cauchy, it follows that the proposed iterative algorithm is convergent, i.e., $X(i) \to X^*$ as $i \to \infty$ for some $X^* \in \mathbb{R}^n$.

3.4.3 Parameter Tuning

The choice of tuning parameters affects the convergence speed of the proposed algorithm. The lower the values for the tuning parameters, the smaller the correction caused by the *innovation* terms, hence, the slower the algorithm converges. Larger values for the tuning parameters generally result in faster convergence. However, the resulting large *innovation* values might result in oscillatory behavior or even divergence. Theorem 3 suggests that our algorithm's convergence is generally structural-dependent, i.e., on the values of the model parameters only. Leveraging this property, in the following, we present some general guidelines, that are based on our observations which may be employed to tune the parameters.

Observations: Analyzing the effects and meaning of the individual terms in the update rules, we can make the following statements about the values for the tuning parameters:

- The λ update (3.14) includes two *innovation* terms: coupling between neighbors and local load balance equation. It is reasonable to choose $\alpha > \beta$, since supplying local

demand should have a higher priority than the coupling perseverance.

- Since θ regulates the ingoing and outgoing flows of a bus, and the previous observation suggests that $\alpha > \beta$, adjusting γ such that $\alpha > \gamma$ is likely to prevent possible oscillatory behaviour.
- A set of tuning parameters for a system should work for a wide range of loading conditions.

Heuristic Parameter Tuning Method: In the following, we present some more specific guidelines to adjust the tuning parameters. The analytical justification for this heuristic method is given in the Appendix, which is based on a specific equivalent reformulation of the original problem.

1. choose β such that $\beta \leq \frac{1}{max_i \sum_{j\in\Omega_i} \frac{1}{X_{ij}}}$.
2. choose γ such that $\gamma \leq \frac{1}{max_i \sum_{j\in\Omega_i} \frac{1}{X_{ij}}}$.
3. choose α such that $\alpha > \beta$ and $\alpha > \gamma$. Larger values of α may be preferred, of course, till the point that increasing α leads to oscillatory behavior or divergence. Increase α until noticing oscillatory behavior.
4. Tuning of δ to achieve faster convergence depends on the loadings of the system. Start with $\delta = 0.5 \times \beta$; larger values of δ may be preferred, of course, till the point that increasing δ leads to oscillatory behavior or divergence.

Note, the above is a heuristic and is not guaranteed to yield optimal choices of the tuning parameters in all system and loading scenarios. Nonetheless, some simulation examples are presented in Sect. 3.5 in which we follow the above guidelines to choose the tuning parameter for a class of realistic power systems.

3.4.4 Justifications for Approximate Tuning Parameter Method

The following subsection justifies the approximate parameter tuning procedure introduced in the pervious subsection. Specifically, we consider a modified system, denoted by $\mathfrak{M}$, (see Assumptions *M.1* and *M.2*) for which we tune the parameters, namely $(\alpha_m, \beta_m, \gamma_m, \delta_m)$. Then, we derive the desirable parameter choices for the original setup, denoted by $\mathfrak{O}$, from the α_m, β_m, γ_m, and δ_m designed for the system $\mathfrak{M}$.

M.1: The generators' cost function parameters of $\mathfrak{O}$, i.e., $a_n^{\mathfrak{O}}, b_n^{\mathfrak{O}}, c_n^{\mathfrak{O}}$, are scaled by a factor ξ such that $\frac{1}{\xi a_n^{\mathfrak{O}}}$ obtain sufficiently small values. It also follows that

$$\forall\ \epsilon > 0,\ \exists\ \xi\ s.t.\ \ \frac{1}{\xi a_n^{\mathfrak{O}}} \leq \epsilon, \quad \forall n \in \Omega_G \tag{3.34}$$

M.2: A fictitious bus, i.e., a bus without generator/load, is added to the $\mathfrak{O}$'s network. This fictitious bus could be connected to any of the buses. Note, the fictitious bus is not equivalent to the slack bus. Later in this section, we discuss the necessity of adding a fictitious bus to the $\mathfrak{O}$'s network.

Remark 3: Let the DC-OPF problem, defined by (3.1)–(3.5), yield $[\lambda^\star, \theta^\star, \mu^\star, P^\star]$ as the optimal primal and dual variables. Then, scaling the objective function of this problem by a factor ξ, results in $[\xi\lambda^\star, \theta^\star, \xi\mu^\star, P^\star]$ as the optimal primal and dual variables.

Justification 1: Let the $\mathcal{I}-\mathcal{DOPF}$ algorithm converge to the optimal solution of DC-OPF for the modified system ($\mathfrak{M}$) using the $(\alpha_m, \beta_m, \gamma_m, \delta_m)$ as tuning parameters. Then, adjusting the tuning parameters to $(\frac{1}{\xi}\alpha_m, \beta_m, \gamma_m, \frac{1}{\xi}\delta_m)$ results in convergence of the $\mathcal{I}-\mathcal{DOPF}$ algorithm for the original system ($\mathfrak{O}$).

Proof: Given that the tuning parameters of $\mathcal{I}-\mathcal{DOPF}$ are adjusted to $(\frac{1}{\xi}\alpha_m, \beta_m, \gamma_m, \frac{1}{\xi}\delta_m)$, the $\mathcal{I}-\mathcal{DOPF}$'s iterative updates for the system $\mathfrak{O}$, namely $[\lambda^{\mathfrak{O}}, \theta^{\mathfrak{O}}, \mu^{\mathfrak{O}}, P^{\mathfrak{O}}]$, are as follows

$$\lambda_i^{\mathfrak{O}}(k+1) = \lambda_i^{\mathfrak{O}}(k) - \beta_m \cdot \left(\lambda_i^{\mathfrak{O}}(k) \sum_{j \in \Omega_i} \frac{1}{X_{ij}} - \sum_{j \in \Omega_i} \lambda_j^{\mathfrak{O}}(k) \frac{1}{X_{ij}} + \sum_{j \in \Omega_i} \left(\mu_{ij}^{\mathfrak{O}}(k) - \mu_{ji}^{\mathfrak{O}}(k) \right) \frac{1}{X_{ij}} \right)$$
$$-\frac{\alpha_m}{\xi} \cdot \left(\sum_{n \in \Omega_{G_i}} P_{G_n}^{\mathfrak{O}}(k) - P_{L_i} - \sum_{j \in \Omega_i} \frac{\theta_i^{\mathfrak{O}}(k) - \theta_j^{\mathfrak{O}}(k)}{X_{ij}} \right) \tag{3.35}$$

$$P_{G_n}^{\mathfrak{O}}(k+1) = \mathbb{P}_n \left[\frac{\lambda_i^{\mathfrak{O}}(k) - b_n^{\mathfrak{O}}}{2a_n^{\mathfrak{O}}} \right] \tag{3.36}$$

$$\theta_i^{\mathfrak{O}}(k+1) = \theta_i^{\mathfrak{O}}(k) - \gamma_m \left(- \sum_{n \in \Omega_{G_i}} P_{G_n}^{\mathfrak{O}}(k) + P_{L_i} + \sum_{j \in \Omega_i} \frac{\theta_i^{\mathfrak{O}}(k) - \theta_j^{\mathfrak{O}}(k)}{X_{ij}} \right) \tag{3.37}$$

$$\mu_{ij}^{\mathfrak{O}}(k+1) = \mathbb{P} \left[\mu_{ij}^{\mathfrak{O}}(k) - \frac{\delta_m}{\xi} \left(\overline{P}_{ij} - \frac{\theta_i^{\mathfrak{O}}(k) - \theta_j^{\mathfrak{O}}(k)}{X_{ij}} \right) \right] \tag{3.38}$$

$$\mu_{ji}^{\mathfrak{O}}(k+1) = \mathbb{P} \left[\mu_{ji}^{\mathfrak{O}}(k) - \frac{\delta_m}{\xi} \left(\overline{P}_{ij} + \frac{\theta_i^{\mathfrak{O}}(k) - \theta_j^{\mathfrak{O}}(k)}{X_{ij}} \right) \right]. \tag{3.39}$$

Now, multiplying (3.35) by ξ results in,

$$\xi\lambda_i^{\mathfrak{O}}(k+1) = \xi\lambda_i^{\mathfrak{O}}(k) - \beta_m \cdot \left(\xi\lambda_i^{\mathfrak{O}}(k) \sum_{j \in \Omega_i} \frac{1}{X_{ij}} - \sum_{j \in \Omega_i} \xi\lambda_j^{\mathfrak{O}}(k) \frac{1}{X_{ij}} + \sum_{j \in \Omega_i} \left(\xi\mu_{ij}^{\mathfrak{O}}(k) - \xi\mu_{ji}^{\mathfrak{O}}(k) \right) \frac{1}{X_{ij}} \right)$$
$$-\alpha_m \cdot \left(\sum_{n \in \Omega_{G_i}} P_{G_n}^{\mathfrak{O}}(k) - P_{L_i} - \sum_{j \in \Omega_i} \frac{\theta_i^{\mathfrak{O}}(k) - \theta_j^{\mathfrak{O}}(k)}{X_{ij}} \right). \tag{3.40}$$

Also, (3.36) could be stated as,

$$P_{G_n}^{\mathfrak{O}}(k+1) = \mathbb{P}_n\left[\frac{\xi\lambda_i^{\mathfrak{O}}(k) - \xi b_n^{\mathfrak{O}}}{2\xi a_n^{\mathfrak{O}}}\right]. \tag{3.41}$$

Furthermore, multiplying (3.38) and (3.39) by ξ results in,

$$\begin{aligned}
\xi\mu_{ij}^{\mathfrak{O}}(k+1) &= \mathbb{P}\left[\xi\mu_{ij}^{\mathfrak{O}}(k) - \delta_m\left(\overline{P}_{ij} - \frac{\theta_i^{\mathfrak{O}}(k) - \theta_j^{\mathfrak{O}}(k)}{X_{ij}}\right)\right] \qquad (3.42)\\
\xi\mu_{ji}^{\mathfrak{O}}(k+1) &= \mathbb{P}\left[\xi\mu_{ji}^{\mathfrak{O}}(k) - \delta_m\left(\overline{P}_{ij} + \frac{\theta_i^{\mathfrak{O}}(k) - \theta_j^{\mathfrak{O}}(k)}{X_{ij}}\right)\right]. \qquad (3.43)
\end{aligned}$$

Note, (3.42) and (3.43) hold because $\mathbb{P}$ projects the updated values onto $[0,\infty)$. In other words, $\mu_{ij}^{\mathfrak{O}}(k+1) = 0$ yields $\xi\mu_{ij}^{\mathfrak{O}}(k+1) = 0$, whereas if $\mu_{ij}^{\mathfrak{O}}(k+1) > 0$ then projection is not needed anymore.

Now, we define transformation $\mathfrak{T}$ as,

$$\begin{cases}
\lambda^{\mathfrak{T}}(k) = \xi\lambda^{\mathfrak{O}}(k), \qquad \theta^{\mathfrak{T}}(k) = \theta^{\mathfrak{O}}(k)\\
\mu^{\mathfrak{T}}(k) = \xi\mu^{\mathfrak{O}}(k), \qquad P_G^{\mathfrak{T}}(k) = P_G^{\mathfrak{O}}(k).
\end{cases} \tag{3.44}$$

Under this transformation (3.40)-(3.43) are stated as,

$$\begin{aligned}
\lambda_i^{\mathfrak{T}}(k+1) &= \lambda_i^{\mathfrak{T}}(k) - \beta_m\cdot\left(\lambda_i^{\mathfrak{T}}(k)\sum_{j\in\Omega_i}\frac{1}{X_{ij}} - \sum_{j\in\Omega_i}\lambda_j^{\mathfrak{T}}(k)\frac{1}{X_{ij}} + \sum_{j\in\Omega_i}\left(\mu_{ij}^{\mathfrak{T}}(k) - \mu_{ji}^{\mathfrak{T}}(k)\right)\frac{1}{X_{ij}}\right)\\
&\quad -\alpha_m\cdot\left(\sum_{n\in\Omega_{G_i}}P_{G_n}^{\mathfrak{T}}(k) - P_{L_i} - \sum_{j\in\Omega_i}\frac{\theta_i^{\mathfrak{T}}(k) - \theta_j^{\mathfrak{T}}(k)}{X_{ij}}\right) \qquad (3.45)
\end{aligned}$$

$$P_{G_n}^{\mathfrak{O}}(k+1) = \mathbb{P}_n\left[\frac{\lambda_i^{\mathfrak{T}}(k) - \xi b_n^{\mathfrak{O}}}{2\xi a_n^{\mathfrak{O}}}\right] \tag{3.46}$$

$$\theta_i^{\mathfrak{T}}(k+1) \;=\; \theta_i^{\mathfrak{T}}(k) - \gamma_m \left(- \sum_{n \in \Omega_{G_i}} P_{G_n}^{\mathfrak{T}}(k) + P_{L_i} + \sum_{j \in \Omega_i} \frac{\theta_i^{\mathfrak{T}}(k) - \theta_j^{\mathfrak{T}}(k)}{X_{ij}} \right) \tag{3.47}$$

$$\mu_{ij}^{\mathfrak{T}}(k+1) \;=\; \mathbb{P}\left[\mu_{ij}^{\mathfrak{T}}(k) - \delta_m \left(\overline{P}_{ij} - \frac{\theta_i^{\mathfrak{T}}(k) - \theta_j^{\mathfrak{T}}(k)}{X_{ij}} \right) \right] \tag{3.48}$$

$$\mu_{ji}^{\mathfrak{T}}(k+1) \;=\; \mathbb{P}\left[\mu_{ji}^{\mathfrak{T}}(k) - \delta_m \left(\overline{P}_{ij} + \frac{\theta_i^{\mathfrak{T}}(k) - \theta_j^{\mathfrak{T}}(k)}{X_{ij}} \right) \right]. \tag{3.49}$$

Equations (3.45)-(3.49) are similar to the iterative updates of $\mathcal{I} - \mathcal{DOPF}$ for system $\mathfrak{M}$ with tuning parameters adjusted to $(\alpha_m, \beta_m, \gamma_m, \delta_m)$, which converges to the optimal solution according to the hypothesis of *Justification 1.*

Finally, let $\mathcal{I} - \mathcal{DOPF}$ achieve the optimal solution, namely $[\xi\lambda^\star, \theta^\star, \xi\mu^\star, P^\star]$ for system $\mathfrak{M}$. Then, due to the transformation, defined by (3.44), $\mathcal{I} - \mathcal{DOPF}$ achieves $[\lambda^\star, \theta^\star, \mu^\star, P^\star]$ as the optimal solution for system $\mathfrak{O}$. This verifies *Remark 3.* Note that adding a fictitious bus does not change the solution of the DC-OPF, since it is not connected to a generator or a load.

We now analytically justify the applicability of our proposed approximate tuning parameter method for the modified test system ($\mathfrak{M}$), namely $(\alpha_m, \beta_m, \gamma_m, \delta_m)$. To this end, we consider system $\mathfrak{M}$ without line limit constraints for which we provide choices of β_m, γ_m and α_m that are guaranteed to lead to convergence of the corresponding $\mathcal{I} - \mathcal{DOPF}$ algorithm. Then, for this system $\mathfrak{M}$, δ is tuned according to the guideline presented in the previous subsection.

Note, by leaving out the μ update the corresponding matrix A, see (3.26), reduces to

A_r as follows,

$$A_r = \begin{bmatrix} \beta B & -\alpha B & \alpha I \\ 0 & \gamma B & -\gamma I \\ -\frac{I}{2a} & 0 & I \end{bmatrix}, \tag{3.50}$$

where we also assume that *M.1* and *M.2* hold for the above reduced modified system. The matrix A_r is then decomposed as

$$A_r = \overbrace{\begin{bmatrix} \beta B & -\alpha B & \alpha I \\ 0 & \gamma B & -\gamma I \\ 0 & 0 & I \end{bmatrix}}^{A_r^I} + \overbrace{\begin{bmatrix} 0 & 0 & 0 \\ 0 & 0 & 0 \\ -\frac{I}{2a} & 0 & 0 \end{bmatrix}}^{A_r^{II}}. \tag{3.51}$$

Remark 4: Using standard eigenvalue perturbation results, namely the Bauer–Fike theorem [21], since *M.1* ensures that all entries of A_r^{II} are less than ϵ, we have $\rho(A_r) \leq \rho(A_r^I) + O(\epsilon)$, where the order notation $O(\epsilon)$ denotes that the quantity goes to zero as $\epsilon \to 0$. Here, $\rho(.)$ denotes the spectral radius.

Moreover, A_r^I is an upper triangular matrix. Therefore the eigenvalues of A_r^I are the eigenvalues of its diagonal blocks, namely βB, γB and I.

Justification 2: Let *M.1* and *M.2* hold for the reduced modified system. Then there exists a set of tuning parameters such that $\rho(I - A_r) < 1$.

Proof: The three diagonal blocks of A_r^I are symmetric diagonally dominant matrices with positive diagonal entries, hence, they are positive semi-definite. Furthermore, *M.2* guarantees the positive definiteness of A_r^I's diagonal blocks. Although our system's set up includes a slack bus, a fictitious bus is required to remove singularity of the βB block. By adding an additional fictitious bus at least one row of B does not sum to zero, hence,

the resulting B matrix becomes non-singular. Note, the fictitious bus merely updates θ to ensure that its corresponding line flow stays zero. Using standard relations between matrix traces and eigenvalues, it may then be shown that

$$\rho(I - A_r^I) \;\leq\; max\left[1 - max(\beta \times \sum_{j\in\Omega_i} \frac{1}{X_{ij}}), 1 - max(\gamma \times \sum_{j\in\Omega_i} \frac{1}{X_{ij}})\right].$$

provided β and γ are sufficiently small. Specifically, by adjusting β and γ such that,

$$\begin{cases} \beta \leq \frac{1}{max_i \sum_{j\in\Omega_i} \frac{1}{X_{ij}}} \\ \\ \gamma \leq \frac{1}{max_i \sum_{j\in\Omega_i} \frac{1}{X_{ij}}}. \end{cases} \tag{3.52}$$

we would have $\rho(I - A_r^I) < 1$. In (3.34), the constant ϵ can be made arbitrary small by properly scaling the cost parameters in *M.1*, which results in $\rho(I - A_r^I) + O(\epsilon) < 1$, hence, $\rho(I - A_r) < 1$.

Remark 5: For any $\varsigma > 0$ there exists an ℓ_p-norm such that $\rho(A_r) \leq \|A_r\|_p \leq \rho(A_r) + \varsigma$.

Justification 3: Let β and γ hold in (3.52), then there exists an ℓ_p-norm such that $\|I - A_r\|_p < 1$.

Proof: Since β and γ hold in (3.52), *Justification 2* implies that $\rho(I - A_r) < 1$. Then, we can pick an $\varsigma > 0$ such that $\rho(I - A_r) + \varsigma < 1$ and, by *Remark 5*, we can find an ℓ_p-norm such that $\|I - A_r\|_p \leq \rho(I - A_r) + \varsigma < 1$.

After tuning β and γ, we choose α such that $\alpha > \beta$ and $\alpha > \gamma$. Then, we increase α until $\mathcal{I} - \mathcal{DOPF}$ does not converge any more. Finally, to tune δ we start with $\delta = 0.5 \times \beta$ and then increase δ until noticing oscillatory behavior.

Remark 6: Justification 1 further implies that assumption *M.1* does not affect the choice of β and γ for a system. Therefore, in order to tune the parameters one can follow

the steps provided in the previous subsection.

3.5 Simulation Results

3.5.1 Test System Set up

We use the IEEE 118-bus (see Appendix) [22] and 994-bus test systems to carry out simulations to test the $\mathcal{I}-\mathcal{DOPF}$, $\mathcal{AI}-\mathcal{DOPF}$ and $\mathcal{EI}-\mathcal{DOPF}$ algorithms. For the $\mathcal{I}-\mathcal{DOPF}$, $\mathcal{AI}-\mathcal{DOPF}$ algorithms the communication network, i.e., which bus is communicating and exchanging information with which bus, has the same topology as the physical system. The consumption of the loads is set to be equal to the values given in the original systems, while the synchronous condensers are removed. Also, following the guidelines in Sect. 3.4.3, the tuning parameters are set to the values given in Table 3.2. The chosen line limits for the IEEE 118-bus test system result in three congested lines namely #4-#5, and #25-#27, and #49-#50.

We use cold start for the simulations. In the cold start, all variables except the λ's are set to zero at the start of the simulation, which is reasonable due to the fact that the λ's represent the locational marginal prices and are generally strictly bounded away from zero. Also, for an actual implementation, reasonable initial settings for all of these variables could be the optimal values computed for the previous time step.

Table 3.2: Tuning Parameter Values

Parameter	IEEE 118-bus
α	0.15
β	0.0032
γ	0.0032
δ	0.08

3.5.2 Convergence Measurements

In order to evaluate the performance of the proposed distributed approach, two measures are introduced. The first measure determines the relative distance of the objective function from the optimal value over the iterations,

$$rel = \frac{|f - f^*|}{f^*}, \tag{3.53}$$

where f^* is the optimal objective function value calculated by solving the centralized DC-OPF problem. In order to calculate f^*, the centralized problem is implemented in MATLAB environment and solved using the optimization package Tomlab. Moreover, the value of load balance, as one of the optimality conditions, is potentially another indication of the distance from the optimal value, since the value of the load balance at the optimal point is equal to zero. Thus, we propose using the sum over the residuals of all power flow equations over the course of the iterations as the second measure of convergence, and is given by:

$$res = \sum_i \sqrt{g_i^2}, \tag{3.54}$$

where g_i corresponds to the local power flow balance at bus i, which enforces supply/demand balance.

3.5.3 Case Study 1: Synchronous Update

In this subsection, we use synchronous updates for all buses. Figure. 3.3(a) shows the evolution of the power output of the generator buses over 7500 iterations for the IEEE RTS. Figures 3.3(b) and 3.3(c) show the evolution of λ and μ, respectively. Also, Fig. 3.4 shows the rel, and the res for the same simulation set up. At the final iteration, the maximum power balance constraint violation is 0.0048. Note that, occasional oscillations appear which could be prevented by reducing some of the tuning parameters further but

this would also lead to a larger number of iterations until convergence. It can be seen that the three Lagrange multipliers associated with the line constraints of the congested lines are non-zero and the locational marginal prices λ are not equal to the same value.

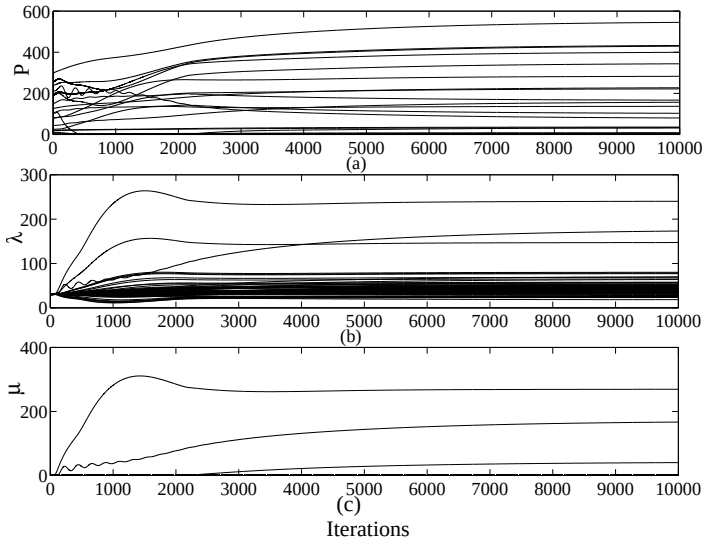

Figure 3.3: (a) Generation output (b) Lagrangian multiplier λ (c) Lagrangian multiplier μ for the IEEE 118-bus system with synchronous update

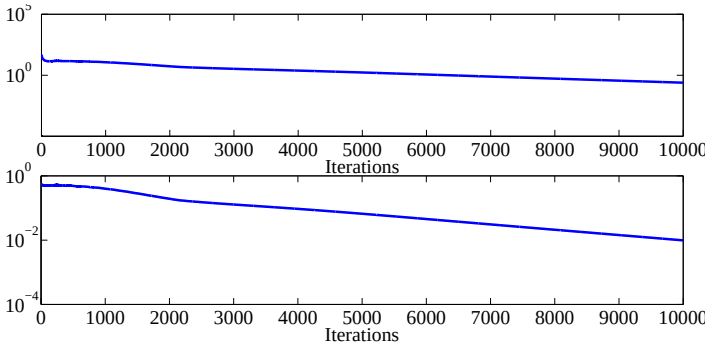

Figure 3.4: (a) Objective function value $\frac{|f-f^*|}{f^*}$ and (b) residual of equality constraints $\sum_i \sqrt{g_i^2}$ for the IEEE 118-bus system with synchronous update.

Note that each iteration is computationally very inexpensive as it only requires the evaluation of algebraic functions which are done in parallel at the individual buses. In the above figures, each iteration merely corresponds to updating the variables according to updates (3.14)-(3.18). The resulting intermediate values do not necessarily constitute a feasible solution of the power flow equations.

3.5.4 Case Study 2: Synchronous Update with extra links

Figure 3.5 shows the evolution of the *rel* and *res* values for the set up that is introduced in Sect. 3.5.2, in which three of the system lines are congested, for 10000 iterations with four additional communication links as given in Table 3.3. This figure clearly illustrates the effect of added communication links on the convergence towards the optimal solution from the centralized DC-OPF.

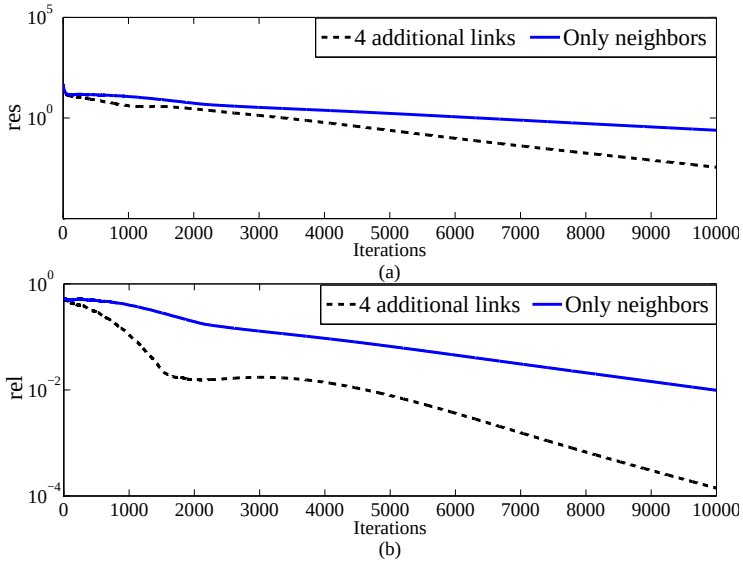

Figure 3.5: (a) Residual of equality constraint $\sum_i \sqrt{g_i^2}$ (b) Relative distance to solution $(\frac{|f-f^*|}{f^*})$

Table 3.3: added communication links for the congested case

ID	Added communication links
0AL	No link
1AL	65-4
2AL	65-15 & 65-4
3AL	100-4 & 65-15 & 65-4
4AL	65-50 & 100-4 & 65-15 & 65-4

Figure. 3.6 illustrates the impact of adding new communication links with more details. Based on these simulations, as the number of new communication links increases, the efficacy of new additional communication links reduces. In other words, the influence of new communication links on the convergence rate decreases.

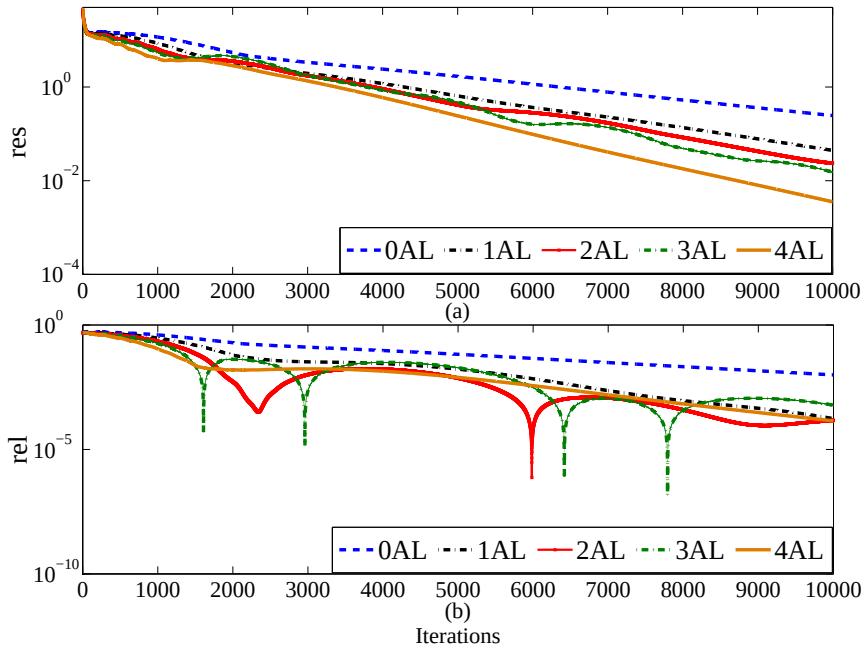

Figure 3.6: (a) Residual of equality constraint $\sum_i \sqrt{g_i^2}$ (b) Relative distance to solution $(\frac{|f-f^*|}{f^*})$

3.5.5 Case Study 3: Asynchronous Update

Figure. 3.7 presents the simulation results for the IEEE 118-bus test system when it is divided into two areas, and updated values are exchanged among buses within each area at every iteration and between buses in separate areas only once every 30 iterations. This figure illustrate the results for the generation settings and for the Lagrangian multipliers, where the evolution at the outer iterations are shown, i.e., every 30th inner iteration, hence, the total number of inner iterations conducted is actually 5000. Furthermore, Fig.3.8 illustrates the introduced convergence measures, i.e., *rel* and *res*, over the course of iterations for this case.

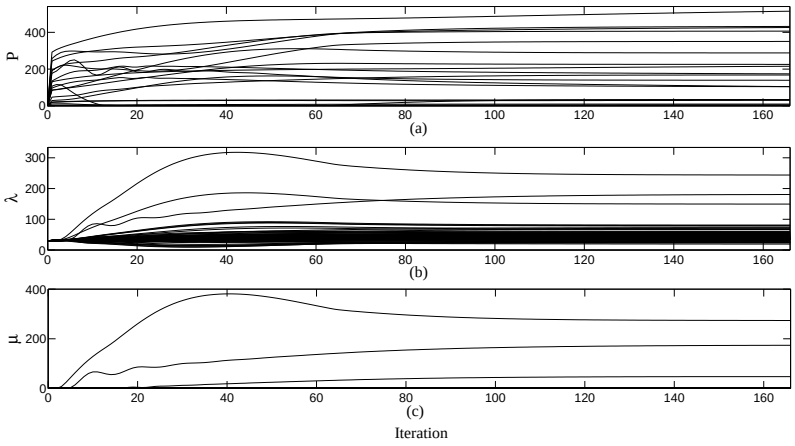

Figure 3.7: (a) Generation output (b) Lagrangian multiplier λ (c) Lagrangian multiplier μ for IEEE 118-bus with asynchronous update, 2 areas.

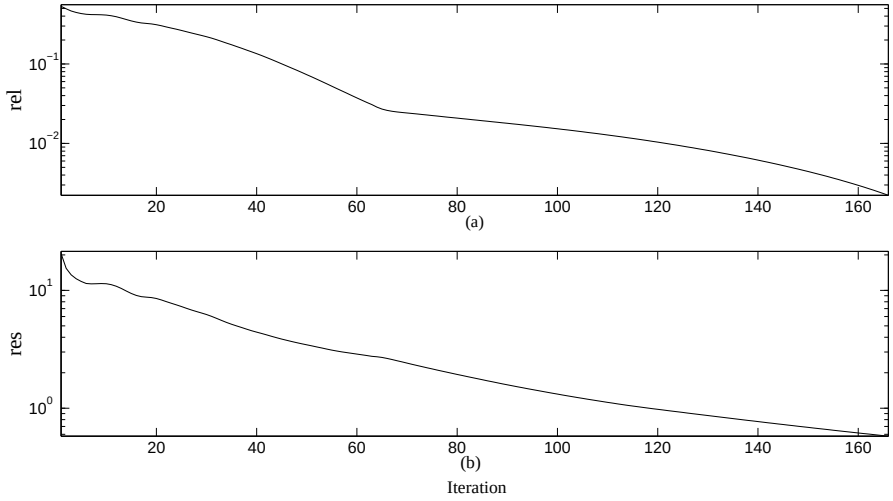

Figure 3.8: (a) Objective function value $\frac{|f-f^*|}{f^*}$ and (b) residual of equality constraints $\sum_i \sqrt{g_i^2}$ for IEEE 118-bus with asynchronous update, 2 areas.

Now, the IEEE 118-bus test system is divided into four areas, and inter-area information exchange takes place every 20 iterations. Figure 3.9 shows the P_G, λ, and μ over the course of 5000 inner iterations. Moreover, Fig. 3.10 depicts the *rel* and *res* for the same system settings. The speed of convergence with respect to inner iterations depends on the number of areas and how often these areas exchange update information. Generally, if number of areas increases but the communication gap stays the same, convergence speed reduces.

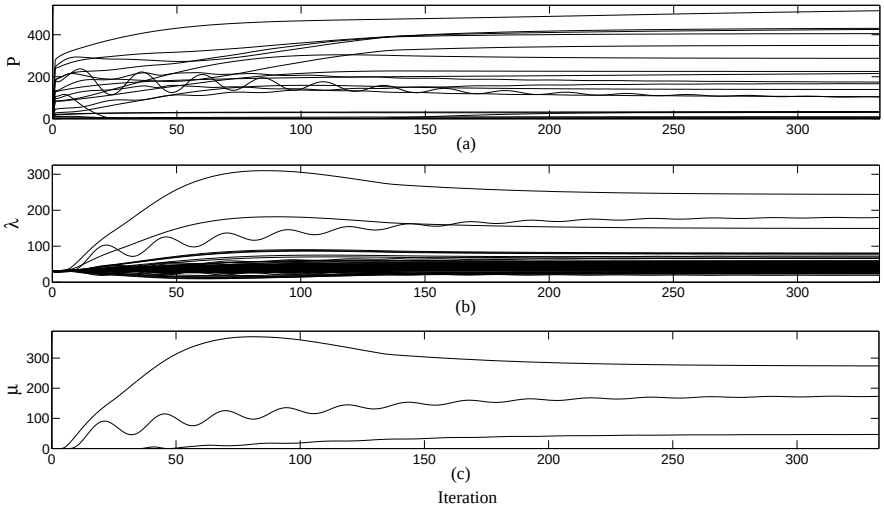

Figure 3.9: (a) Generation output (b) Lagrangian multiplier λ (c) Lagrangian multiplier μ for IEEE 118-bus with asynchronous update, 4 areas.

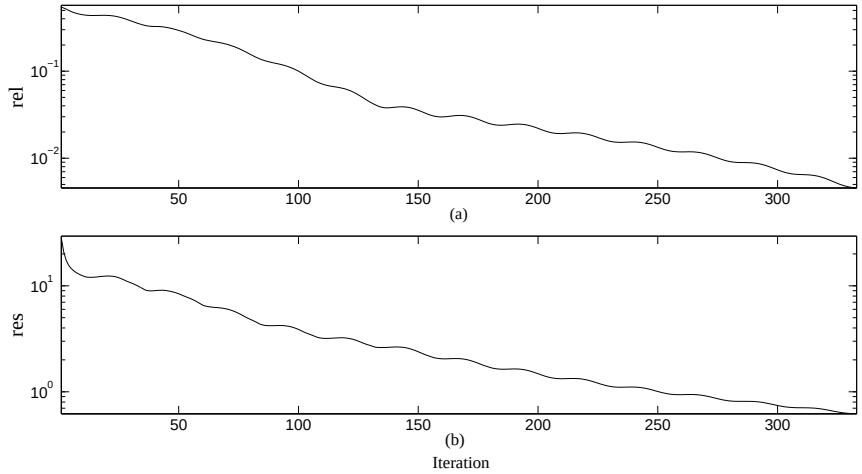

Figure 3.10: (a) Objective function value $\frac{|f-f^*|}{f^*}$ and (b) residual of equality constraints $\sum_i \sqrt{g_i^2}$ for IEEE 118-bus with asynchronous update, 4 areas.

It can be assumed that inner iterations do not require any communication if carried out centrally inside the region thereby reducing the communication needs significantly.

Also note, although as the outer communication time gap increases, the frequency of outer data exchange decreases, a big outer communication time gap could result in divergence of the algorithm. For example, based on our simulations for IEEE 118-bus, with 4 areas, $\mathcal{AI}-\mathcal{DOPF}$ diverges if time gap is larger than 200 iterations.

Moreover, asynchronous updates are carried out for 994-bus test system. To this end, eight 118-bus test systems, i.e., each of them considered as an area, are attached to each other to form the 944-bus test system. Updated values are exchanged between agents within the area after each iteration and between agents in separate areas once every 20 iterations. The tuning parameters are presented in Table 3.4. Figure 3.11 presents the outer iteration results for the generation settings P_G, Lagrangian multiplier μ and res. Note, it is assumed that inner iterations do not require any communication if carried out at a central regional location thereby reducing the communication needs significantly.

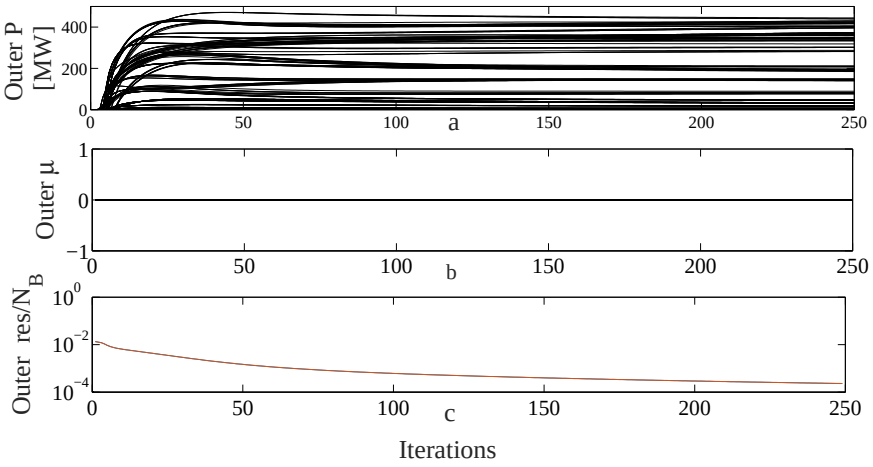

Figure 3.11: (a) Generation output, (b) Lagrangian multiplier μ and (c) Residual of equality constraint $\sum_i \sqrt{(g_i^c)^2}/N_B$, $\mathcal{AI} - \mathcal{DOPF}$, 944 bus test system.

Table 3.4: Tuning Parameter Values

Parameter	944-bus
α	0.0040
β	0.0024
γ	0.0004
δ	0.3

3.5.6 Case Study 4: Asynchronous Update with Additional Communication

Table 3.5 presents the achieved *res* for the IEEE 118-bus test system after 5000 iterations under various partitioning and two different communication topologies, i.e., with and without additional communication links. Note, that two additional communication links are utilized in addition to the communication links in the physical neighborhood. These new links connect two major generators (buses #65 and #4) and a major generator and major load (buses #65 and #50) across the system. The tuning parameters are kept the same for the sake of comparison.

Based on this table, as the number of areas increases and equal communication gap, the convergence gets slower. This makes intuitive sense, since coordination overhead is proportional to the number of areas. Also, this table clearly shows the effectiveness of the additional communication links.

Table 3.5: Achieved *res* under different communication topology and portioning, IEEE 118 system

# areas	Outer area communication gap	*res* without additional links	*res* with two additional links
1	1	0.51	0.45
2	30	0.57	0.55
4	20	0.73	0.69
6	20	0.85	0.8

3.6 Summary

In this chapter, we presented a distributed approach to solve the DC Optimal Power Flow problem, i.e., the generation dispatch is determined which minimizes the cost to supply the

load in a distributed manner taking into account limited line capacities. The main features of the algorithm are that it allows for a fully distributed implementation down to the bus level without the need for a coordinating central entity; the individual updates per iteration consist of simple function evaluations and exchange of information is limited to bus angles and Lagrange multipliers associated with power flow equations and line constraints among the neighboring buses. In particular, there is no need to share information about generation cost parameters or generation settings.

We discussed synchronous and asynchronous implementations of the proposed algorithm. The asynchronous version not only allows to model multiple information exchange modalities in the system but also communication delays. The asynchronous updates enable a more realistic implementation to optimally coordinate across geographically distinct areas and/or to improve computation speed by parallelizing calculations. Moreover in order to improve convergence rate of our developed method, we proposed to add additional communication links between distant buses in the system and provided a way to make beneficial use of the information exchanged between these distant buses in the local variable update. These additional links improve the flow of information in the system, which leads to faster agreements between the buses across the system on the values for the control variables. In particular, we suggested that adding communication links between the influential buses across the network to exchange the supply/demand imbalance enhances the convergence rate. Along this line, investigating impact of communication graph's connectivity on the convergence properties of our proposed algorithm is a valuable research direction. The proposed algorithms were tested in the IEEE 118-bus and 944-bus test systems showing that it converges to the overall optimal solution. Moreover, this chapter discusses the convergence criteria for the proposed distributed method, and analytically proves that the limit point of our innovation-based approach is the optimal solution of the OPF problem.

Chapter 4

Distributed Security Constrained Optimal Power Flow

4.1 Introduction

4.1.1 Motivation and Related Work

In this chapter, we propose a distributed energy management procedure with focus on security of power network operation. Today's centralized controllers have to deal with the large scale problem of coordinating geographically scattered energy resources while ensuring reliable operation of the power system in accordance with the N-1 security criteria. To fulfill the N-1 security requirement, generation is dispatched such that no operational constraints are violated in normal conditions or in any credible contingency case involving the failure of at most one system component. The respective generation dispatch is found by solving the Security Constrained Optimal Power Flow (SCOPF) problem. Traditionally, this problem is solved in a centralized fashion.

However, current coordination practices are incapable of coping with challenges caused by evolving power grid's new technologies and capabilities. Majority of industry leaders

have reached consensus on the need for transitioning from existing centralized control to a hybrid central/distributed control structure. To address this need, an alternative control structure should be designed to provide features such as regional authorization of entities, coordinated control of regional entities, and scalability to work seamlessly with other elements of the existing grid [23]. This need has motivated the Seams Issues Subcommittee of the Western Electricity Coordinating Council (WECC) to search for coordination approaches to perform virtual consolidation for wide-area security constrained economic dispatch over multiple balancing areas while accounting for seams problems [24]. In this chapter, we present an off-line distributed coordination method that could be used to enable SCOPF for virtual consolidation of multiple balancing areas.

In the proposed multi-agent context, the DC-SCOPF[1] problem is viewed as a collaborative distributed optimization problem in which the network agents collectively aim to minimize the global cost of secure power system operation. In our approach denoted by $\mathcal{I}-\mathcal{DSCOPF}$ (Innovation based Distributed Security Constrained Optimal Power Flow), each agent is responsible for updating its local variables pertaining to normal operation as well as contingency cases. As it was discussed in chapter 3, our proposed innovation based update structure is based on the fact that each of the optimality conditions constitutes equalities or inequalities with only local variable coupling. The local updates are built on the local Lagrange multipliers relationships and the fact that the power flow equation should hold at every bus.

In $\mathcal{I}-\mathcal{DSCOPF}$, an agent corresponds to a power system bus, thereby representing a collection of generator/load/storage entities connected to that bus. The $\mathcal{I}-\mathcal{DSCOPF}$ requires buses to exchange variable updates after every iteration, which might be prohibitive for an actual implementation. Like chapter 3 we also propose a more realistic version of our proposed algorithm, denoted by $\mathcal{AI}-\mathcal{DSCOPF}$ (Asynchronous *Innova-*

[1]Using DC approximation for N-1 calculations is a common practice in today's power system operation, e.g., Midwest Independent Transmission System Operator and Southwest Power Pool [25].

tion based Distributed Security Constrained Optimal Power Flow), which does not require every bus to exchange information with all of its neighbors after every single iteration. Similar to the $\mathcal{AI}-\mathcal{DOPF}$ method in chapter 3, the $\mathcal{AI}-\mathcal{DSCOPF}$ groups buses into areas where the exchange between buses within the areas may take place every iteration while communication with buses in another area might take place only every x-th iteration.

Moreover, $\mathcal{AI}-\mathcal{DSCOPF}$ structure allows for assigning an agent to each area to perform the intra-area computations at a central location within the area which makes the intra-area communications redundant. Therefore, $\mathcal{AI}-\mathcal{DSCOPF}$ can be employed to achieve improved coordination among control areas thereby leading to optimal overall system utilization or to address what is commonly referred to as the seams problem, i.e., enabling coordination among areas to exchange energy while executing their own policies locally in their own areas.

Prior distributed approaches to solve the SCOPF have mostly been based on decomposition theory [26]. A widely used decomposition technique to tackle the computational complexity of the SCOPF problem is Benders decomposition technique e.g., [27, 28, 29]. Benders decomposition facilitates parallel computing and copes with the large scale nature of the original SCOPF optimization problem by decomposing the SCOPF into a master problem corresponding to normal operation (pre-contingency, $c = 0$) and N_c subproblems, each corresponding to a contingency case ($c \in \{1, \cdots, N_c\}$).

Lagrangian based methods are also applied to find regionally decomposed solution approaches for the SCOPF problem. In these regionally decomposed techniques the SCOPF is divided into subproblems where each subproblem corresponds to a region, e.g., [30, 31]. In order to solve the SCOPF problem, [30, 31] proposed decoupling the problem at tie-lines connecting neighboring areas, and leaving each area with an autonomous area SCOPF problem to solve. On the other hand, [32] suggested an Alternating Direction Method of Multipliers (ADMM) which decouples the SCOPF problem into subproblems associated

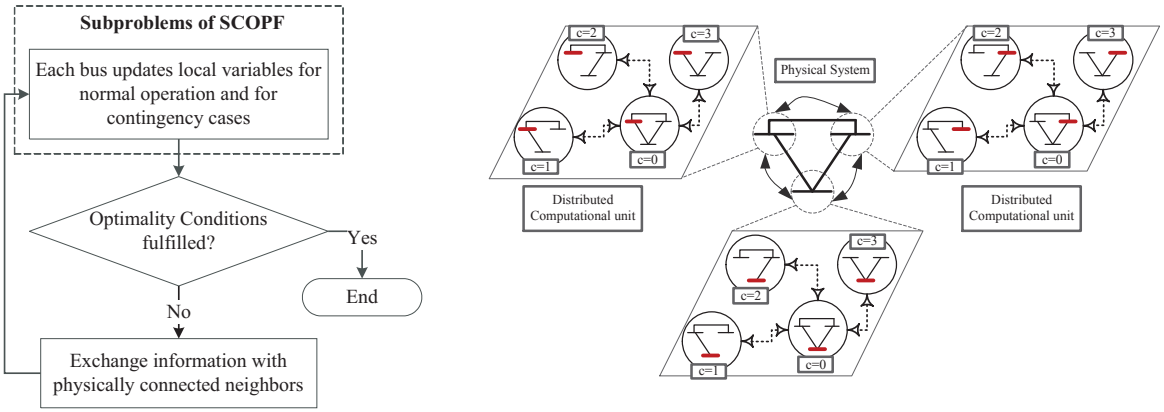

(a) Local bus level computation

(b) Communication and computation structure of the Innovation-based distributed approach

Figure 4.1: The $\mathcal{I}-\mathcal{DSCOPF}$ distributed structure, the dashed line represents inner data exchange, and the solid line represents outer communication. The $c=0$ refers to normal operation (pre-contingency) while $c \neq 0$ refers to the post-contingency cases

with each bus. Although, ADMM addresses the large scale of the SCOPF problem, it requires a central coordination of the subproblems because of the update of the multipliers. In [33], the authors proposed a fully distributed algorithm to solve the SCOPF using the proximal message passing method, where each network device solves an optimization problem at each iteration, and exchanges information with connected neighbors.

This chapter expands our previous work presented in chapter 3, which focused on the OPF problem, to the SCOPF problem. Similarly to the $\mathcal{I}-\mathcal{DOPF}$ (see Sect. 3.3.1), the proposed $\mathcal{I}-\mathcal{DSCOPF}$ approach assigns an agent to each bus. Each agent is not only responsible for the update of a few local variables for normal operation but also the local variables for the contingency cases. Each agent further exchanges information about the normal and the contingency cases with other neighboring agents. Our algorithm directly solves the first order optimality conditions for the security constrained optimal power flow problem, i.e., reduces the original optimization problem into solving a coupled system of linear equations.

The key features of $\mathcal{I}-\mathcal{DSCOPF}$ are as follows:

- Implemented in a fully distributed fashion (see Fig. 4.1(a)).

- Parallelized computation at all buses without centralized entity, as illustrated in Fig. 4.1(a).
- Parallelized computation of normal operation and all contingency cases with contingency cases impacting normal operation only if contingency cases become binding, (will be discussed in detail in Sect. 4.3)

Note, although the structure of $\mathcal{I}-\mathcal{DSCOPF}$ allows for parallel computations, tackling the computational complexity of the SCOPF problem is not the primary focus of this chapter. Additionally, while $\mathcal{I}-\mathcal{DSCOPF}$ allows for a fully distributed calculation of the solution to the DC-SCOPF problem, that does not mean that the implementation has to be done in a geographically distributed way. In fact, the introduced $\mathcal{AI}-\mathcal{DSCOPF}$ provides flexibility in choosing the level of distributedness for the actual implementation of the proposed distributed algorithm.

4.1.2 Notation

Parameters and Constants

P_{L_i}	Load at bus i
a_n, b_n, c_n	Cost function parameters of generator n
$\overline{P}_{G_n}$	Maximum generation of generator n
$\underline{P}_{G_n}$	Minimum generation of generator n
Ω_G	Set of all generators
Ω_B	Set of all buses
Ω_{G_i}	Set of all generators at bus i
Ω_L^c	Set of all lines in operation during contingency c
Ω_C	index set corresponding to the set of normal operation and all contingencies ($\Omega_C = \{0, \cdots, NC\}$),

Ω_i^c	Set of all buses that bus i communicates with in additions to its physical neighbors in contingency c
Ω_{i^+}	Set of all buses connected to bus i through additional communication links
X_{ij}	Reactance of line ij
$\overline{P}_{ij}$	Line flow limit of line ij
$\alpha, \beta, \gamma, \tau, \eta$	Tuning paramters
N_B	Number of buses

Variables

P_{G_n}	Power output of generator n
θ_i^c	Voltage angle at bus i in contingency c
μ_n^+, μ_n^-	Lagrangian multipliers related to upper and lower generation limits of generator n
μ_{ij}^c	Lagrangian multiplier of the line flow constraint of line ij in contingency c
λ_i^c	Lagrangian multiplier of the load balance equation of bus i in contingency c

4.2 DC Security Constrained OPF

4.2.1 Problem Formulation

The objective of the SCOPF problem is to determine the generation dispatch which supplies the load at the least cost while ensuring that the system is N-1 secure. Consequently, the SCOPF problem has a set of line flow constraints for the pre-contingency case ($c = 0$) and a set of constraints for each post-contingency case ($c \in \{1, \cdots, N_C\}$). Using the DC power flow approximation the problem formulation is therefore given by

$$
\begin{aligned}
&\min_{P_G,\theta} \sum_{n\in\Omega_G} (a_n P_{G_n}^2 + b_n P_{G_n} + c_n) \\
\text{s.t. } & P_{G_i} - P_{L_i} = \sum_{j\in\Omega_i^c} \frac{\theta_i^c - \theta_j^c}{X_{ij}}, \quad \forall i \in \Omega_B, \ \ \forall c \in \Omega_C \\
& \theta_1 = 0 \\
& \underline{P}_{G_n} \le P_{G_n} \le \overline{P}_{G_n}, \quad \forall n \in \Omega_G \\
& -\overline{P}_{ij} \le \frac{\theta_i^c - \theta_j^c}{X_{ij}} \le \overline{P}_{ij}, \ \forall ij \in \Omega_L^c. \ \ \forall c \in \Omega_C
\end{aligned} \tag{4.1}
$$

The above formulation is another instance of the compact problem formulation in Sect. 2.1, where $\mathfrak{G}$ enforces the power balance constraint at all buses for all contingency cases, and and $\mathfrak{H}$ corresponds to limits on decision variables and operational constraints. Here, $i = 1$ is taken to be the slack bus.

4.2.2 Optimality Conditions

The Lagrangian function for this convex optimization problem can be written as:

$$
\begin{aligned}
L = & \sum_{n\in\Omega_G} (a_n P_{G_n}^2 + b_n P_{G_n} + c_n) \\
& + \sum_{n\in\Omega_G} \mu_n^+ (P_{G_n} - \overline{P}_{G_n}) + \sum_{n\in\Omega_G} \mu_n^- (-P_{G_n} + \underline{P}_{G_n}) \\
& + \sum_{c=0}^{N_C} \sum_{i\in\Omega_B} \lambda_i^c \cdot (-P_{G_i} + P_{L_i} + \sum_{j\in\Omega_i^c} \frac{\theta_i^c - \theta_j^c}{X_{ij}}) \\
& + \sum_{c=0}^{N_C} \sum_{ij\in\Omega_L^c} \mu_{ij}^c \cdot (\frac{\theta_i^c - \theta_j^c}{X_{ij}} - \overline{P}_{ij}) \\
& + \sum_{c=0}^{N_C} \sum_{ji\in\Omega_L^c} \mu_{ji}^c \cdot (-\frac{\theta_i^c - \theta_j^c}{X_{ij}} - \overline{P}_{ij}),
\end{aligned}
$$

where the λ's and the μ's correspond to the Lagrange multipliers of the equality and inequality constraints of the SCOPF problem, respectively. Since our proposed approach is based on solving the optimality conditions of the DC-SCOPF problem in a distributed manner, the rest of this subsection is devoted to the derivation of the first order optimality conditions which are given as follows:

$$\frac{\partial L}{\partial P_{G_n}} = 2a_n P_{G_n} + b_n - \sum_{c=0}^{N_c} \lambda_n^c + \mu_n^+ - \mu_n^- = 0 \tag{4.2}$$

$$\frac{\partial L}{\partial \theta_i^c} = \lambda_i^c \sum_{j \in \Omega_i^c} \frac{1}{X_{ij}} - \sum_{j \in \Omega_i^c} \lambda_j^c \frac{1}{X_{ij}} + \sum_{j \in \Omega_i^c} (\mu_{ij}^c - \mu_{ji}^c) \frac{1}{X_{ij}} = 0 \tag{4.3}$$

$$\frac{\partial L}{\partial \lambda_i^c} = -P_{G_i} + P_{Li} + \sum_{j \in \Omega_i^c} \frac{\theta_i^c - \theta_j^c}{X_{ij}} = 0 \tag{4.4}$$

$$\frac{\partial L}{\mu_n^+} = P_{G_n} - \overline{P}_{G_n} \leq 0 \tag{4.5}$$

$$\frac{\partial L}{\mu_n^-} = -P_{G_n} + \underline{P}_{G_n} \leq 0 \tag{4.6}$$

$$\frac{\partial L}{\mu_{ij}^c} = \frac{\theta_i^c - \theta_j^c}{X_{ij}} - \overline{P}_{ij} \leq 0 \tag{4.7}$$

$$\frac{\partial L}{\mu_{ji}^c} = -\frac{\theta_i^c - \theta_j^c}{X_{ij}} - \overline{P}_{ij} \leq 0, \tag{4.8}$$

for all $i \in \Omega_B$, $c \in \Omega_C$, $n \in \Omega_G$, and $ij \in \Omega_L^c$. Additionally, the complementary slackness conditions for the inequality constraints and the positivity constraints on the μ's need to hold. In order to find a solution for the DC-SCOPF problem, the above constrained equation system needs to be solved. Given that the choice of the slack bus does not have any influence on the result of the underlying optimization problem, $\theta_1 = 0$ is omitted from the Lagrangian function and first order optimality conditions. Since the discussed DC-SCOPF is convex and also satisfies the strong duality conditions, any solution that fulfills all of the discussed first order optimality conditions is the optimal solution of the DC-SCOPF problem. Here, we assume that the primal optimization problem is strictly feasible.

4.3 Distributed Approach

This section presents the distributed updates for $\mathcal{I}-\mathcal{DSCOPF}$ and $\mathcal{AI}-\mathcal{DSCOPF}$. These proposed iterative procedures solve the constrained system given in Sect. 4.2.

4.3.1 The $\mathcal{I}-\mathcal{DSCOPF}$ Algorithm

This section presents the $\mathcal{I}-\mathcal{DSCOPF}$ iterative algorithm to solve the first order optimality conditions of the SCOPF problem, where each agent (bus) merely exchanges information with its physically connected neighbors during the course of the iterations. The set of variables that each agent i updates include the estimates of the setting of the generator at bus i, all Lagrange multipliers and bus angles associated with bus i for normal operation and contingency cases. The general format of the local updates follows the format given in Sect. 2.3.1.

In our distributed $\mathcal{I}-\mathcal{DSCOPF}$ approach, agent i takes care of updating and finding the optimal values for the variables associated with it, namely λ_i^c, θ_i^c, P_{G_i}, and μ_{ij}^c for $j \in \Omega_i$ but receives the updates for $\lambda_j^c, \theta_j^c, \mu_{ji}^c$ from the neighboring agents j. The remainder of this section is devoted to introducing the distributed updates for each of the variables, i.e, λ_i^c, θ_i^c, P_{G_i}, and μ_{ij}^c for all i and $j \in \Omega_i$.

The proposed update for λ_i^c iterate is given as:

$$\begin{aligned}
\lambda_i^c(k+1) &= \lambda_i^c(k) - \beta\left(\frac{\partial L}{\partial \theta_i^c}\right) + \alpha\left(\frac{\partial L}{\partial \lambda_i^c}\right) \\
&= \lambda_i^c(k) - \beta\left(\lambda_i^c(k)\sum_{j\in\Omega_i^c}\frac{1}{X_{ij}} - \sum_{j\in\Omega_i^c}\lambda_j^c(k)\frac{1}{X_{ij}} + \sum_{j\in\Omega_i^c}(\mu_{ij}^c(k)-\mu_{ji}^c(k))\frac{1}{X_{ij}}\right) \\
&\quad - \alpha\left(P_{G_i}(k) - P_{L_i} - \sum_{j\in\Omega_i^c}\frac{\theta_i^c(k)-\theta_j^c(k)}{X_{ij}}\right),
\end{aligned} \tag{4.9}$$

where $\alpha, \beta > 0$ are tuning parameters and k denotes the iteration index. In this update rule, the first term, which corresponds to the optimality condition (4.3), preserves the coupling between the neighboring Lagrange multipliers, whereas the local power flow equation (4.4) constitutes the second term to enforce the supply/demand balance at each bus. This update has the same structure as λ update that is presented in Sect. 3.3.1, hence, the same argument justifies its intuition.

Then, given the value of the Lagrange multiplier estimates $\lambda_i^c(k+1)$, the P_G iterates are updated by:

$$P_{G_i}(k+1) = \mathbb{P}_i \left[\frac{\sum_{c=0}^{N_c} \lambda_i^c(k+1) - b_n}{2a_n} \right], \tag{4.10}$$

where the operator $\mathbb{P}_i$ denotes projection onto the interval $[\underline{P}_{G_i}, \overline{P}_{G_i}]$, i.e., if the value is greater than $\overline{P}_{G_i}$, the $P_{G_i}(k+1)$ estimate is set to that upper limit and similarly for the lower limits. This update is derived based on the intuition that was discussed in Sect. 3.3.1 for the P_G update. A detailed convergence analysis is presented in Sect. 4.4 where we analytically prove that the $\mathcal{I} - \mathcal{DSCOPF}$ converges to the optimal solution of the SCOPF even without directly updating μ_n^+ and μ_n^-.

The angles of the buses are updated according to

$$\begin{aligned} \theta_i^c(k+1) &= \theta_i^c(k) - \gamma \left(\frac{\partial L}{\partial \lambda_i^c} \right), \\ &= \theta_i^c(k) - \gamma \left(-P_{G_i}(k) + P_{L_i} + \sum_{j \in \Omega_i} \frac{\theta_i^c(k) - \theta_j^c(k)}{X_{ij}} \right), \end{aligned} \tag{4.11}$$

with $\gamma > 0$ being a tuning parameter. Again, this update is based on the same intuition as the θ update in the previous chapter (see (3.16)).

The Lagrange multiplier iterates corresponding to the line limits are updated as follows:

$$\begin{aligned}\mu_{ij}^c(k+1) &= \mathbb{P}_{ij}\left[\mu_{ij}^c(k) + \delta\left(\frac{\partial L}{\partial \mu_{ij}^c}\right)\right] \\ &= \mathbb{P}_{ij}\left[\mu_{ij}^c(k) - \delta\left(\overline{P}_{ij} - \frac{\theta_i^c(k) - \theta_j^c(k)}{X_{ij}}\right)\right],\end{aligned} \tag{4.12}$$

where $\delta > 0$ is a tuning parameter and the projection $\mathbb{P}_{ij}$ ensures the positivity of μ_{ij}^c, the Lagrange multiplier estimates obtained in (4.12), by projecting the resulting updated values onto the interval $[0, \infty)$.

The update rules of the $\mathcal{I} - \mathcal{DSCOPF}$ algorithm, (4.9)-(4.12), meet the requirement for a distributed solution approach, since each agent i performs the updates for local variables using only local information, i.e., its and its neighbors' previous iterates. Moreover, the fact that the updates depend only on the previous iterates enables the parallel computation of the updates for all agents across the system.

The update (4.10) for the generator outputs is the only update which involves variables from multiple system states, i.e., normal state and contingency states ($c \in \{0, \cdots, N_C\}$). However, as long as all line flows in a particular contingency case c are below their limits, the optimal generation setting is actually not affected by contingency c and therefore the Lagrange multiplier values λ_i^c turn out to be zero. While iterating towards the solution, however, the Lagrange multipliers are non-zero and may unnecessarily impact the update of the P_{G_i} iterates. Consequently, we can adjust the update such that we only include the estimate λ_i^c for contingency c in update (4.10) if any of the iterate μ_{ij}^c for that contingency are non-zero. This will require spreading the information about if any of these Lagrange multipliers have become non-zero throughout the network. We call this approach the version **B** of the distributed algorithm and the original formulation, i.e., taking into account the λ_i^cs even if no line constraint becomes binding for contingency c, version **A** of the algorithm. Given that the power generation update (4.10) is the only update which takes into account the interaction between different system conditions ($c \in \{0, \cdots, N_C\}$),

the updates for the normal and contingency cases can be solved concurrently (one step). Particularly, if approach **B** is used for the update of the generator settings, then the updates for the contingency cases can basically run in the background without affecting the iterations of the normal operation if none of the μ_{ij} iterate become greater than zero.

The P_G update for the version **B** of the $\mathcal{I}-\mathcal{DSCOPF}$ is given as

$$P_{G_i}(k+1)=\mathbb{P}_i\left[\frac{\sum_{c=0}^{N_c}(1-e^{-\varkappa\sum_{ij\in\Omega_L^c}\mu_{ij}^c})\cdot\lambda_i^c(k+1)-b_n}{2a_n}\right].$$

where $\varkappa$ is a large positive number. As long as the μ_{ij}^c's are zero the λ_i^c does not have any impact on P_{G_i}, but as soon as they become non-zero, the term in the first parentheses becomes close to one due to the large value of $\varkappa$. Therefore, using the exponential term leads to proper incorporation of the λ_i^c iterates associated with non-zero μ_{ij}^c estimates.

4.3.2 The $\mathcal{AI}-\mathcal{DSCOPF}$ Algorithm

In the $\mathcal{AI}-\mathcal{DSCOPF}$'s procedure, some buses only exchange information after every x-th iteration, whereas $\mathcal{I}-\mathcal{DSCOPF}$ requires every bus to exchange information with all of its neighbors after every single iteration. The asynchronous implementation may be used in a situation in which the goal is to coordinate multiple areas, each area, for instance being operated by a single central entity: the internal iterations for the buses within each area could be done at a central location within the area and the designated area centers exchange information with each other, referred to as outer iterations, after every few of these inner iterations. We introduce an iteration counter k_i for each bus and iteration counter n_{ij} for the update of the information between buses i and j, assuming that n_{ij} only increases after every x-th increase of k_i and k_j. Hence, updates (4.9), (4.11) and (4.12) are adjusted to

$$\lambda_i^c(k_i+1) = \lambda_i^c(k_i) - \beta \left(\lambda_i^c(k_i) \sum_{j\in\Omega_i} \frac{1}{X_{ij}} - \sum_{j\in\Omega_i} \lambda_j^c(n_{ij}) \frac{1}{X_{ij}} + \sum_{j\in\Omega_i} \left(\mu_{ij}^c(k_i) - \mu_{ji}^c(n_{ij}) \right) \frac{1}{X_{ij}} \right)$$
$$-\alpha \cdot \left(\sum_{n\in\Omega_{G_i}} P_{G_n}(k_i) - P_{L_i} - \sum_{j\in\Omega_i} \frac{\theta_i^c(k_i) - \theta_j^c(n_{ij})}{X_{ij}} \right)$$

$$\theta_i^c(k_i+1) = \theta_i^c(k_i) - \gamma \left(- \sum_{n\in\Omega_{G_i}} P_{G_n}(k_i) + P_{L_i} + \sum_{j\in\Omega_i} \frac{\theta_i^c(k_i) - \theta_j^c(n_{ij})}{X_{ij}} \right)$$

$$\mu_{ij}^c(k_i+1) = \mathbb{P} \left[\mu_{ij}^c(k_i) - \delta \left(\overline{P}_{ij} - \frac{\theta_i^c(k_i) - \theta_j^c(n_{ij})}{X_{ij}} \right) \right].$$

Note, the proposed $\mathcal{AI} - \mathcal{DSCOPF}$ algorithm could be potentially used to enable SCOPF for virtual consolidation of balancing areas. The structure of $\mathcal{AI} - \mathcal{DSCOPF}$ allows for assigning an agent to each area. The intra-area computations for the buses within each area could be done at a central location within the area by an agent. Then, designated area agents exchange information with each other. The properties of our proposed asynchronous implementation, such as assigning control of each area to an agent, and requiring limited non-sensitive information exchange between agents, match with the characteristics of a desired virtual coordination framework [23].

4.4 Convergence Analysis

This section discusses the convergence properties of the proposed $\mathcal{I} - \mathcal{DSCOPF}$ algorithm for version **A** as described in Sect. 4.3. Although, the convergence analysis follows the same steps as presented in Sect. 3.4, for the sake of completeness we reiterate some of the analytical arguments discussed in Sect. 3.4. In order to derive the convergence properties for the $\mathcal{I} - \mathcal{DSCOPF}$ algorithm, we first introduce the compact form the distributed updates.

The update rules for the all variables in $\mathcal{I}-\mathcal{DSCOPF}$ can be written in a dense form as

$$\begin{aligned} X(k+1) &= \widetilde{X}(k) - A\widetilde{X}(k) + C \\ \widetilde{X}(k+1) &= \mathbb{P}[X(k+1)], \end{aligned} \tag{4.13}$$

where X is the vector of the stacked variables $(\lambda_i^c, \theta_i^c, \mu_{ij}^c, \mu_{ji}^c, P_{G_i})$ for all buses $\{1,\ldots,N_B\}$, $j \in \Omega_i$ and all contingency cases $c = \{1,\ldots,N_C\}$. Also, $\mathbb{P}$ is the projection operator which ensures that the Lagrange multipliers for the line constraints stay positive and the generation outputs stay within the given bound. Hence, $\widetilde{X}$ is the vector of the stacked projected variables. Equation (4.15) presents (4.13) in more detail.

$$X(k+1) = \left(I - \begin{bmatrix} -\alpha & \beta & 0 & 0 \\ \gamma & 0 & 0 & 0 \\ 0 & 0 & -\delta & 0 \\ 0 & 0 & 0 & \frac{1}{2a} \end{bmatrix} \right) \begin{bmatrix} \frac{\partial L}{\partial \lambda^c} \\ \frac{\partial L}{\partial \theta^c} \\ \frac{\partial L}{\partial \mu^c} \\ \frac{\partial L}{\partial P_G} \end{bmatrix} \tag{4.14}$$

$$X(k+1) = \left(I - \overbrace{\begin{bmatrix} \beta\mathsf{B} & -\alpha\mathsf{B} & \beta(\mathsf{B_y})^T & \alpha I \\ 0 & \gamma\mathsf{B} & 0 & -\gamma I \\ 0 & -\delta\mathsf{B_y} & 0 & 0 \\ -\frac{\mathsf{Z}}{2a} & 0 & 0 & I \end{bmatrix}}^{\mathrm{A}} \right) \widetilde{X}(k) + \overbrace{\begin{bmatrix} \alpha\mathsf{P_L} \\ -\gamma\mathsf{P_L} \\ -\delta\overline{\mathsf{P}}_{\mathsf{ij}} \\ -\frac{b}{2a} \end{bmatrix}}^{\mathrm{C}}. \tag{4.15}$$

In (4.15), B is a block diagonal matrix that its diagonal elements are B^c (bus admittance matrices associated with contingency c). Also, I is identity matrix. Moreover, $\mathsf{B_y}$ is a block diagonal matrix and its diagonal elements are B_y^c. Here, $B_y^c = H \cdot (\mathcal{I}^c \cdot diag\frac{1}{X_{ij}})^T$, where $\mathcal{I}^c$ is the incidence matrix associated with contingency c, and $H = [I, -I]^T$. Furthermore,

$\mathsf{Z} = [I \dots I]$, and it has N_B columns and N_C rows. Finally, $\mathsf{P_L} = [P_L \dots P_L]$ and $\overline{\mathsf{P}}_{\mathsf{ij}} = [\overline{P}_{ij}^{0} \dots \overline{P}_{ij}^{N_c}]$.

4.4.1 Optimality of the Solution

At first, Theorem 1 presents the formal proof that any fixed point of the proposed approach satisfies the optimality conditions (4.2)–(4.8) of the SCOPF problem. Then, Theorem 2 discusses the optimality of the achieved limit point.

Theorem 1: Let X^* be a fixed point of the proposed $\mathcal{I} - \mathcal{DSCOPF}$ algorithm. Then, $X^\star$ satisfies all of the optimality conditions of the SCOPF problem (4.2)–(4.8).

Proof: The formal proof of Theorem 1, includes the verifications of the set of claims which show that $X^\star$ fulfills all of the first order optimality conditions. Note that, the vector of stacked variables $(\lambda_i^{c\star}, \theta_i^{c\star}, \mu_{ij}^{c\star}, P_{G_i}^{\star})$ for all buses (agents) $i = \{1, \dots, N_B\}$ is denoted by $X^\star$.

Claim 1: $X^\star$ satisfies the optimality conditions that correspond to the positivity of the Lagrangian multipliers of the line limits, i.e., $\mu_{ij}^{c\star} \geq 0$.

Verification by contradiction: Let us assume, on the contrary, that the above claim does not hold, i.e., one of the line limit multiplier variables in $X^\star$, say $\mu_{ij}^{c\star}$, is negative. Assessing (4.12) at $X^\star$ leads to a non-negative value for μ_{ij}^{c}, because the projection operator enforces the positivity of the μ_{ij}^{c}, therefore,

$$\mu_{ij}^{c\star} \neq \mathbb{P}\left[\mu_{ij}^{c\star} - \delta \cdot \left(\overline{P}_{ij} - \frac{\theta_i^{c\star}(k) - \theta_j^{c\star}(k)}{X_{ij}}\right)\right].$$

The above clearly contradicts the fact that X^* is a fixed point of (4.12).

Claim 2: $X^\star$ fulfills the optimality conditions that correspond to the line limit constraints, (4.7)–(4.8).

Verification by contradiction: Let us assume, on the contrary, that the above claim does not hold, i.e., $X^\star$ does not fulfill (4.7) for all i and j. In other words, there exists

(i,j) such that $\left(\theta_i^{c\star} - \theta_j^{c\star}\right)/X_{ij} > \overline{P}_{ij}$, which results in a negative innovation term in the assessment of (4.12) at $X^\star$. Since $\mu_{ij}^{c}{}^\star \geq 0$ (see claim 1), evaluating (4.12) at $X^\star$ results in a value greater than $\mu_{ij}^{c}{}^\star \geq 0$, i.e.,

$$\mu_{ij}^{c}{}^\star < \mathbb{P}\left[\mu_{ij}^{c}{}^\star - \delta \cdot \left(\overline{P}_{ij} - \frac{\theta_i^{c\star}(k) - \theta_j^{c\star}(k)}{X_{ij}}\right)\right],$$

which contradicts the fact that X^* is a fixed point of (4.12). Similar discussion proves that $X^\star$ fulfills (4.8).

Claim 3: The complementary slackness condition holds at $X^\star$, i.e., for all pairs (i,j),

$$\mu_{ij}^{c}{}^\star \cdot \left(\frac{\theta_i^{c\star} - \theta_j^{c\star}}{X_{ij}} - \overline{P}_{ij}\right) = 0.$$

Verification by contradiction: Let us assume, on the contrary, that the above claim does not hold, i.e., there exists a pair (i,j) such that both $\mu_{ij}^{c}{}^\star$ and $\left(\theta_i^{c\star} - \theta_j^{c\star}\right)/X_{ij} - \overline{P}_{ij}$ are non-zero. Based on the verified claims 1 and 2, $\mu_{ij}^{c}{}^\star > 0$ and $\left(\theta_i^{c\star} - \theta_j^{c\star}\right)/X_{ij} < \overline{P}_{ij}$ for all pairs (i,j), respectively. Now, note that evaluating (4.12) at $X^\star$, results in a value less than $\mu_{ij}^{c}{}^\star$, which contradicts the fact that X^* is a fixed point of (4.12).

Claim 4: The local load balance equation (4.4) is preserved at $X^\star$.

Verification by contradiction: Let us assume, on the contrary, that the above claim does not hold, i.e., the load balance equation doesn't hold at $X^\star$. In other words, there exists i such that the value of the innovation term in (4.11) is non-zero when evaluated at $X^\star$, i.e.,

$$\theta_i^{c\star} \neq \theta_i^{c\star} - \gamma\left(-\sum_{n\in\Omega_{G_i}} P_{G_n}^\star + P_{L_i} + \sum_{j\in\Omega_i} \frac{\theta_i^{c\star} - \theta_j^{c\star}}{X_{ij}}\right),$$

which contradicts the fact that X^* is a fixed point of (4.11).

Claim 5: The coupling between the Lagrangian multipliers, given by (4.3), is maintained at $X^\star$.

Verification by contradiction: Let us assume, on the contrary, that the above claim

does not hold, i.e., $X^\star$ does not fulfill (4.3) for some i. Note that (4.9) consists of two types of innovation terms: the innovation term that preserves the Lagrangian multipliers' coupling, (4.3), and the innovation terms which takes into account the local power balance equations at each bus across the system, (4.4). The verification of claim 4 indicates that the local power balance equation residues are zero at $X^\star$. Therefore, the contradiction hypothesis, i.e., the Lagrangian multipliers' coupling is not preserved at $X^\star$, implies that that the the value of (4.9) is not equal to $\lambda_i^{c\star}$ when evaluated at $X^\star$. This contradicts with the fact that X^* is a fixed point of (4.9).

Claim 6: $X^\star$ fulfills the optimality conditions associated with the generation limits, (4.5)–(4.6).

Verification by contradiction: Let us assume, on the contrary, that the above claim does not hold, i.e., there exists i such that $P^\star_{G_i}$ does not lie in $[\underline{P}_{G_i}, \overline{P}_{G_i}]$. Therefore, evaluating (4.10) at $X^\star$ acheives a value different from $P^\star_{G_i}$, due to the presence of the projection operator that enforces the value of P_{G_i} to stay in the specified region, $[\underline{P}_{G_i}, \overline{P}_{G_i}]$. This result in a contradiction with the fact that X^* is a fixed point of (4.10).

Here, we discuss the outcomes of Theorem 1. Due to the fact, that $\mathcal{I} - \mathcal{DSCOPF}$ consists of continuous transformations of the iterates, it follows that, if $\mathcal{I} - \mathcal{DSCOPF}$ converges, the limit point is necessarily a fixed point of the iterative mapping. Therefore, based on Theorem 1, any limit point of the $\mathcal{I} - \mathcal{DSCOPF}$ satisfies the first order optimality conditions, (4.2)–(4.8), of the DC-SCOPF problem. Moreover, the following Theorem 2 discusses the optimality of limit points of the proposed $\mathcal{I} - \mathcal{DSCOPF}$ method.

Theorem 2: Let the SCOPF problem (4.1) have a feasible solution within the interior of the associated constraint set, and, further, assume that the proposed $\mathcal{I} - \mathcal{DSCOPF}$ algorithm converges to a point $X^\star$. Then X^* is the optimal solution of the SCOPF problem (4.1).

Proof: By Theorem 1, $X^\star$ satisfies the optimality conditions (4.2)–(4.8). Due to the

fact that the DC-SCOPF is a convex problem, and assumed to be strictly feasible, the primal variables ($P^{\star}$,$\theta^{c\star}$) in X^{*} constitutes an optimal solution to the SCOPF problem (4.1).

To wrap up, note that Theorems 1 and 2 guarantee that any fixed point of the proposed $\mathcal{I}-\mathcal{DSCOPF}$ algorithm version **A** constitutes an optimal solution to the SCOPF problem. In other words, if the $\mathcal{I}-\mathcal{DSCOPF}$ version **A** attains convergence, the limit point is necessarily an optimal solution of the SCOPF problem. Finally, we note, that whether the scheme converges or not depends on several design factors, in particular, the tuning parameters α, β, γ and δ. Hence, a general sufficient condition for convergence is presented in the following subsection.

4.4.2 Sufficient Condition for Convergence

In order to derive general sufficient condition for convergence of $\mathcal{I}-\mathcal{DSCOPF}$, the following assumption on the matrix A as defined in (4.15) is imposed:
A.1: There exists an ℓ_p-norm such that the tuning parameters α, β, γ and δ can be designed to achieve $\|I-A\|_p < 1$.

Theorem 3: Let *A.1* hold, then the algorithm presented in (4.13) achieves convergence.

Proof: Proof of this theorem is the same as proof of Theorem 3 in Sect. 3.4.2.

4.4.3 Parameter Tuning

We note, that the convergence of our distributed scheme depends on several design factors, in particular, the tuning parameters α, β, γ and δ. This section analytical derives a heuristic method to adjust the tuning parameters. At first we discuss the steps of this tuning method, and later we present the analytical justification for these steps.

1. choose β such that $\beta \leq \frac{1}{max_i \sum_{j\in\Omega_i} \frac{1}{X_{ij}}}$.

2. choose γ such that $\gamma \leq \frac{1}{max_i \sum_{j \in \Omega_i} \frac{1}{X_{ij}}}$.

3. choose α such that $\alpha > \beta$ and $\alpha > \gamma$. Increase α until noticing oscillatory behavior.

4. Tuning of δ depends on the loadings of the system. Start with $\delta = 0.5 \times \beta$; Increase δ until noticing oscillations.

Note, the above heuristic method is not guaranteed to yield optimal tuning parameters in all system and loading scenarios.

4.4.4 Justifications for Approximate Tuning Parameter Method

This subsection is devoted to justifying the proposed approximate parameter tuning procedure. Specifically, we consider a modified system, denoted by $\mathfrak{M}$, (see Assumptions *M.1* and *M.2*) for which we tune the parameters, namely $(\alpha_m, \beta_m, \gamma_m, \delta_m)$. Then, we derive the desirable parameter choices for the original setup, denoted by $\mathbb{O}$, from the α_m, β_m, γ_m, and δ_m designed for the system $\mathfrak{M}$.

M.1: The generators' cost function parameters of $\mathbb{O}$, i.e., $a_n^{\mathbb{O}}, b_n^{\mathbb{O}}, c_n^{\mathbb{O}}$, are scaled by a factor ξ such that $\frac{1}{\xi a_n^{\mathbb{O}}}$ obtain sufficiently small values. It also follows that

$$\forall\ \epsilon > 0,\ \exists\ \xi\ s.t.\ \ \frac{1}{\xi a_n^{\mathbb{O}}} \leq \epsilon, \quad \forall n \in \Omega_G \tag{4.16}$$

M.2: A fictitious bus, i.e., a bus without generator/load, is added to the $\mathbb{O}$'s network. This fictitious bus could be connected to any of the buses.

Remark 3: Let the DC-SCOPF problem, defined by (4.1), yield $[\lambda^{c,\star}, \theta^{c,\star}, \mu^{c,\star}, P^{\star}]$ as the optimal primal and dual variables. Then, scaling the objective function of this problem by a factor ξ, results in $[\xi\lambda^{c,\star}, \theta^{c,\star}, \xi\mu^{c,\star}, P^{\star}]$ as the optimal primal and dual variables.

Justification 1: Let the $\mathcal{I} - \mathcal{DSCOPF}$ algorithm converge to the optimal solution of DC-SCOPF for the modified system ($\mathfrak{M}$) using the $(\alpha_m, \beta_m, \gamma_m, \delta_m)$ as tuning parameters.

Then, adjusting the tuning parameters to $(\frac{1}{\xi}\alpha_m, \beta_m, \gamma_m, \frac{1}{\xi}\delta_m)$ results in convergence of the $\mathcal{I}-\mathcal{DSCOPF}$ algorithm for the original system $(\mathbb{O})$.

Proof: Given that the tuning parameters of $\mathcal{I}-\mathcal{DSCOPF}$ are adjusted to $(\frac{1}{\xi}\alpha_m, \beta_m, \gamma_m, \frac{1}{\xi}\delta_m)$, the $\mathcal{I}-\mathcal{DSCOPF}$'s iterative updates for the system $\mathbb{O}$, namely $[\lambda^{c,\mathbb{O}}, \theta^{c,\mathbb{O}}, \mu^{c,\mathbb{O}}, P^{\mathbb{O}}]$, are as follows

$$\begin{aligned}\lambda_i^{c,\mathbb{O}}(k+1) = \lambda_i^{c,\mathbb{O}}(k) - \beta_m \cdot \left(\lambda_i^{c,\mathbb{O}}(k) \sum_{j\in\Omega_i} \frac{1}{X_{ij}} - \sum_{j\in\Omega_i} \lambda_j^{c,\mathbb{O}}(k) \frac{1}{X_{ij}} + \sum_{j\in\Omega_i} \left(\mu_{ij}^{c,\mathbb{O}}(k) - \mu_{ji}^{c,\mathbb{O}}(k) \right) \frac{1}{X_{ij}} \right) \\ - \frac{\alpha_m}{\xi} \cdot \left(\sum_{n\in\Omega_{G_i}} P_{G_n}^{\mathbb{O}}(k) - P_{L_i} - \sum_{j\in\Omega_i} \frac{\theta_i^{c,\mathbb{O}}(k) - \theta_j^{c,\mathbb{O}}(k)}{X_{ij}} \right)\end{aligned} \tag{4.17}$$

$$P_{G_n}^{\mathbb{O}}(k+1) = \mathbb{P}_n \left[\frac{\sum_{c=0}^{N_c} \lambda_i^{c,\mathbb{O}}(k) - b_n^{\mathbb{O}}}{2a_n^{\mathbb{O}}} \right] \tag{4.18}$$

$$\theta_i^{c,\mathbb{O}}(k+1) = \theta_i^{c,\mathbb{O}}(k) - \gamma_m \left(- \sum_{n\in\Omega_{G_i}} P_{G_n}^{\mathbb{O}}(k) + P_{L_i} + \sum_{j\in\Omega_i} \frac{\theta_i^{c,\mathbb{O}}(k) - \theta_j^{c,\mathbb{O}}(k)}{X_{ij}} \right) \tag{4.19}$$

$$\begin{aligned}\mu_{ij}^{c,\mathbb{O}}(k+1) = \mathbb{P} \left[\mu_{ij}^{c,\mathbb{O}}(k) - \frac{\delta_m}{\xi} \left(\overline{P}_{ij} - \frac{\theta_i^{c,\mathbb{O}}(k) - \theta_j^{c,\mathbb{O}}(k)}{X_{ij}} \right) \right] \\ \mu_{ji}^{c,\mathbb{O}}(k+1) = \mathbb{P} \left[\mu_{ji}^{c,\mathbb{O}}(k) - \frac{\delta_m}{\xi} \left(\overline{P}_{ij} + \frac{\theta_i^{c,\mathbb{O}}(k) - \theta_j^{c,\mathbb{O}}(k)}{X_{ij}} \right) \right].\end{aligned} \tag{4.20}$$

Now, multiplying (4.17) by ξ results in,

$$\xi\lambda_i^{c,\mathbb{O}}(k+1) = \xi\lambda_i^{c,\mathbb{O}}(k) - \beta_m \cdot \left(\xi\lambda_i^{c,\mathbb{O}}(k) \sum_{j\in\Omega_i} \frac{1}{X_{ij}} - \sum_{j\in\Omega_i} \xi\lambda_j^{c,\mathbb{O}}(k) \frac{1}{X_{ij}} + \sum_{j\in\Omega_i} \left(\xi\mu_{ij}^{c,\mathbb{O}}(k) - \xi\mu_{ji}^{c,\mathbb{O}}(k) \right) \frac{1}{X_{ij}} \right)$$
$$- \alpha_m \cdot \left(\sum_{n\in\Omega_{G_i}} P_{G_n}^{\mathbb{O}}(k) - P_{L_i} - \sum_{j\in\Omega_i} \frac{\theta_i^{c,\mathbb{O}}(k) - \theta_j^{c,\mathbb{O}}(k)}{X_{ij}} \right). \tag{4.21}$$

Also, (4.18) could be stated as,

$$P_{G_n}^{\mathbb{O}}(k+1) = \mathbb{P}_n \left[\frac{\xi \sum_{c=0}^{N_c} \lambda_i^{c,\mathbb{O}}(k) - \xi b_n^{\mathbb{O}}}{2\xi a_n^{\mathbb{O}}} \right]. \tag{4.22}$$

Furthermore, multiplying (4.20) by ξ results in,

$$\begin{aligned} \xi\mu_{ij}^{c,\mathbb{O}}(k+1) &= \mathbb{P}\left[\xi\mu_{ij}^{c,\mathbb{O}}(k) - \delta_m \left(\overline{P}_{ij} - \frac{\theta_i^{c,\mathbb{O}}(k) - \theta_j^{c,\mathbb{O}}(k)}{X_{ij}} \right) \right] \\ \xi\mu_{ji}^{c,\mathbb{O}}(k+1) &= \mathbb{P}\left[\xi\mu_{ji}^{c,\mathbb{O}}(k) - \delta_m \left(\overline{P}_{ij} + \frac{\theta_i^{c,\mathbb{O}}(k) - \theta_j^{c,\mathbb{O}}(k)}{X_{ij}} \right) \right]. \end{aligned} \tag{4.23}$$

Note, (4.23) hold because $\mathbb{P}$ projects the updated values onto $[0, \infty)$. In other words, $\mu_{ij}^{c,\mathbb{O}}(k+1) = 0$ yields $\xi\mu_{ij}^{c,\mathbb{O}}(k+1) = 0$, whereas if $\mu_{ij}^{c,\mathbb{O}}(k+1) > 0$ then projection is not needed anymore.

Now, we define transformation $\mathfrak{T}$ as,

$$\begin{cases} \lambda^{c,\mathfrak{T}}(k) = \xi\lambda^{c,\mathbb{O}}(k), & \theta^{c,\mathfrak{T}}(k) = \theta^{c,\mathbb{O}}(k) \\ \mu^{c,\mathfrak{T}}(k) = \xi\mu^{c,\mathbb{O}}(k), & P_G^{\mathfrak{T}}(k) = P_G^{\mathbb{O}}(k), \end{cases} \tag{4.24}$$

Under this transformation (4.19),(4.21),(4.22),(4.23) are stated as,

$$\lambda_i^{c,\mathfrak{T}}(k+1) = \lambda_i^{c,\mathfrak{T}}(k) - \beta_m \cdot \left(\lambda_i^{c,\mathfrak{T}}(k) \sum_{j\in\Omega_i} \frac{1}{X_{ij}} - \sum_{j\in\Omega_i} \lambda_j^{c,\mathfrak{T}}(k) \frac{1}{X_{ij}} + \sum_{j\in\Omega_i} \left(\mu_{ij}^{c,\mathfrak{T}}(k) - \mu_{ji}^{c,\mathfrak{T}}(k) \right) \frac{1}{X_{ij}} \right)$$
$$- \alpha_m \cdot \left(\sum_{n\in\Omega_{G_i}} P_{G_n}^{\mathfrak{T}}(k) - P_{L_i} - \sum_{j\in\Omega_i} \frac{\theta_i^{c,\mathfrak{T}}(k) - \theta_j^{c,\mathfrak{T}}(k)}{X_{ij}} \right) \tag{4.25}$$

$$P_{G_n}^{\mathfrak{T}}(k+1) = \mathbb{P}_n \left[\frac{\sum_{c=0}^{N_c} \lambda_i^{c,\mathfrak{T}}(k) - \xi b_n^{\mathbb{O}}}{2\xi a_n^{\mathbb{O}}} \right] \tag{4.26}$$

$$\theta_i^{c,\mathfrak{T}}(k+1) = \theta_i^{c,\mathfrak{T}}(k) - \gamma_m \left[-\sum_{n\in\Omega_{G_i}} P_{G_n}^{\mathfrak{T}}(k) + P_{L_i} + \sum_{j\in\Omega_i} \frac{\theta_i^{c,\mathfrak{T}}(k) - \theta_j^{c,\mathfrak{T}}(k)}{X_{ij}} \right] \tag{4.27}$$

$$\begin{aligned} \mu_{ij}^{c,\mathfrak{T}}(k+1) &= \mathbb{P} \left[\mu_{ij}^{c,\mathfrak{T}}(k) - \delta_m \left(\overline{P}_{ij} - \frac{\theta_i^{c,\mathfrak{T}}(k) - \theta_j^{c,\mathfrak{T}}(k)}{X_{ij}} \right) \right] \\ \mu_{ji}^{c,\mathfrak{T}}(k+1) &= \mathbb{P} \left[\mu_{ji}^{c,\mathfrak{T}}(k) - \delta_m \left(\overline{P}_{ij} + \frac{\theta_i^{c,\mathfrak{T}}(k) - \theta_j^{c,\mathfrak{T}}(k)}{X_{ij}} \right) \right]. \end{aligned} \tag{4.28}$$

Equations (4.25),(4.26),(4.27),(4.28) are similar to the iterative updates of $\mathcal{I} - \mathcal{DSCOPF}$ for system $\mathfrak{M}$ with tuning parameters adjusted to $(\alpha_m, \beta_m, \gamma_m, \delta_m)$, which converges to the optimal solution according to the hypothesis of *Justification 1.*

Finally, let $\mathcal{I} - \mathcal{DSCOPF}$ achieve the optimal solution, namely $[\xi\lambda^{c,\star}, \theta^{c,\star}, \xi\mu^{c,\star}, P^{\star}]$ for system $\mathfrak{M}$. Then, due to the transformation, defined by (4.24), $\mathcal{I} - \mathcal{DSCOPF}$ achieves $[\lambda^{c,\star}, \theta^{c,\star}, \mu^{c,\star}, P^{\star}]$ as the optimal solution for system $\mathbb{O}$. This verifies *Remark 3.* Note that adding a fictitious bus does not change the solution of the DC-SCOPF, since it is not connected to a generator or a load.

We now analytically justify the applicability of our proposed approximate tuning parameter method for the modified test system ($\mathfrak{M}$), namely $(\alpha_m, \beta_m, \gamma_m, \delta_m)$. To this end, we consider system $\mathfrak{M}$ without line limit constraints for which we provide choices of β_m, γ_m and α_m that are guaranteed to lead to convergence of the corresponding $\mathcal{I} - \mathcal{DSCOPF}$ algorithm. Then, for this system $\mathfrak{M}$, δ is tuned according to the guideline presented earlier in this section.

Note, by leaving out the μ^c update the corresponding matrix A, see (4.15), reduces to A_r as follows,

$$A_r = \begin{bmatrix} \beta\mathsf{B} & -\alpha\mathsf{B} & \alpha I \\ 0 & \gamma\mathsf{B} & -\gamma I \\ -\frac{\mathsf{Z}}{2a} & 0 & I \end{bmatrix},$$

where we also assume that *M.1* and *M.2* hold for the above reduced modified system. The matrix A_r is then decomposed as

$$A_r = \overbrace{\begin{bmatrix} \beta\mathsf{B} & -\alpha\mathsf{B} & \alpha I \\ 0 & \gamma\mathsf{B} & -\gamma I \\ 0 & 0 & I \end{bmatrix}}^{A_r^I} + \overbrace{\begin{bmatrix} 0 & 0 & 0 \\ 0 & 0 & 0 \\ -\frac{\mathsf{Z}}{2a} & 0 & 0 \end{bmatrix}}^{A_r^{II}}.$$

Remark 4: Using standard eigenvalue perturbation results, namely the Bauer–Fike theorem [21], since *M.1* ensures that all entries of A_r^{II} are less than ϵ, we have $\rho(A_r) \leq \rho(A_r^I) + O(\epsilon)$, where the order notation $O(\epsilon)$ denotes that the quantity goes to zero as $\epsilon \to 0$. Here, $\rho(.)$ denotes the spectral radius.

Moreover, A_r^I is an upper triangular matrix. Therefore the eigenvalues of A_r^I are the

eigenvalues of its diagonal blocks, namely βB, γB and I.

Justification 2: Let *M.1* and *M.2* hold for the reduced modified system. Then there exists a set of tuning parameters such that $\rho(I - A_r) < 1$.

Proof: The assumption *M.2* guarantees the diagonal dominance of A_r^I's diagonal blocks [34]. Also, by adding an additional fictitious bus at least one row of B does not sum to zero, hence, the resulting B matrix becomes non-singular. Consequently, A_r^I becomes non-singular. Note, the fictitious bus merely updates θ^c to ensure that its corresponding line flow stays zero. Therefore, the three diagonal blocks of A_r^I are symmetric diagonally dominant matrices with positive diagonal entries, hence, they are positive definite.

The remainder of this proof is devoted to finding upper bounds for β and γ such that $\rho(I - A_r) < 1$ holds.

Let us define $\mathfrak{e}(I - \beta\mathsf{B})$ as the eigenvalue of the matrix block $(I - \beta\mathsf{B})$, then based on *Remark 4*

$$\rho(I - A_r^I) \quad < \quad 1,$$

which further implies that

$$\begin{cases} |\mathfrak{e}_j(I - \beta\mathsf{B})| < 1 \\ \\ |\mathfrak{e}_j(I - \gamma\mathsf{B})| < 1. \end{cases} \tag{4.29}$$

First we discuss the existence of an upper bound for β such that $\rho(I - \beta\mathsf{B}) < 1$ holds. A similar argument would establish an upper bound for γ such that $\rho(I - \gamma\mathsf{B}) < 1$ holds. The above equation leads to

$$0 < 1 - \mathfrak{e}_j(I - \beta\mathsf{B}) < 2 \quad \forall j \in \{1, \ldots, N_B \times N_c\}. \tag{4.30}$$

Note, B is a block diagonal matrix that its diagonal elements are B^c (bus admittance matrices associated with contingency c). Using the Gershgorin circle theorem, it may be shown that

$$|\mathfrak{e}_j(I-\beta B^c)-1+\beta B^c_{ii}| \leq \beta B^c_{ii} \quad \forall j \in \{1,\ldots,N_B\} \quad \forall c \in \{0,\ldots,N_c\}.$$

Therefore,

$$0 \leq 1-\mathfrak{e}_j(I-\beta B^c) \leq 2\beta B^c_{ii} \quad \forall j \in \{1,\ldots,N_B\} \quad \forall c \in \{0,\ldots,N_c\}. \tag{4.31}$$

As it was discussed earlier *M.2* ensures the non-singularity of each block of B, hence, $0 < 1-\mathfrak{e}_j(I-\beta B^c)$ holds. Combining (4.30) and (4.31) further implies,

$$\exists\ \beta\ s.t.\ \ 0 < 1-\mathfrak{e}_j(I-\beta B^c) < 2\beta B^c_{ii} < 2 \quad \forall j \in \{1,\ldots,N_B\}. \quad \forall c \in \{0,\ldots,N_c\}.$$

A similar discussion justifies the existence of γ

$$\exists\ \gamma\ s.t.\quad 0 < 1-\mathfrak{e}_j(I-\gamma B^c) < 2\gamma B^c_{ii} < 2 \quad \forall j \in \{1,\ldots,N_B\} \quad \forall c \in \{0,\ldots,N_c\}.$$

Finally, provided β and γ are sufficiently small, specifically, by adjusting β and γ such that,

$$\begin{cases} \beta \leq \frac{1}{max_i \sum_{j \in \Omega_i} \frac{1}{X_{ij}}} \\ \\ \gamma \leq \frac{1}{max_i \sum_{j \in \Omega_i} \frac{1}{X_{ij}}}. \end{cases} \tag{4.32}$$

we would have $\rho(I - A_r^I) < 1$. Note, (4.32) only involve B_{ii}^0 since $B_{ii}^0 > B_{ii}^c$. In (4.16), the constant ϵ can be made arbitrary small by properly scaling the cost parameters in *M.1*, which results in $\rho(I - A_r^I) + O(\epsilon) < 1$, hence, $\rho(I - A_r) < 1$.

Remark 5: For any $\varsigma > 0$ there exists an ℓ_p-norm such that $\rho(A_r) \leq \|A_r\|_p \leq \rho(A_r) + \varsigma$.

Justification 3: Let β and γ hold in (4.32), then there exists an ℓ_p-norm such that $\|I - A_r\|_p < 1$.

Proof: Since β and γ hold in (4.32), *Justification 2* implies that $\rho(I - A_r) < 1$. Then, we can pick an $\varsigma > 0$ such that $\rho(I - A_r) + \varsigma < 1$ and, by *Remark 5*, we can find an ℓ_p-norm such that $\|I - A_r\|_p \leq \rho(I - A_r) + \varsigma < 1$.

After tuning β and γ, we choose α such that $\alpha > \beta$ and $\alpha > \gamma$. Then, we increase α until $\mathcal{I} - \mathcal{DSCOPF}$ does not converge any more. Finally, to tune δ we start with $\delta = 0.5 \times \beta$ and then increase δ until noticing oscillatory behavior.

Remark 6: Justification 1 further implies that assumption *M.1* does not affect the choice of β and γ for a system. Therefore, in order to tune the parameters one can follow the steps provided in earlier in this section.

4.5 Simulation Results

4.5.1 Test System Set up

The simulations are carried out for the IEEE-14 bus, IEEE-57 bus [22] and 944-bus (consisting of 8 IEEE 118-bus systems) test systems (see Appendix). To test for cases in which contingencies affect the optimal settings of the generator outputs, line limits are deter-

mined which lead to a set of severe congestions in case of contingencies. Given the chosen line limits for the IEEE-14 bus test system, the faults in the lines connecting buses 1 and 5 and buses 2 and 3 will result in bottlenecks in the lines connecting buses 1 and 2 and buses 3 and 4, respectively. Also, in the IEEE-57 bus test system the line limits are adjusted such that the failure of the lines connecting buses 7 and 29, and buses 1 and 16 lead to congestions in the lines connecting buses 8 and 9 and buses 12 and 17, respectively. Finally, in the 944-bus the considered contingencies lead to two congested lines. Note, none of the considered line failures lead to disconnection of a bus from the rest of the system. The cost function parameters of the generators are calculated based on the heat rate curves given in the IEEE Reliability Test System [35] and recent fuel prices. Also, the tuning parameters are set to the values given in Table 4.1. The tuning parameters are adjusted following the guidelines presented in Sect. 4.4.3. It should be noted that we used a cold start for all simulations, i.e., all the variables except the λ's, which represent the locational marginal prices, are set to zero at the start of the simulation.

Table 4.1: Tuning Parameter Values

Parameter	IEEE 14-bus	IEEE 57-bus	944-bus
α	0.0002	0.0019	0.0040
β	0.04	0.0081	0.0024
γ	0.01	0.0050	0.0004
δ	0.01	0.0250	0.3

4.5.2 Convergence Measurements

In order to evaluate the performance of the proposed algorithm we introduce two measures. These measures quantify the performance the proposed algorithms. The first measure determines the relative distance of the objective function from the optimal value over the

iterations, i.e.,

$$rel = \frac{|f - f^*|}{f^*},$$

where f^* is the optimal objective function value calculated by solving the centralized DC-SCOPF problem. Moreover, the value of the load balance, as one of the optimality conditions, is another indication of the distance from the optimal solution, since the value of the load balance at the optimal point is equal to zero. Thus, we use the normalized sum over the residuals of all power flow equations over the course of the iterations for the normal operation (pre-contingency, $c = 0$), and each contingency case ($c \in \{1, \cdots, N\}$) as the second measure of convergence.

Hence, this measure is given by:

$$res^c = \frac{\sum_i \sqrt{(g_i^c)^2}}{N_B}.$$

where g_i^c is the local power flow equation at bus i in contingency c, and N_B is the number of buses.

4.5.3 Case Study 1: IEEE 14-bus Test System

This section presents the performance of the $\mathcal{I} - \mathcal{DSCOPF}$ for the IEEE-14 bus test system taking into account N-1 failures of all lines. Therefore, the contingency set includes all possible line failures. Using version **A** of the $\mathcal{I} - \mathcal{DSCOPF}$ algorithm, Fig. 4.2 shows the evolution of the total power output of the generator buses, μ and λ over 4000 iterations. Given that two of the lines reach their limits, two Lagrange multipliers associated with the line constraints of the congested lines are non-zero and the locational marginal prices (λ) are no longer equal to the same value.

Also, Fig. 4.3 shows rel and res for the contingencies of the same setup using version **A** of our proposed algorithm. Each iteration is computationally very inexpensive as it only

requires the evaluation of algebraic functions, which are done in parallel at the individual buses. Furthermore, Fig. 4.4 and Fig. 4.5 depict the evolution of variables and convergence measures for the same test system setup using version **B** of the $\mathcal{I} - \mathcal{DSCOPF}$ algorithm. Comparing the two versions of $\mathcal{I} - \mathcal{DSCOPF}$, version **B** outperforms version **A** with respect to convergence speed.

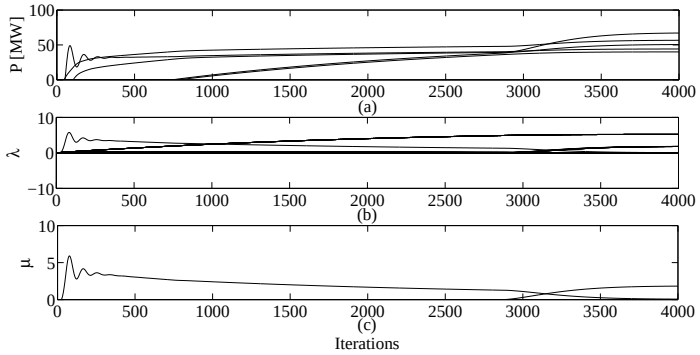

Figure 4.2: (a) Generation output, (b) Lagrangian multiplier λ and (c) Lagrangian multiplier μ for version **A**, $\mathcal{I} - \mathcal{DSCOPF}$, IEEE-14 bus test system

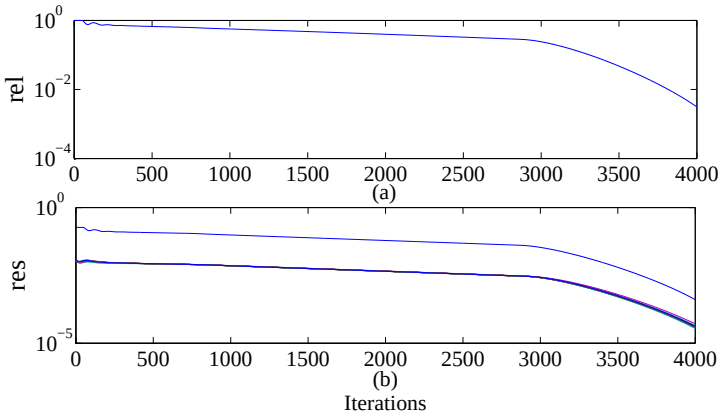

Figure 4.3: (a) Relative distance to solution ($|f - f^*| / f^*$) and (b) Residual of equality constraint $\sum_i \sqrt{(g_i^c)^2}/N_B$ for version **A**, $\mathcal{I} - \mathcal{DSCOPF}$, IEEE-14 bus test system.

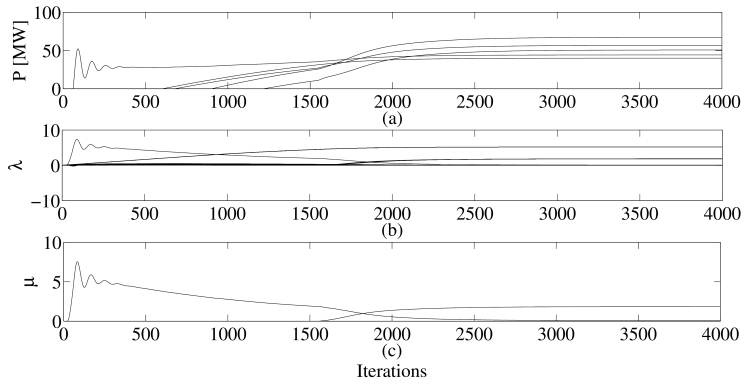

Figure 4.4: (a) Generation output, (b) Lagrangian multiplier λ and (c) Lagrangian multiplier μ for version **B**, $\mathcal{I}-\mathcal{DSCOPF}$, IEEE-14 bus test system

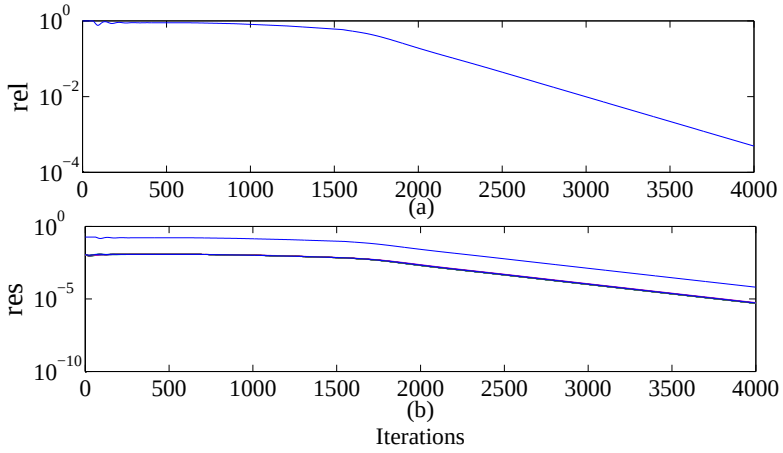

Figure 4.5: (a) Relative distance to solution ($|f-f^*|/f^*$) and (b) Residual of equality constraint $\sum_i \sqrt{(g_i^c)^2}/N_B$ for version **B**, $\mathcal{I}-\mathcal{DSCOPF}$, IEEE-14 bus test system.

4.5.4 Case Study 2: IEEE 57-bus Test System

This section illustrates the performance of the proposed distributed $\mathcal{I}-\mathcal{DSCOPF}$ algorithm for the IEEE-57 bus test system. Figure. 4.6(a) shows the evolution of the power output of the generators over 10000 iterations for the $\mathcal{I}-\mathcal{DSCOPF}$ version **A** algorithm. Figures 4.6(b) and 4.6(c) show the evolution of λ and μ, respectively. Oscillations appear which could be prevented by reducing some of the tuning parameters, but this would also lead to a larger number of iterations until convergence. Also, Fig. 4.7 shows *rel* and *res* for the considered contingencies. Since in this case that the set of contingencies is not

complete, the performance of versions **A** and **B** of the $\mathcal{I}-\mathcal{DSCOPF}$ algorithm is similar. Therefore, using the version **B** of $\mathcal{I}-\mathcal{DSCOPF}$ would more or less lead to a replica of the already included figure for version **A**. Note, the values of *rel* and *res* for the version **B** of $\mathcal{I}-\mathcal{DSCOPF}$ algorithm after 10000 iterations are 5.47e-6 and 0.001, respectively.

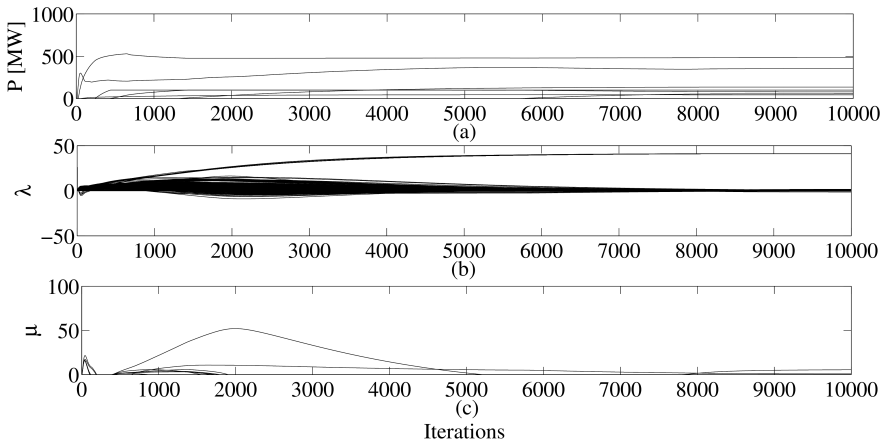

Figure 4.6: (a) Generation output, (b) Lagrangian multiplier λ and (c) Lagrangian multiplier μ for version **A**, $\mathcal{I}-\mathcal{DSCOPF}$, IEEE-57 bus test system

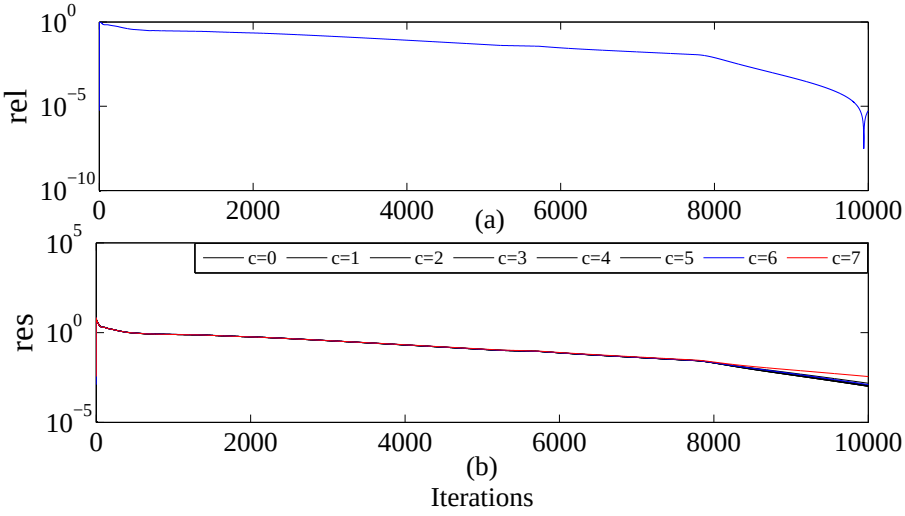

Figure 4.7: (a) Relative distance to solution ($|f-f^*|/f^*$) and (b) Residual of equality constraint $\sum_i \sqrt{(g_i^c)^2}/N_B$ for version **A**, $\mathcal{I}-\mathcal{DSCOPF}$, IEEE-57 bus test system.

4.5.5 Case Study 3: 944-bus Test System

This section presents the simulation results for the $\mathcal{AI}-\mathcal{DSCOPF}$ algorithm where asynchronous updates are carried out between areas. To this end, eight 118-bus test systems, i.e., each of them considered as an area, are attached to each other to form the 944-bus test system. Note, the contingency set includes failure of the lines connecting buses 5 and 8 and buses 15 and 19 inside each area in addition to lines that connect the areas to each other. Updated values are exchanged between agents within the area after each iteration and between agents in separate areas once every 20 iterations. The tuning parameters are presented in Table 4.1. Figure 4.8 presents the outer iteration results for the generation settings P_G, Lagrangian multiplier μ and res. Note, it is assumed that inner iterations do not require any communication if carried out at a central regional location thereby reducing the communication needs significantly.

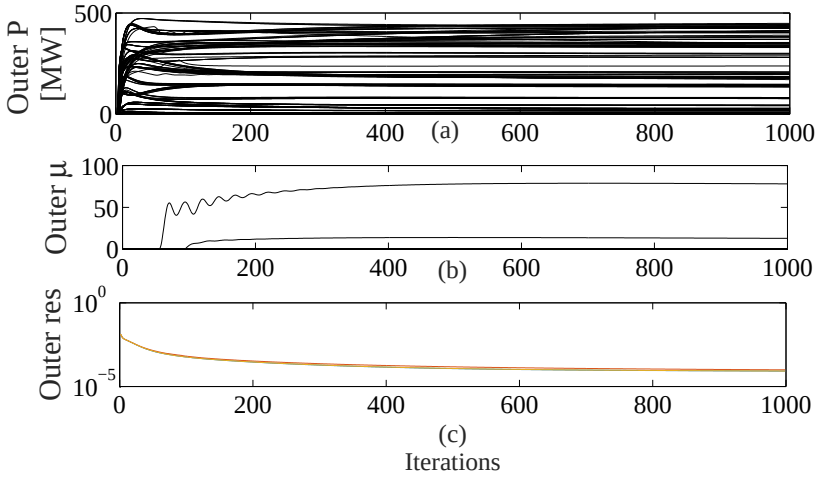

Figure 4.8: (a) Generation output, (b) Lagrangian multiplier μ and (c) Residual of equality constraint $\sum_i \sqrt{\left(g_i^c\right)^2}/N_B$, $\mathcal{AI}-\mathcal{DSCOPF}$, 944 bus test system.

4.5.6 Case Study 4: Sensitivity Analysis

This section investigates the impact of distributedness, i.e., number of areas, and number of buses on the convergence of the $\mathcal{AI}-\mathcal{DSCOPF}$ algorithm. Simulations are carried out for different numbers of areas and different number of buses and the results are presented in Table 4.2. Here, the *res* of $\mathcal{AI}-\mathcal{DSCOPF}$ is reported after 5000 inner iterations. Note, the contingency set includes failure of the lines connecting buses 5 and 8 and buses 15 and 19 inside each area in addition to lines that connect the areas to each other. Based on this table, as the number of buses increases the convergence slows down. Moreover, the speed of convergence with respect to inner iterations depends on the number of areas and how often these areas exchange updated information. Generally, if the number of areas increases but the communication gap stays the same, convergence speed reduces. Again, as previously mentioned, it can be assumed that inner iterations do not require any communication if carried out centrally inside the region thereby reducing the communication needs significantly.

Table 4.2: Required number of iterations to achieve convergence with various number of areas, and various number of attached IEEE 118-bus

# attached 118 buses	# areas	inner iter. per outer iter.	$res \times N_B$
2	2	10	0.1215
3	3	10	0.1434
4	4	10	0.1624
	8	10	0.1627
	8	40	0.1628
8	8	20	0.2152
	16	20	0.2153

4.6 Summary

In this chapter, we have presented two multi-agent distributed approaches to solve the DC-SCOPF problem, namely the $\mathcal{I}-\mathcal{DSCOPF}$ and $\mathcal{AI}-\mathcal{DSCOPF}$, in a distributed manner. In the DC-SCOPF problem, the generation dispatch is determined which minimizes the cost to supply the load taking into account limited line capacities both in normal and contingency cases. The main features of the $\mathcal{I}-\mathcal{DSCOPF}$ algorithm are that it allows for a fully distributed implementation down to the bus level without the need for a coordinating central entity. Each bus is represented by an agent and the individual agent updates per iteration consist of simple function evaluations and exchange of information is limited to bus angles and Lagrange multipliers associated with power flow equations and line constraints among the neighboring agents. In particular, there is no need to share information about generation cost parameters or generation settings. Moreover, we have presented two versions of the $\mathcal{I}-\mathcal{DSCOPF}$; version **A** which utilizes the original optimality conditions in the update functions, and version **B** that effectively modifies the update functions to improve the convergence rate of the $\mathcal{I}-\mathcal{DSCOPF}$ algorithm.

Furthermore, we discussed synchronous and asynchronous implementations of the proposed algorithm. The asynchronous version, denoted by $\mathcal{AI}-\mathcal{DSCOPF}$, not only allows to model multiple information exchange modalities in the system but also the impact of communication. The asynchronous updates enable a more realistic implementation to optimally coordinate across geographically distinct areas and/or to improve computation speed by parallelizing calculations. The proposed algorithms were tested in the IEEE 14-bus, IEEE 57-bus and the 944-bus test systems showing that it converges to the overall optimal solution. Moreover, this chapter discusses the convergence criteria for the proposed distributed methods. Finally, in order to adjust the tuning parameters, we suggested a set of guidelines which is backed by analytical justifications.

Chapter 5

Distributed Approach For Power Flow Control

5.1 Introduction

5.1.1 Motivation and Related Work

Today's transmission grid is operated closer to its capacity limits due to the increased penetration of renewable resources, ever increasing electricity consumption, and lack of investment in transmission assets. The resulting bottlenecks in this interconnected system may result in a suboptimal usage of the generation assets. A possible way to resolve this issue is to better utilize the existing transmission system such as by installing and operating power flow control devices that allow directing power flows to desired paths. This could alleviate congestions of transmission lines by essentially increasing the transfer capacity of the grid.

Flexible AC Transmission Systems (FACTS) are capable of steering power flows by altering parameters of the transmission grid, e.g., line reactances. The newly developed distributed version of FACTS devices [36], namely Distributed FACTS (D-FACTS), not

just serve the purpose of increasing the transfer capacity of the grid but also offer a more reliable and cost effective option compared with traditional FACTS devices. In this regard, the effect of D-FACTS adoption in the transmission grid is discussed in detail in [36].

A distributed control scheme could decrease the complexity of optimal coordination of these power flow control devices and hence improve the operation of the future electric grid which is envisioned to be penetrated by a range of distributed components and generation resources. To address this need and to implement an autonomous structure for power flow control, in [37, 38, 39] multi agent distributed control strategies for FACTS devices are proposed which are based on sensitivity analysis. Moreover, [40] proposed a sensitivity based distributed control of FACTS devices against line overloading. However, sensitivity based approaches could lead to a conflicting behavior of FACTS devices in the case that the control areas assigned to these devices overlap which indicates mutual influences [41]. In this regards, [42] presented a distributed model predictive control for automatic generation control of a multi-systems grid where inter-system tie-lines are equipped with FACTS devices. Furthermore, [43] utilized an alternating direction method of multipliers to solve the power flow control problem, in which at each iteration every bus has to solve multiple optimization problems.

Motivated by the same cause, the focus of this chapter is on finding a distributed solution for the DC-OPF where the D-FACTS are incorporated into the problem formulation to allow for power flow control (PFC). Our proposed distributed scheme, denoted by $\mathcal{I}-\mathcal{DPFC}$ (Innovation based Distributed Power Flow Control) integrates first order optimality conditions of the PFC problem as *local innovation-gradient*s into the local variable updates as presented in chapter 3 for the case without power flow control devices. To our knowledge, this is the first time this type of approach is proposed for distributed power flow control.

As mentioned in Sect. 2.3.1, the $\mathcal{I}-\mathcal{DPFC}$ reduces the original PFC's optimization

problem to solving a coupled system of equations in a fully distributed manner. The $\mathcal{I}-\mathcal{DPFC}$'s local update rules, which include linear combinations of the discussed optimality conditions, require each bus to update a few local variables and exchange information with neighboring physically connected buses. Also, our proposed $\mathcal{I}-\mathcal{DPFC}$ method could be further extended to allow for asynchronous implementation (see 3.3.2 for more details). However, unlike chapters 3 and 4, the incorporation of power flow control variables make the formulation non-convex and by solving the first order optimality conditions we aim to obtain a local optimum, in general, for the PFC problem studied in this chapter.

5.1.2 Notation

Parameters and Constants

P_{L_i}	Load at bus i
a_n, b_n, c_n	Cost function parameters of generator n
$\overline{P}_{G_n}, \underline{P}_{G_n}$	Maximum and minimum generation of generator n
X_{ij}, Y_{ij}	Reactance and admittance of line ij
$\Delta\overline{X}_{ij}, \Delta\underline{X}_{ij}$	Maximum and minimum reactance of D-FACTS in line ij
$\overline{Y}_{ij}, \underline{Y}_{ij}$	Upper and lower limit for the admittance of line ij that is equipped with D-FACTS
$\overline{P}_{ij}$	Line flow limit of line ij
Ω_G, Ω_B	Set of all generators and set of all buses
Ω_{G_i}	Set of all generators at bus i
Ω_L	Set of all lines in the grid
Ω_i	Set of all buses physically connected to bus i
N_B	Number of buses
$\alpha, \beta, \gamma, \tau, \eta$	Tuning paramters

Variables

P_{G_n}	Power output of generator n
θ_i	Voltage angle at bus i
$X_{ij,T}$,	Total reactance of line ij
$Y_{ij,T}$	Total admittance of line ij
λ_i	Lagrangian multiplier of the load balance equation of bus i
μ_{ij}	Lagrangian multiplier of the line flow constraint of line ij
μ_n^+, μ_n^-	Lagrangian multipliers related to upper and lower generation limits of generator n
ν_n^+, ν_n^-	Lagrangian multipliers related to upper and lower admittance limits of the lines equipped with D-FACTS

5.2 Power Flow Control

5.2.1 D-FACTS modeling

In this chapter, a D-FACTS device is modeled as a variable reactance ΔX_{ij} in series with the line reactance X_{ij} [36]. Note, this paper assumes that a D-FACTS is capable of decreasing and increasing the overall reactance of the line. Increasing a line's reactance steers power away from that line while decreasing the reactance draws power into the line. Incorporating D-FACTS, the total reactance of a line is modeled as

$$X_{ij,T} = X_{ij} + \Delta X_{ij} \tag{5.1}$$

$$\Delta \underline{X}_{ij} \leq \Delta X_{ij} \leq \Delta \overline{X}_{ij}. \tag{5.2}$$

5.2.2 Problem Formulation

The *PFC* problem is aimed at finding the generation dispatch and the settings for the power flow control devices which supply the load in the system at the least cost while taking into account operational constraints such as line flow limits and limits on generation outputs. Mathematically this problem is formulated as:

$$\min_{P_G} \sum_{n \in \Omega_G} (a_n P_{G_n}^2 + b_n P_{G_n} + c_n) \tag{5.3}$$

$$\text{s.t.} \quad \sum_{n \in \Omega_{G_i}} P_{G_n} - P_{Li} = \sum_{j \in \Omega_i} Y_{ij,T} \cdot (\theta_i - \theta_j) \quad \forall i \in 1, \cdots, N_B \tag{5.4}$$

$$\theta_1 = 0 \tag{5.5}$$

$$-\overline{P}_{ij} \leq Y_{ij,T} \cdot (\theta_i - \theta_j) \leq \overline{P}_{ij} \ \forall ij \in \Omega_L \tag{5.6}$$

$$\underline{P}_{G_n} \leq P_{G_n} \leq \overline{P}_{G_n} \quad \forall n \in \Omega_n \tag{5.7}$$

$$\underline{Y}_{ij} \leq Y_{ij,T} \leq \overline{Y}_{ij}, \quad \forall ij \in \Omega_L \tag{5.8}$$

where $Y_{ij,T} = 1/X_{ij,T}$ and the upper and lower limits $\overline{Y}_{ij}, \underline{Y}_{ij}$ for the admittance of line ij are derived from (5.1), (5.2) resulting in

$$\underline{Y}_{ij} = \frac{1}{X_{ij} + \Delta \overline{X}_{ij}} \quad \text{and} \quad \overline{Y}_{ij} = \frac{1}{X_{ij} + \Delta \underline{X}_{ij}}.$$

Therefore, instead of controlling the reactance of the DFACTS, the admittance of line ij ($Y_{ij,T}$) is considered as a control variable. Here, $i = 1$ is taken to be the slack bus and its angle θ_1 is set to zero. Note, the above formulation can be casted as an instance of the general optimization form (2.1)-(2.3), with equations (5.3), (5.4), and (5.6)-(5.8) corresponding to $\mathfrak{F}$, $\mathfrak{G}$ and $\mathfrak{H}$, respectively. Here, $i = 1$ is taken to be the slack bus.

5.2.3 Optimality Conditions

The Lagrangian function for this optimization problem is given by:

$$\begin{aligned} L = & \sum_{n\in\Omega_G}(a_n P_{G_n}^2 + b_n P_{G_n} + c_n) + \sum_{n\in\Omega_G}\mu_n^+(P_{G_n} - \overline{P}_{G_n}) + \sum_{n\in\Omega_G}\mu_n^-(-P_{G_n} + \underline{P}_{G_n}) \\ & + \nu_{ij}^+(Y_{ij,T} - \overline{Y}_{ij}) + \nu_{ij}^-(-Y_{ij,T} + \underline{Y}_{ij}) \\ & + \sum_{i=1}^{N_B}\lambda_i(-\sum_{n\in\Omega_{G_i}} P_{G_n} + P_{Li} + \sum_{j\in\Omega_i} Y_{ij,T}\cdot(\theta_i - \theta_j)) \\ & + \sum_{ij\in\Omega_L}\mu_{ij}(Y_{ij,T}\cdot(\theta_i - \theta_j) - \overline{P}_{ij}) + \sum_{ji\in\Omega_L}\mu_{ji}(-Y_{ij,T}\cdot(\theta_i - \theta_j) - \overline{P}_{ij}). \end{aligned} \tag{5.9}$$

and the corresponding first order optimality conditions are derived as follows:

$$\frac{\partial L}{\partial P_{G_n}} = 2a_n P_{G_n} + b_n - \lambda_n + \mu_n^+ - \mu_n^- = 0 \tag{5.10}$$

$$\frac{\partial L}{\partial \theta_i} = \lambda_i \sum_{j\in\Omega_i} Y_{ij,T} - \sum_{j\in\Omega_i}\lambda_j Y_{ij,T} + \sum_{j\in\Omega_i}(\mu_{ij} - \mu_{ji})Y_{ij,T} = 0 \tag{5.11}$$

$$\frac{\partial L}{\partial \lambda_i} = -\sum_{n\in\Omega_{G_i}} P_{G_n} + P_{Li} - \sum_{j\in\Omega_i} Y_{ij,T}\cdot(\theta_i - \theta_j) = 0 \tag{5.12}$$

$$\begin{aligned} \frac{\partial L}{Y_{ij,T}} = & (\theta_i - \theta_j)\cdot\lambda_i + (\theta_j - \theta_i)\cdot\lambda_j + \nu_n^+ - \nu_n^- \\ & + (\theta_i - \theta_j)\cdot\mu_{ij} + (\theta_j - \theta_i)\cdot\mu_{ji} = 0 \end{aligned} \tag{5.13}$$

$$\frac{\partial L}{\mu_n^+} = P_{G_n} - \overline{P}_{G_n} \le 0 \tag{5.14}$$

$$\frac{\partial L}{\mu_n^-} = -P_{G_n} + \underline{P}_{G_n} \le 0 \tag{5.15}$$

$$\frac{\partial L}{\nu_{ij}^+} = Y_{ij,T} - \overline{Y}_{ij} \le 0 \tag{5.16}$$

$$\frac{\partial L}{\nu_{ij}^-} = Y_{ij,T} - \underline{Y}_{ij} \le 0 \tag{5.17}$$

$$\frac{\partial L}{\mu_{ij}} = Y_{ij,T}\cdot(\theta_i - \theta_j) - \overline{P}_{ij} \le 0 \tag{5.18}$$

$$\frac{\partial L}{\mu_{ji}} = -Y_{ij,T}\cdot(\theta_i - \theta_j) - \overline{P}_{ij} \le 0, \tag{5.19}$$

for all $i \in \Omega_B$, and $ij \in \Omega_L$ plus the complementary slackness conditions for the inequality constraints and the positivity constraints on the μ's and ν's.

5.3 Distributed Approach

This chapter presents the $\mathcal{I}-\mathcal{DPFC}$ algorithm to solve the first order optimality conditions of the PFC. This iterative scheme follows the *innovation*-based update formulation that is introduced in Sect. 2.3.1. Here, each bus (agent) i is responsible for updating the variables associated with it, namely λ_i, θ_i, P_{G_n} for $n \in \Omega_{G_i}$, $Y_{ij,T}$, and μ_{ij} for $j \in \Omega_i$. The rest of this section is devoted to formulating the updates for the local variables. As will be seen, updates for $\mu_n^+, \mu_n^-, \nu_n^+,$ and ν_n^- are not required as we use projections to enforce the limits on the generation outputs and the line reactances. Hence, $\mathcal{I}-\mathcal{DPFC}$ does not include any updates for these Lagrange Multipliers.

The proposed update for λ_i is given as:

$$\begin{aligned}\lambda_i(k+1) = \lambda_i(k) - \beta \cdot \Bigg(& \lambda_i(k) \sum_{j\in\Omega_i} Y_{ij,T}(k) - \sum_{j\in\Omega_i} \lambda_j(k) Y_{ij,T}(k) \\ & + \sum_{j\in\Omega_i} Y_{ij,T}(k) \cdot (\mu_{ij}(k) - \mu_{ji}(k)) \Bigg) \\ & - \alpha \cdot \Bigg(\sum_{n\in\Omega_{G_i}} P_{G_n}(k) - P_{L_i} - \sum_{j\in\Omega_i} Y_{ij,T}(k) \cdot (\theta_i(k) - \theta_j(k)) \Bigg),\end{aligned} \tag{5.20}$$

where $\alpha, \beta > 0$ are tuning parameters. This update rule is based on the same intuition that was presented for (3.14).

Knowing the value of λ_i, the power outputs of the generators $P_{G_n}, n \in \Omega_{G_i}$ are updated as follows:

$$P_{G_n}(k+1) = \mathbb{P}_n \left[\frac{\lambda_i(k+1) - b_n}{2a_n} \right]. \tag{5.21}$$

Note, the projection operator $\mathbb{P}_n$ in the update rule ensures that the obtained value lies in the feasible range $[\underline{P}_{G_n}, \overline{P}_{G_n}]$, i.e., if the updated value is greater than the capacity of the generator, the value is set to that upper bound and similarly for the lower generation limit. The above update and its intuition matches the one for (3.15).

The angles of the buses are updated as

$$\theta_i(k+1) = \theta_i(k) - \gamma \left(-\sum_{n \in \Omega_{G_i}} P_{G_n}(k) + P_{L_i} + \sum_{j \in \Omega_i} Y_{ij,T}(k) \cdot (\theta_i(k) - \theta_j(k)) \right), \tag{5.22}$$

where $\gamma > 0$ is a tuning parameter. Using the local supply/demand balance equation in (5.22) intuitively follows the same argument that is presented for (3.16).

The corresponding update for μ_{ij}, i.e., the Lagrange multiplier associated with line limits is given as:

$$\mu_{ij}(k+1) = \mathbb{P}_{ij} \left[\mu_{ij}(k) - \delta \cdot \left(\overline{P}_{ij} - Y_{ij,T}(k) \cdot (\theta_i(k) - \theta_j(k)) \right) \right], \tag{5.23}$$

with $\delta > 0$. Note, this update always results in positive values for the Lagrange multipliers due to the projection $\mathbb{P}_{ij}$ onto the feasible region $[0, \infty)$ (see discussion related to (3.18) for more details).

The update for the admittance $Y_{ij,T}$ of the line is given as:

$$\begin{aligned} Y_{ij,T}(k+1) = \mathbb{P}_{ij,y} \big[& Y_{ij}(k) - \tau((\theta_i(k) - \theta_j(k)) \cdot \lambda_i(k) + \\ & (\theta_j(k) - \theta_i(k)) \cdot \lambda_j(k) + (\theta_i(k) - \theta_j(k)) \cdot \mu_{ij}(k) + (\theta_j(k) - \theta_i(k)) \cdot \mu_{ji}(k)) \big]. \end{aligned} \tag{5.24}$$

Here, $\tau > 0$ is again a tuning parameter. The projection operator $\mathbb{P}_{ij,y}$ projects the corresponding updated value onto the feasible space defined by $[\underline{Y}_{ij}, \overline{Y}_{ij}]$. The aforementioned update rule is based on (5.13), where the effect of the ν^+ and ν^- are captured in terms of

the projections.

Also, note that due to the non-convexity of the PFC, the $\mathcal{I}-\mathcal{DPFC}$ is not guaranteed to achieve a globally optimal solution, but by solving the first order optimality conditions we aim to obtain a local optimum.

5.4 Convergence Analysis

5.4.1 Properties of the Solution

In the following Theorem 1, we first show that a fixed point of the proposed iterative scheme necessarily satisfies the optimality conditions (5.10)–(5.19) of the PFC problem.

Theorem 1: Let X^* be a fixed point of the proposed $\mathcal{I}-\mathcal{DPFC}$ algorithm. Then, $X^\star$ satisfies all of the optimality conditions of the PFC problem (5.10)–(5.19).

Proof: The formal proof of Theorem 1 includes the verifications of the set of claims which show that $X^\star$ fulfills all of the first order optimality conditions. Note that the vector of stacked variables $(\lambda_i{}^\star, \theta_i{}^\star, \mu_{ij}{}^\star, P^\star_{G_i}, Y^\star_{ij,T})$ for all buses (agents) $i=\{1,\ldots,N_B\}$ is denoted by $X^\star$.

Claim 1: $X^\star$ fulfills the optimality conditions which enforce the positivity of the Lagrangian multipliers associated with the line limits, i.e., $\mu^\star_{ij}\geq 0$.

Verification by contradiction: Let us assume on the contrary that in $X^\star$ one of the line limit multiplier variables, say $\mu^\star_{ij}$, is negative. Now, note that, evaluating (5.23) at $X^\star$ results in a non-negative value for μ_{ij} due to the projection of μ_{ij} into the set of positive reals. In other words, we have

$$\mu^\star_{ij} \neq \mathbb{P}\left[\mu^\star_{ij}-\delta\cdot\left(\overline{P}_{ij}-Y^\star_{ij,T}\cdot(\theta^\star_i-\theta^\star_j)\right)\right],$$

which contradicts the fact that X^* is a fixed point of (5.23). A similar argument establishes that $\mu^\star_{ji}\geq 0$.

Claim 2: $X^\star$ satisfies the optimality conditions associated with the line limit constraints, (5.18)–(5.19).

Verification by contradiction: Let us assume that $X^\star$ does not fulfill (5.18) for all i and j, i.e., there exists (i,j) such that $Y^\star_{ij,T} \cdot (\theta^\star_i - \theta^\star_j) > \overline{P}_{ij}$. This implies that the value of the innovation term in (5.23) is negative when evaluated at $X^\star$. Also, note that, based on claim 1, $\mu^\star_{ij} \geq 0$. Therefore, evaluating (5.23) at $X^\star$ results in a value greater than $\mu^\star_{ij}$, i.e.,

$$\mu^\star_{ij} < \mathbb{P}\left[\mu^\star_{ij} - \delta \cdot \left(\overline{P}_{ij} - Y^\star_{ij,T} \cdot (\theta^\star_i - \theta^\star_j)\right)\right],$$

which contradicts the fact that X^* is a fixed point of (5.23). Similar arguments can be used to prove that $X^\star$ fulfills (5.19).

Claim 3: $X^\star$ satisfies the optimality conditions associated with the complementary slackness condition, i.e., for all pairs (i,j),

$$\mu^\star_{ij} \cdot \left(Y^\star_{ij,T} \cdot (\theta^\star_i - \theta^\star_j) - \overline{P}_{ij}\right) = 0.$$

Verification by contradiction: Let us assume on the contrary that X^* does not satisfy the above complementary slackness condition, i.e., there exists a pair (i,j) such that both $\mu^\star_{ij}$ and $Y^\star_{ij,T} \cdot (\theta^\star_i - \theta^\star_j)$ are non-zero. Hence, according to the claims 1 and 2, we must have, $\mu^\star_{ij} > 0$ and $Y^\star_{ij,T} \cdot (\theta^\star_i - \theta^\star_j) < \overline{P}_{ij}$, respectively. Now, note that evaluating (5.23) at $X^\star$, results in a value less than $\mu^\star_{ij}$, which clearly contradicts the fact that X^* is a fixed point of (5.23).

Claim 4: $X^\star$ satisfies the local load balance equation (5.12).

Verification by contradiction: Let us assume on the contrary that $X^\star$ does not fulfill (5.12), i.e., there exists i such that the value of the innovation term in (5.22) is non-zero

when evaluated at $X^\star$. Clearly, this would lead to

$$\theta_i^\star \neq \theta_i^\star - \gamma \left(-\sum_{n \in \Omega_{G_i}} P_{G_n}^\star + P_{L_i} + \sum_{j \in \Omega_i} Y_{ij,T}^\star \cdot (\theta_i^\star - \theta_j^\star) \right),$$

thus contradicting the fact that X^* is a fixed point of (5.22).

Claim 5: The coupling between the Lagrangian multipliers, given by (5.11), is maintained at $X^\star$.

Verification by contradiction: Let us assume on the contrary that $X^\star$ does not fulfill (5.11) for some i. Note that (5.20) includes two innovation terms: the innovation term associated with the Lagrangian multipliers' coupling and the innovation term which represents the local power balance equation. We already verified that the local power balance equation is zero at $X^\star$ (see claim 4). Thus, the contradiction hypothesis necessarily implies that the innovation term associated with the Lagrangian multipliers' coupling attains a non-zero value at $X^\star$. This, in turn, implies that the the value of (5.20) is not equal to $\lambda_i^\star$ when evaluated at $X^\star$, which clearly contradicts the fact that X^* is a fixed point of (5.20).

Claim 6: $X^\star$ satisfies the optimality conditions associated with the generation limits, (5.14)–(5.15).

Verification by contradiction: Let us assume on the contrary that there exists i such that $P_{G_i}^\star$ does not lie in $[\underline{P}_{G_i}, \overline{P}_{G_i}]$. Now, note that, plugging in $\lambda^\star$ in (5.21), would then result in a value different from $P_{G_i}^\star$, since the projection operator enforces the value of P_{G_i} to stay in the specified region, $[\underline{P}_{G_i}, \overline{P}_{G_i}]$. This, in turn, clearly contradicts the fact that X^* is a fixed point of (5.21).

Claim 7: $X^\star$ satisfies the optimality conditions associated with the admittance limits of line ij equipped with D-FACTS, (5.16)–(5.17).

Verification by contradiction: Let us assume on the contrary that there exists i such that $Y_{ij,T}^\star$ does not lie in $[\underline{Y}_{ij}, \overline{Y}_{ij}]$. Now, note that, plugging in $Y_{ij,T}^\star$ in (5.24), would then

result in a value different from $Y^{\star}_{ij,T}$, since the projection operator enforces the value of $Y^{\star}_{ij,T}$ to stay in the specified region, $[\underline{Y}_{ij}, \overline{Y}_{ij}]$. This, in turn, clearly contradicts the fact that X^* is a fixed point of (5.24).

Claim 8: $X^{\star}$ satisfies (5.13).

Verification by contradiction: Let us assume on the contrary that $X^{\star}$ does not fulfill (5.13), i.e., there exists (i, j) such that the value of the innovation term in (5.24) is non-zero when evaluated at $X^{\star}$. Also, based on *Claim 7* $Y^{\star}_{ij,T}$ is in the specified region, $[\underline{Y}_{ij}, \overline{Y}_{ij}]$, hence the projection operator in (5.24) is redundant. Clearly, our assumption would lead to

$$Y^{\star}_{ij,T} \neq Y^{\star}_{ij,T} - \tau((\theta^{\star}_i - \theta^{\star}_j) \cdot \lambda^{\star}_i + (\theta^{\star}_j - \theta^{\star}_i) \cdot \lambda^{\star}_j + (\theta^{\star}_i - \theta^{\star}_j) \cdot \mu^{\star}_{ij} + (\theta^{\star}_j - \theta^{\star}_i) \cdot \mu^{\star}_{ji}).$$

thus contradicting the fact that X^* is a fixed point of (5.24).

Here, we discuss the outcomes of Theorem 1. Due to the fact, that $\mathcal{I} - \mathcal{DPFC}$ consists of continuous transformations of the iterates, it follows that, if $\mathcal{I} - \mathcal{DPFC}$ converges, the limit point is necessarily a fixed point of the iterative mapping. Therefore, based on Theorem 1, any limit point of the $\mathcal{I} - \mathcal{DPFC}$ satisfies the first order optimality conditions, (5.10)–(5.19), of the PFC problem. Moreover, the following Theorem 2 discusses the optimality of limit points of the proposed $\mathcal{I} - \mathcal{DPFC}$ method.

Remark 1: Let us assume that $X^{\star}$ fulfills first order optimality conditions of the PFC problem. Then, $X^{\star}$ is a local optimum of the underlaying optimization problem only if optimality conditions at $X^{\star}$ satisfy constraint qualifications.

Theorem 2: Let the PFC problem (5.3)-(5.8) have a feasible solution within the interior of the associated constraint set, and, further, assume that the proposed $\mathcal{I} - \mathcal{DPFC}$ algorithm converges to a point $X^{\star}$. Then X^* is a local optimal solution of the PFC problem.

Proof: By Theorem 1, $X^{\star}$ satisfies the optimality conditions (5.10)–(5.19) of the PFC problem. Also, first order optimality conditions of the PFC problem are linearly inde-

pendent, hence, they satisfy linear independent constraint qualification at X^*. Therefore, based on Remark 1 X^* is a local optimal solution of the PFC problem.

Finally, note that the discussed PFC problem is a non-convex problem, hence, a solution that fulfills its associated first order optimality conditions may not constitute an optimal solution for the original problem.

5.5 Simulation Results

5.5.1 Test System Set up

We evaluate the $\mathcal{I}-\mathcal{DPFC}$ using the IEEE 14-Bus system and IEEE 118-Bus system (see Appendix). The topology of the communication network is the same as the physical system, i.e., each bus only exchanges information with its physically connected buses. In the IEEE 14-Bus system, the power flow control devices are placed in lines connecting buses 3 and 4 and connecting buses 4 and 9. The line limits are chosen such that the lines connecting buses 1 and 2 and connecting buses 3 and 4 reach their limits in the optimal solution. In the IEEE 118-Bus system, the power flow control devices are placed in lines connecting buses 3 and 5 and also buses 25 and 27. At the optimal solution, the lines connecting buses 4 and 5, buses 25 and 27 and buses 49 and 50 reach their limits.

The cost parameters for the generators are derived from the heat rate curves given in the IEEE Reliability Test System and recent fuel costs. The simulations are performed using a cold start, i.e., all the variables except the Lagrange multipliers λ_i are set to zero at the start.

5.5.2 Convergence Measurements

The performance of the $\mathcal{I}-\mathcal{DPFC}$ is evaluated using the same two measures as in previous chapters. The first corresponds to the relative distance of the objective function

value f from the solution of the centralized problem (f^*) using the KNITRO solver of the commercial optimization package Tomlab,

$$rel = \frac{|f - f^*|}{f^*}, \tag{5.25}$$

The second measure quantifies the fulfillment of the load balance equations. Hence, we denote g_i as the residual of the supply/demand balance at bus i. The sum over these residuals over the course of the iterations provides this second measure and is given as

$$res = \sum_i \sqrt{g_i^2}, \tag{5.26}$$

5.5.3 Case Study 1: IEEE 14-bus Test System

We first discuss the results for the IEEE 14-bus test system. Figure 5.1(a) depicts the evolution of the generation outputs over 2000 iterations, while Fig. 5.1(b) shows the evolution of the λ's for the same number of iterations.

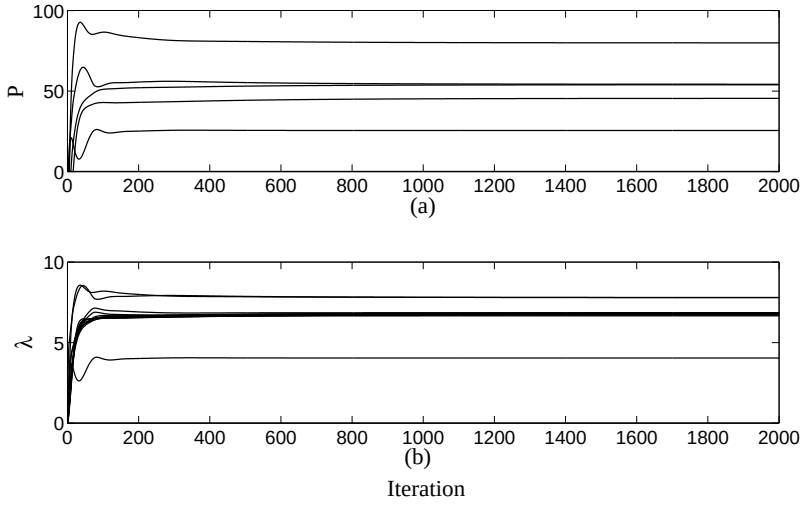

Figure 5.1: (a) Generation output, and (b) Lagrangian multiplier λ (IEEE 14-Bus test system).

Moreover, Figs. 5.2(a) and (b) give the evolution of the μ's of all lines, and the line admittances which are equipped with D-FACTS for 2000 iterations, respectively. Since two of the lines are congested at the optimal solution, their associated μ_{ij}'s obtain non-zero values. Furthermore, again due to the congestions, the λ's for the buses deviate from each other at the final solution.

Figure 5.3(a) shows the relative distance from the optimal value of the objective function over the course of the iterations. Although the PFC problem is non-convex, for the IEEE-14 bus the Tomlab's solution is globally optimal(based on the output flag of the solver).

The sum over the residual of all supply/demand equations is given in Fig. 5.3(b). It is clear that the $\mathcal{I} - \mathcal{DPFC}$ algorithm gets closer to the optimal solution as more iterations are carried out. Also, the obtained values from the $\mathcal{I} - \mathcal{DPFC}$ are seen to satisfy the first order optimality conditions. Note that, in particular, at the limiting convergence point, the value of the power flow equations residual, and consequently the res, is equal to zero.

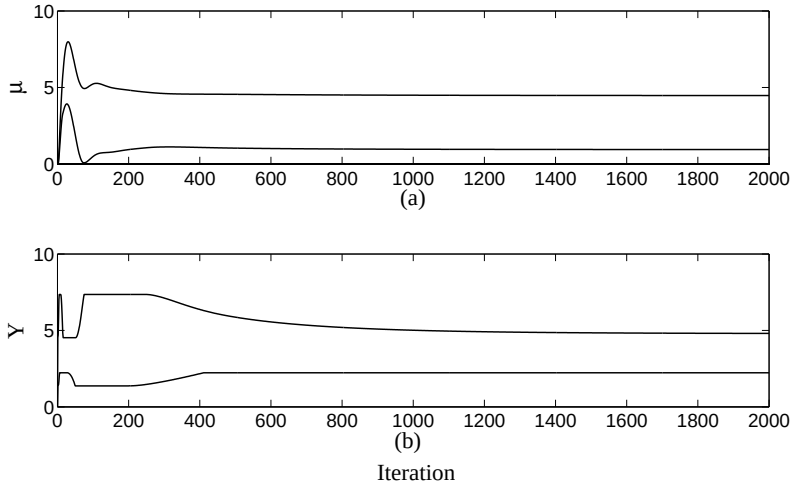

Figure 5.2: (a) Lagrangian multiplier μ, and (b) Variable Admittance Y (IEEE 14-Bus test system).

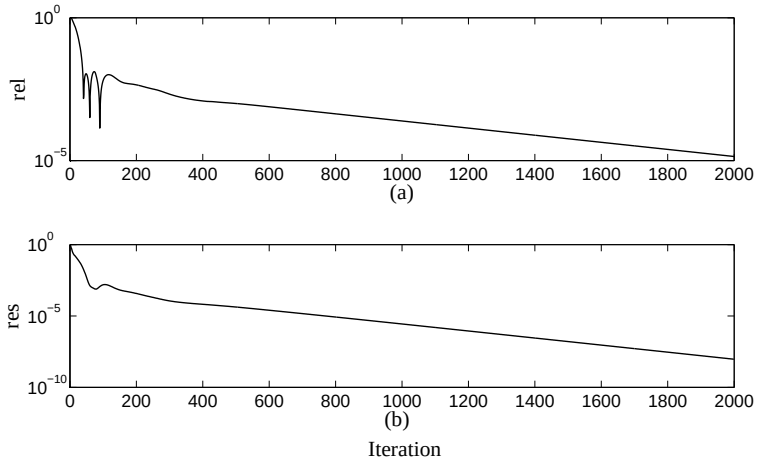

Figure 5.3: (a) Relative distance to solution $\frac{|f-f^*|}{f^*}$, and (b) Residual of load balance constraints $\sum_i \sqrt{g_i^2}$ (IEEE 14-Bus test system).

5.5.4 Case Study 2: IEEE 118-bus Test System

Figure 5.4 shows the simulation results (generation outputs, Lagrange multiplier, and variable admittance) for the IEEE-118 bus test system over 5000 iterations.

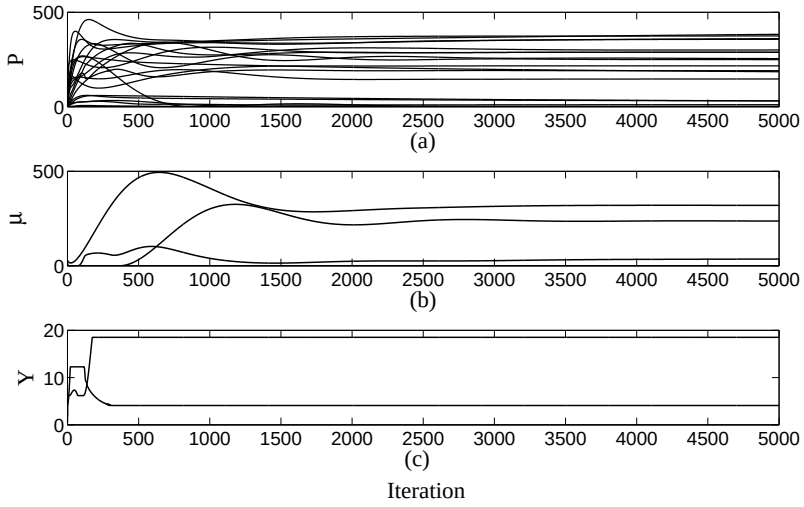

Figure 5.4: (a) Generation output, (b) Lagrangian multiplier μ, and (c) Variable Admittance Y (IEEE 118-Bus test system).

Moreover, in order to show the performance of our proposed algorithm we implemented the $\mathcal{I}-\mathcal{DPFC}$ algorithm for the case that all lines of the IEEE-118 bus test system are

equipped with power flow control devices. Figure 5.5 presents the generation outputs, Lagrange multipliers μ, and variable admittance Y of all lines. The res and rel are given in Fig. 5.6. The achieved value for rel after 5000 iteration is 0.0028. Similarly to the IEEE-14 bus test system, the optimization variables converge towards the same solution as the centralized solver.

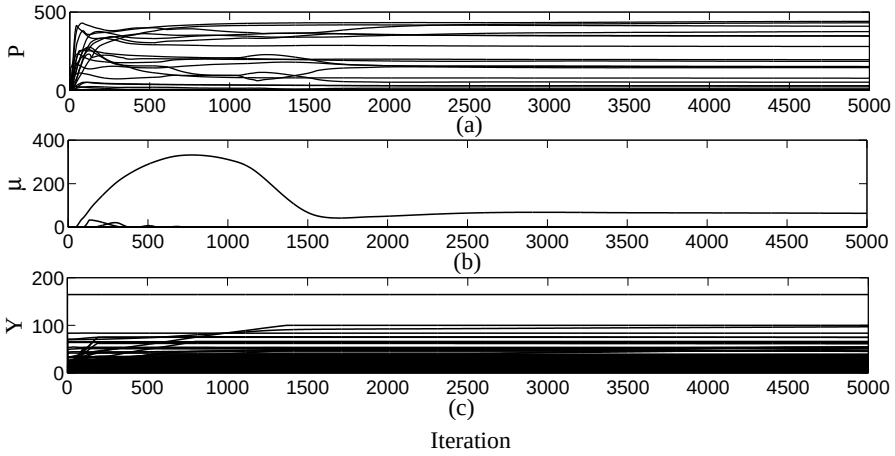

Figure 5.5: (a) Generation output, (b) Lagrangian multiplier μ, and (c) Variable Admittance Y (IEEE 118-Bus test system).

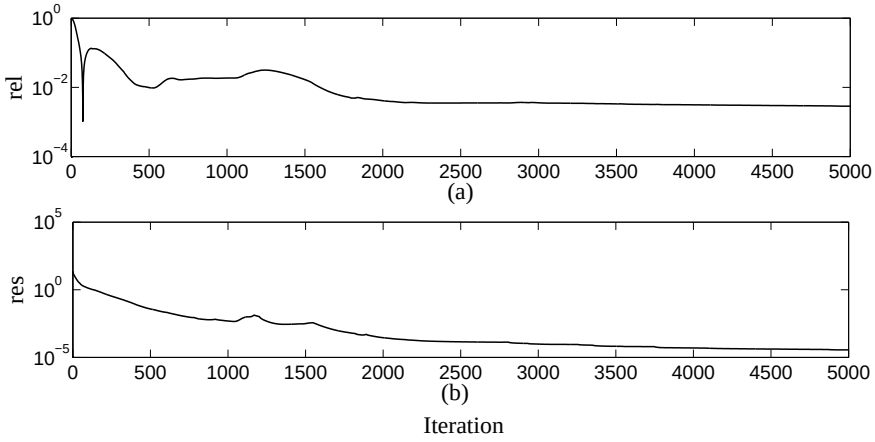

Figure 5.6: (a) Generation output, (b) Lagrangian multiplier μ, and (c) Variable Admittance Y (IEEE 118-Bus test system).

5.6 Summary

In this chapter, we have presented a distributed approach to solve the DC Optimal Power Flow problem with D-FACTS placed in some of the transmission lines. The approach defines local updates for the variables which use combinations of the first order optimality conditions of the corresponding optimization problem as innovation terms. This algorithm allows for a fully distributed implementation down to the bus level without the need for a coordinating entity. The update rules just involve simple function evaluations and the information exchange is limited to a few neighboring buses. Furthermore, this algorithm does not require sharing information about generation cost parameters or generation settings. The performance of the algorithm was tested in the IEEE 14-bus and 118-bus test systems providing proof of concept by showing convergence to the centralized solution. Finally, we analytically justified that any solution achieved by our proposed algorithm is a local optimal solution to the underlying optimization problem.

Chapter 6

Distributed Cooperative Charging of Plug-in Electric Vehicles

6.1 Introduction

6.1.1 Motivation and Related Work

Plug-in electric vehicles (PEVs) are considered as flexible loads since their charging schedules can be shifted over the course of a day without impacting drivers mobility. This property can be exploited to reduce charging costs and adverse network impacts. However, the uncoordinated charging of PEVs could potentially overburden the electricity network at certain times [44].

Prior approaches to coordinated charging of PEVs have mostly been based on assigning coordination responsibilities to an entity, indicated as an aggregator. The aggregator is an intermediary agent between the PEVs and other power system entities, such as network operators or energy providers. An aggregator's role varies depending on the features of a coordination approach, e.g., a more passive role in decentralized[1]/distributed approaches

[1]In the literature, the term "decentralized" is used to refer to approaches that do not rely on communication, i.e., where charging decisions are taken by PEVs solely based on local information. It can also

compared with centralized ones.

It should be noted that a centralized control structure is not suitable to handle the coordination problem of a large PEV fleet, since this problem is inherently distributed and computationally complex [45, 46, 47, 48, 49, 50, 51]. Moreover, a centralized control scheme may require communication of sensitive information (arrival and departure times, energy requirements) from PEVs to an aggregator. Distributed control strategies are a scalable alternative for solving the PEV-CC problem as they distribute the responsibility of finding optimal settings among multiple entities and additionally they also protect to a certain extent private information such as the driving behavior. Moreover, if the algorithm is implemented in a truly distributed fashion using intelligent agents throughout the network, it generally can be expected that a distributed approach is more robust than a centralized approach with respect to communication failures and cyber attacks.

Most of the existing communication-based decentralized approaches in the literature require an exchange of information (mostly information of charging schedules) with an aggregator, i.e., coordinating entity, to some extent [52, 53, 54, 55, 56, 57, 58]. Generally, a control scheme's underlying structure depends on the agents' cooperation strategy. The approach in [52] consider non-cooperative agents and is based on mean field game theory. Moreover, [54, 58] utilize a price-based scheme to achieve a desired aggregated behavior for a fleet of non-cooperative PEVs in a decentralized manner. On the other hand, the approaches in [53, 55, 56, 57] are based on the agents' cooperation. As an example, the alternating direction method of multipliers is one of the popular approaches to solve the PEVs cooperative charging problem, which decomposes the original problem into smaller subproblems that are assigned to each PEV and an aggregator [55, 56]. Note that, the discussed decentralized approaches require each PEV to exchange information with a central agent and are therefore less robust towards failure than peer-to-peer based distributed

refer to approaches where PEVs take their own charging scheduling decisions based on information shared with a central coordinator.

schemes. In other words, in this setup every communication link failure could render a central coordinator incapable of solving the original optimization problem, whereas a distributed control approach only requires a sparsely connected communication network to achieve the optimal solution. Moreover, [58] proposed a decentralized approach for PEV charging coordination while taking into account tradeoff between total generation cost and the local costs associated with overloading and battery degradation. To this end, the authors restructured the original optimization problem as an unconstrained optimization problem and then solved the first order optimality conditions of the restructured optimization problem in a decentralized manner.

With regards to consensus based approaches, [57] proposes a consensus-based method to solve the PEVs' cooperative charging problem in a distributed fashion, which requires one of the agents to access the total charging demand information. Also, [59] proposes a consensus-based distributed charging rate control scheme for PEVs to minimize total charging power loss, which overlooks the PEVs' individual constraints. Here we propose a *consensus+innovations* based approach to find a distributed solution for the PEV-CC problem (see Sect. 2.3.2). In this chapter, the *consensus* update term of the algorithm enforces an agreement on an incremental price for the energy provided, while the *innovation* term ensures that the local constraints of the individual PEVs are satisfied at the minimum cost.

Given the inherent uncertainty of PEVs' driving pattern, i.e., arrival/departure times and energy consumption during the trips, multi-step receding horizon optimization approaches lend themselves as suitable options for solving cooperative charging problems. In this chapter, we utilize the model proposed in [56] to optimize over several possible driving pattern realizations for each PEV. To solve the respective optimization problem, we have developed a distributed receding horizon optimization technique. Receding horizon approaches compute the optimal action over a horizon period, and then apply the imme-

diate time step solution. To compute the optimal actions for the succeeding time step, the variables and driving pattern scenarios are updated first, and then the multi-time step optimization is executed for the subsequent time horizon [60, 61, 62].

Our method is referred to as $\mathcal{CI}-\mathcal{PEVCC}$, i.e., *consensus+innovations* based PEV Coordinated Charging. Our *consensus+innovations* based method is inherently different from existing decomposition theory-based methods in many ways: methodologically, the proposed *consensus+innovations* based approach directly solves the first order optimality conditions of the PEV-CC problem. Hence, it technically reduces the original optimization problem to finding solutions for a coupled system of (constrained linear) equations in a fully distributed manner. In contrast with primal-dual distributed methods, our solution approach does not require updating all Lagrange multipliers (see Sect. 6.3).

The $\mathcal{CI}-\mathcal{PEVCC}$ is based on the general *consensus+innovations* framework [1] (see Sect. 2.3.2), and the iterative updates are designed to achieve a feasible solution for the PEV-CC problem at each iteration. Therefore, the $\mathcal{CI}-\mathcal{PEVCC}$ algorithm ensures that all the intermediate iterates are feasible solutions to the PEV-CC problem, and hence, is naturally robust to unexpected events such as premature termination of the algorithm or communication failures leading to loss of network connectivity. Also, the proposed $\mathcal{CI}-\mathcal{PEVCC}$ algorithm provides a receding horizon optimization framework which is suitable for optimizing over several driving pattern scenarios for each PEV. The $\mathcal{CI}-\mathcal{PEVCC}$ allows for a fully distributed solution for the PEV-CC problem which does not require sensitive information exchange among the PEVs. Additionally, the inter-agent communication graph is merely required to be connected in order to achieve accurate convergence, i.e., in particular, the communication topology might be very sparse. Finally, the proposed $\mathcal{CI}-\mathcal{PEVCC}$ is a scalable solution to the PEV coordination problem since it distributes the computation and communication burden among the PEVs. Figure 6.1 illustrates a sample communication topology that may be employed to implement the $\mathcal{CI}-\mathcal{PEVCC}$

method.

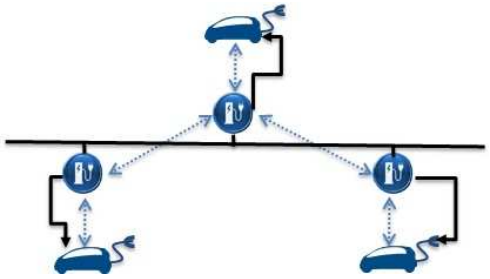

Figure 6.1: Proposed distributed PEVs' coordinated charging scheme (the dashed line represents data exchange, and the solid line represents charing power)

6.1.2 Notation

$\mathbf{x}_{v,s}$	Charging power schedule of PEV v under scenario s over a given time horizon $[0, T]$, $\mathbf{x}_{v,s} \in \mathbb{R}^{T\times 1}$
$\mathbf{L}_s$	Aggregated load of PEVs under scenario s over a given time horizon $[0, T]$, $\mathbf{L}_s \in \mathbb{R}^{T\times 1}$
Ω_v	Set of neighboring charging stations connected to charging station v
c_1, c_2	Cost function parameters, $c_1 \in \mathbb{R}$, $c_2 \in \mathbb{R}^{1\times T}$
A, $b_{v,s}$	Matrix and vector defining the energy constraints of PEV v under scenario s
$\underline{x}_{v,s}$, $\overline{x}_{v,s}$	Upper and lower bounds defining the power constraints of an individual PEV v under scenario s
λ_s, $\mu_{v,s}$	Lagrangian multipliers associated with equality and inequality constraints under scenario s
$\mu_{v,s,-}$, $\mu_{v,s,+}$	Lagrangian multipliers associated with decision variables' upper and lower bounds under scenario s
V, S	Total number of PEVs and driving pattern scenarios
γ_v	Lagrangian multipliers associated with consistency equation for PEV v, $\gamma_v \in \mathbb{R}^{S-1\times 1}$
$\mathcal{S}$	Set of driving pattern realizations $\mathcal{S} = \{1, \cdots, S\}$

6.2 PEV's Coordinated Charging

6.2.1 Problem Formulation

Here we consider a cooperative charging problem for a fleet of PEVs that aims at minimizing a common cost function, which is quadratic with respect to PEVs' aggregated load $\mathbf{L}_s$ under scenario s and over horizon T [56], subject to the PEVs' power and energy constraints under different scenarios, i.e.,

$$\text{minimize}_{\mathbf{x}_{v,s},\mathbf{L_s}} \quad \frac{1}{S}\sum_{s=1}^{S}\left(\mathbf{L_s}^{\top}\cdot c_1\cdot\mathbf{L_s}+c_2^{\top}\cdot\mathbf{L_s}\right) \tag{6.1}$$

$$\text{s.t.} \quad \mathbf{L_s}=\sum_{v\in V}\mathbf{x}_{v,s} \qquad \forall s\in\{1,\cdots,S\} \tag{6.2}$$

$$A\cdot\mathbf{x}_{v,s}\le b_{v,s} \quad \forall v\in\{1,\cdots,V\} \quad \forall s\in\{1,\cdots,S\} \tag{6.3}$$

$$\underline{x}_{v,s}\le\mathbf{x}_{v,s}\le\overline{x}_{v,s} \quad \forall v\in\{1,\cdots,V\} \quad \forall s\in\{1,\cdots,S\} \tag{6.4}$$

$$\mathbf{x}_{v,s}(1)=\mathbf{x}_{v,s'}(1). \quad \forall v\in\{1,\cdots,V\} \quad \forall s,s'\in\{1,\cdots,S\} \tag{6.5}$$

Here, it is assumed that we can extract different scenarios from observed driving behavior $s\in\{1,\cdots,S\}$ [56]. Each sample is associated with a system realization scenario for the fleet and it is referred to using subscript s. In (6.1), c_1 and c_2 representing electricity tariff rates are functions of the total predicted inelastic load (inflexible load other than PEV load). Specifically, as in [56], we assume that the goal is to minimize the costs of serving both the flexible (PEV) and inflexible loads, and that these costs are a quadratic function of accumulated PEVs' consumption and inelastic load.[2]

[2]The cost of serving PEV demand $\mathbf{L}$ and inelastic demand $\mathbf{L}_{\text{in}}$ has the form $\widetilde{a}\mathbf{1}^{\top}(\mathbf{L}+\mathbf{L}_{\text{in}})+\widetilde{b}(\mathbf{L}+\mathbf{L}_{\text{in}})^{\top}(\mathbf{L}+\mathbf{L}_{\text{in}})$, where $\widetilde{a}$ and $\widetilde{b}$ are scalars. This is equivalent to minimizing (6.1) with proper c_1 and c_2.

Energy constraints under scenario s, i.e., constraints on the cumulative demand of an individual load under realization s, are modelled with (6.3). These constraints prevent violation of the upper and lower bounds on the State-Of-Charge (SOC) of the PEV batteries. These bounds are calculated based on individual PEV's connection times and trip energy consumption under each scenario.

In this problem setup, $\mathbf{L}_s$ is the only global variable that couples the charging schedules of all PEVs in a fleet under realization s, hence, (6.2) plays an essential role in finding a distributed solution for this problem setup.

Equation (6.3) presents an abstract model for the energy limitation of PEV batteries. In order to derive this constraint, the following equation is used to determine the energy content of a PEV battery at a given time step:

$$E_{v,s}(t) = E_v(0) + \eta_v \Delta t \sum_{\tau=1}^{t} \mathbf{x}_{v,s}(\tau) - \sum_{\tau=1}^{t} E_{v,s}^{\text{cons}}(\tau), \tag{6.6}$$

where the initial energy content of the battery is given by $E_v(0)$ and the charging efficiency and time step duration are denoted by η_v and Δt, respectively. Finally, $E_{v,s}^{\text{cons}}(t)$ indicates the energy consumption at each time step t under scenario s.

The constraint on energy content is derived using the battery capacity C_v and the minimum state of charge $\underline{\text{SOC}}_v$ requirements as upper and lower bounds, which results in,

$$\underline{\text{SOC}}_v \leq \frac{E_{v,s}(t)}{C_v} \leq 1. \tag{6.7}$$

In order to derive the energy limitation constraint (6.3), the energy content of a PEV, which is presented by (6.6), is replaced in (6.7),

$$\underline{\text{SOC}}_v \times C_v \leq E_v(0) + \eta_v \Delta t \sum_{\tau=1}^{t} \mathbf{x}_{v,s}(\tau) - \sum_{\tau=1}^{t} E_{v,s}^{\text{cons}}(\tau) \leq C_v. \tag{6.8}$$

Note, (6.8) further implies the following two constraints. The lower limit,

$$\frac{1}{\eta_v \Delta t} \times \left(\underline{\text{SOC}}_v \times C_v - E_v(0) + \sum_{\tau=1}^{t} E_{v,s}^{\text{cons}}(\tau) \right) \leq \sum_{\tau=1}^{t} \mathbf{x}_{v,s}(\tau),$$

and the upper limit as follows,

$$\sum_{\tau=1}^{t} \mathbf{x}_{v,s}(\tau) \leq \frac{1}{\eta_v \Delta t} \times \left(C_v - E_v(0) + \sum_{\tau=1}^{t} E_{v,s}^{\text{cons}}(\tau) \right).$$

These two constraints could be presented using the following abstract equations,

$$A_1 \cdot \mathbf{x}_{v,s} \leq b_{v,s}^1$$

$$A_2 \cdot \mathbf{x}_{v,s} \leq b_{v,s}^2,$$

where A_1 and A_2 are lower triangular matrices with all elements being 1. These two equations could be merged into one equation as follows,

$$A \cdot \mathbf{x}_{v,s} \leq b_{v,s},$$

where $A = [A_1; A_2]$ and $b_v = [b_{v,s}^1; b_{v,s}^2]$.

The power constraints (6.4) define the upper and lower bounds on the charging power. In this chapter we merely consider uni-directional charging, hence, the lower bound on the charging power is set to zero ($\underline{x}_{v,s} = 0$). The upper bound $\overline{x}_{v,s}$ is zero during the time steps when the vehicle is not connected, while it is equal to the maximum charging rate of the charging infrastructure or the battery, $\overline{P}_v$, when the vehicle is connected, i.e.,

$$\overline{x}_{v,s}(t) = \begin{cases} \overline{P}_v, & cs_{v,s}(t) = 1 \\ 0, & cs_{v,s}(t) = 0. \end{cases}$$

Here, $cs_{v,s}(t)$ is a binary parameter describing the connection status at time step t under scenario s. Therefore, the timing of PEV trips affects the value of the upper bound. This binary parameter further means that a PEV can plug in and out several times during the optimization horizon. Here, we assumed that the maximum charge power of PEVs is independent of the state of charge.

Furthermore, (6.5) ensures consistency of optimal actions of PEV v across all scenarios at the first time step, which is essential for the implementation of the immediate action. Note we do not model the self discharge of batteries. Comparing with (2.1)-(2.3), $\mathfrak{G}$ is the compact from for (6.2) and (6.5), while (6.3) and (6.4) correspond to $\mathfrak{H}$.

In the PEV-CC problem setup (6.3) and (6.4) are local constraints, i.e., merely involve variables of an individual PEV, while (6.2) is considered as the global constraint, i.e., includes variables from all PEVs.

We propose a receding time horizon optimization framework and solve this optimization problem over a horizon of T time steps. In other words, in our problem, the PEVs optimize their schedules over the optimization horizon rather than optimizing for a single parking instance, but we merely implement the optimal action for the immediate time step. Then the configuration realizations $(b_{v,s}, \underline{x}_{v,s}, \overline{x}_{v,s})$ can be updated based on newly available information. Finally, the horizon is shifted by one time step and the optimization is carried out anew for this shifted horizon.

6.2.2 Optimality Conditions

The Lagrangian function for the aforementioned optimization problem is given by

$$\mathfrak{L} \;=\; \frac{1}{S}\sum_{s\in\mathcal{S}}\left(\mathbf{L_s}^{\top}\cdot c_1\cdot\mathbf{L_s}+c_2^{\top}\cdot\mathbf{L_s}\right)$$

$$
\begin{aligned}
&+\sum_{s\in\mathcal{S}}\lambda_s^{\top}\cdot\left(-\mathbf{L_s}+\sum_{v\in V}\mathbf{x}_{v,s}\right)+\sum_{v\in V}\sum_{s\in\mathcal{S}}\mu_{v,s}^{\top}\cdot\left(A\cdot\mathbf{x}_{v,s}-b_{v,s}\right)\\
&+\sum_{v\in V}\sum_{s\in\mathcal{S}}\mu_{v,s,-}^{\top}\cdot\left(\underline{x}_{v,s}-\mathbf{x}_{v,s}\right)+\mu_{v,s,+}^{\top}\cdot\left(\mathbf{x}_{v,s}-\overline{x}_{v,s}\right)\\
&+\sum_{v\in V}\sum_{s=2}^{S}\gamma_v(s-1)\cdot\left(\mathbf{x}_{v,1}(1)-\mathbf{x}_{v,s}(1)\right),
\end{aligned}
$$

where λ's, μ's and γ's are Lagrange multipliers. Note, $\gamma_v(s-1)$ denotes the $s-1$ element of the γ_v vector. Following the steps presented in Sect. 2.2, the corresponding first order optimality conditions are derived as follows:

$$\frac{\partial\mathfrak{L}}{\partial\mathbf{L_s}}=\frac{1}{S}\left(2c_1\cdot\mathbf{L_s}+c_2\right)-\lambda_s=0 \tag{6.9}$$

$$\frac{\partial\mathfrak{L}}{\partial\mathbf{x}_{v,s=1}}=\lambda_s+A^{\top}\cdot\mu_{v,s}+\left(\mu_{v,s,+}-\mu_{v,s,-}\right)+\sum_{s=2}^{S}\gamma_v(s)=0 \tag{6.10}$$

$$\frac{\partial\mathfrak{L}}{\partial\mathbf{x}_{v,s\neq1}}=\lambda_s+A^{\top}\cdot\mu_{v,s}+\left(\mu_{v,s,+}-\mu_{v,s,-}\right)-\gamma_v(s)=0 \tag{6.11}$$

$$\frac{\partial\mathfrak{L}}{\partial\lambda_s}=-\mathbf{L_s}+\sum_{v\in V}\mathbf{x}_{v,s}=0 \tag{6.12}$$

$$\frac{\partial\mathfrak{L}}{\partial\mu_{v,s}}=A\cdot\mathbf{x}_{v,s}-b_{v,s}\leq0 \tag{6.13}$$

$$\frac{\partial\mathfrak{L}}{\partial\mu_{v,s,+}}=\mathbf{x}_{v,s}-\overline{x}_{v,s}\leq0 \tag{6.14}$$

$$\frac{\partial\mathfrak{L}}{\partial\mu_{v,s,-}}=-\mathbf{x}_{v,s}+\underline{x}_{v,s}\leq0 \tag{6.15}$$

$$\frac{\partial\mathfrak{L}}{\partial\gamma_v}=\begin{bmatrix}\mathbf{x}_{v,1}(1)-\mathbf{x}_{v,2}(1)\\ \vdots\\ \mathbf{x}_{v,1}(1)-\mathbf{x}_{v,S}(1)\end{bmatrix}=0, \tag{6.16}$$

for all $v\in\{1,\ldots,V\}$ and $s\in\mathcal{S}$ plus the complementary slackness conditions for the

inequality constraints. In addition, we enforce positivity of the $\mu_{v,s}$, $\mu_{v,s,+}$, and $\mu_{v,s,-}$'s. In Sect. 6.4 we justify that any solution that fulfills the above system of equations yields an optimal solution for the PEV-CC problem.

6.3 Distributed Approach

The updates for the proposed $\mathcal{CI}-\mathcal{PEVCC}$ algorithm are derived following the *consensus+innovations* method presented in Sect. 2.3.2. In the $\mathcal{CI}-\mathcal{PEVCC}$, we assume that the inter-PEV communication graph is connected, i.e., there is a path (possibly multi-hop) between any pair of agents (charging stations) at each iteration. In our proposed approach, each agent v updates the variables $\mathbf{x}_{v,s}$, $\mathbf{L}_{v,s}$, and $\lambda_{v,s}$ which are directly associated with PEV v. Note, $\mathbf{L}_{v,s}$ and $\lambda_{v,s}$ are agent v's estimation of the global PEVs' load $\mathbf{L}_s$ and Lagrange multiplier λ_s under scenario s, respectively. Here, we denote the iteration counter by k.

The Lagrange multipliers $\lambda_{v,s}$ are updated according to

$$\lambda_{v,s}(k+1)=\mathbb{P}\left[\lambda_{v,s}(k)-\beta_k\left(\sum_{w\in\Omega_v}\left(\lambda_{v,s}(k)-\lambda_{w,s}(k)\right)\right)-\alpha_k\left(\frac{\mathbf{L}_{v,s}(k)}{V}-\mathbf{x}_{v,s}(k)\right)\right]_{[\frac{c_2}{S},\infty)}, \tag{6.17}$$

where α_k, $\beta_k>0$ are tuning parameters. Also, $\mathbb{P}$ is the projection operator that ensures $\lambda_{v,s}\geq c_2/S$. Note, in (6.9), $\mathbf{L}_s\geq 0$, consequently $\lambda_s\geq c_2/S$. Therefore, by using the projection operator we ensure that the local copies of λ satisfy this condition as well.

The first term preserves the coupling between the Lagrange multipliers of agents, while ensuring that the λ's are reaching the same value (*consensus*). The second term, referred to as *innovation*, reflects the accuracy of PEV v's estimation of the total load ($\mathbf{L}_s$) under scenario s. The update makes intuitive sense, e.g., if PEV v's consumption ($\mathbf{x}_{v,s}$) is exceeding its estimated share of overall consumption ($\mathbf{L}_{v,s}(k)/V$), then the innovation term results in an increase in the value of $\lambda_{v,s}(k+1)$. Consequently, using (6.18) to update $\mathbf{L}_{v,s}$,

PEV v's estimation of overall load ($\mathbf{L}_{v,s}$) increases in the next iteration.

Given the value of the Lagrange multiplier $\lambda_{v,s}$, PEV v updates its estimation of the total load ($\mathbf{L}_{v,s}$) using the following update:

$$\mathbf{L}_{v,s}(k+1) = \mathbf{L}_{v,s}(k) - \frac{S}{2c_1}\frac{\partial \mathfrak{L}}{\partial \mathbf{L}_{v,s}(k)} = \frac{S\lambda_{v,s}(k) - c_2}{2c_1}. \tag{6.18}$$

Also, our update structure assumes that all the agents (PEVs) have access to the cost function parameters, which is a reasonable assumption, since the electricity tariffs are generally predetermined (they need to be communicated once in advance and not in real-time).

Finally, a PEV updates the estimation of its charging schedule by following the procedure below. At first, the charging schedule is updated using the following update rule which also ensures the feasibility of updates with respect to (6.3) and (6.4):

$$\widetilde{\mathbf{x}}_{v,s}(k+1) = \mathbb{P}[\mathbf{x}_{v,s}(k) + \delta_k \left(\frac{\mathbf{L}_{v,s}(k)}{V} - \mathbf{x}_{v,s}(k)\right) - \eta_k \left(\lambda_{v,s}(k)\right)]_{\mathcal{F}} \tag{6.19}$$

with $\delta_k > 0$ and $\eta_k > 0$ being tuning parameters. Also, $\mathcal{F}$ the feasible space determined by individual PEV's constraints (see (6.3),(6.4)). Here $\widetilde{\mathbf{x}}_{v,s}$ is an intermediary variable and the projection operator in this case projects $\widetilde{\mathbf{x}}_{v,s}$ onto the feasible space $\mathcal{F}$. The first *innovation* term in (6.19) directs $\widetilde{\mathbf{x}}_{v,s}$ to move towards satisfying its share of global commitment, e.g., if $\mathbf{L}_{v,s}(k)/V < \mathbf{x}_{v,s}(k)$ then $\widetilde{\mathbf{x}}_{v,s}$ increases in the next iteration. Also, the second term in (6.19) makes intuitive sense because it reflects the sensitivity of the Lagrangian function ($\mathfrak{L}$) with respect to $\mathbf{x}_{v,s}$, i.e., $\partial\mathfrak{L}/\partial\mathbf{x}_{v,s}$. Here we neglect the terms related to $\mu_{v,s,+}$ and $\mu_{v,s,-}$ from $\partial\mathfrak{L}/\partial\mathbf{x}_{v,s}$ in the $\mathbf{x}_{v,s}$ update, since these multipliers do not appear in any other constraint and the projection operator ensures the feasibility of the achieved update.

Also we do not update the Lagrange multipliers associated with (6.3), since the projection operator in (6.19) guarantees the feasibility of $\widetilde{\mathbf{x}}_{v,s}$ with respect to individual agent's limitations. Therefore, the $\mathcal{CI} - \mathcal{PEVCC}$ update procedure yields feasible intermediate

iterates.

In the next step, the update rules to enforce the consistency constraint for the initial time step over scenarios of PEV v, i.e., $\mathbf{x}_{v,s}(1) = \mathbf{x}_{v,s'}(1) \quad \forall s, s' \in \mathcal{S}$ are defined.

- Let us denote $\widetilde{\mathcal{X}}_v$ as the collection of all $\widetilde{\mathbf{x}}_{v,s}$s associated with PEV v, i.e., $\widetilde{\mathcal{X}}_v = \begin{bmatrix} \widetilde{\mathbf{x}}_{v,1}, & \cdots & , \widetilde{\mathbf{x}}_{v,S} \end{bmatrix}^\top$
- Let us define $\mathcal{D}$ such that $\mathcal{D} \cdot \widetilde{\mathcal{X}}_v = 0$ satisfies the consistency constraint, i.e., $\widetilde{\mathbf{x}}_{v,s}(1) = \widetilde{\mathbf{x}}_{v,s'}(1) \quad \forall s, s' \in \mathcal{S}$. Note, implementing $\mathcal{D} \cdot \widetilde{\mathcal{X}}_v = 0$ is equivalent to enforcing the consistency constraint (6.5).

This new constraint is further equivalent to projecting $\widetilde{\mathcal{X}_v}$ to the null space of $\mathcal{D}$, i.e., $\mathbb{P}\left[\widetilde{\mathcal{X}_v}\right]_{\mathbb{N}(\mathcal{D})}$ where $\mathbb{N}(\mathcal{D})$ denotes the null space of matrix $\mathcal{D}$. This projection results in $\mathcal{X}_v$ which represents the collection of all $\mathbf{x}_{v,s}$s associated with PEV v, i.e., $\mathcal{X}_v = \begin{bmatrix} \mathbf{x}_{v,1}, & \cdots & , \mathbf{x}_{v,S} \end{bmatrix}^\top$. In our calculations we use the following closed form solution of the aforementioned projection [63],

$$\mathcal{X}_v = \mathbb{P}\left[\widetilde{\mathcal{X}_v}\right]_{\mathbb{N}(\mathcal{D})} = (I - \mathcal{D}^\top(\mathcal{D}\mathcal{D}^\top)^{-1}\mathcal{D})\widetilde{\mathcal{X}_v}. \tag{6.20}$$

The pseudo code for the $\mathcal{CI} - \mathcal{PEVCC}$ algorithm is presented in Table 6.1. The stopping condition can be defined based on some user-defined criterion, e.g., the measurement of *rel*. We have chosen this measure in order to analyze the performance of the algorithm but other stopping conditions can be defined such as the maximum change in the variables to be smaller than a certain threshold.

In this chapter, local agents, i.e., charging stations, receive driving information from PEVs and execute the update rules and data exchange. Given the definition of the updates, it is clear that the $\mathcal{CI} - \mathcal{PEVCC}$ only requires agents to exchange non-sensitive information ($\lambda_{v,s}$) during the course of the iterations. While agents perform computation and communication responsibilities in parallel, the intra-agent updates could be performed in parallel or sequential order. In the sequential implementation, the variables are updated in the

Table 6.1: Pseudo code for the $\mathcal{CI}-\mathcal{PEVCC}$ algorithm

```
Initialize tuning parameters
Initialize variables λ_{v,s}, L_{v,s}, x_{v,s}
    While convergence criteria is not satisfied
        for i=1:number of agents
            Update λ_{v,s} using (6.17)
            Update L_{v,s} using (6.18)
            Update x_{v,s} using (6.19) and (6.20)
            Communicate λ_{v,s} to neighboring agents
        end
        measure rel
    end
```

following order: $\lambda_{v,s}$, $\mathbf{L}_{v,s}$, and $\mathbf{x}_{v,s}$. The sequential implementation uses the most recent updated variables provided by previous update rules in the aforementioned order. For example, in this setup, (6.18) would be $\mathbf{L}_{v,s}(k+1) = (S\lambda_{v,s}(k+1) - c_2)/2c_1$. On the other hand, in the parallel implementation, each agent carries out all of the variable updates at the same time, hence, the update functions use all the values from the previous iteration. For example, $\mathbf{L}_{v,s}$ would be updated according to $\mathbf{L}_{v,s}(k+1) = (S\lambda_{v,s}(k) - c_2)/2c_1$. Therefore, the serial implementation improves convergence speed in terms of the number of iterations required but most likely increases the computation time per agent since the updates at the agents have to be performed in a sequential manner. The $\mathcal{CI}-\mathcal{PEVCC}$ is a fully distributed algorithm since each PEV is represented by one agent that performs computations and it merely requires each agent to communicate with neighboring agents.

Finally, our proposed update structure is designed such that any set of tuning parameters yields a feasible solution for individual PEVs at each iteration. However, tuning parameters influence the speed of reaching the optimal solution of the PEV-CC problem. In the Sect. 6.4, we analytically justify the optimality of our algorithm's achieved solution.

6.4 Convergence Analysis

While [64] discusses convergence properties of the general projected *consensus+innovation* approach in details, in this section we specifically justify convergence properties of the proposed $\mathcal{CI}-\mathcal{PEVCC}$ algorithm as described in Sect. 6.3. To this end, Lemma 1 justifies that the local copies of λ reach consensus or agreement asymptotically as $k \to \infty$. Then, subsection 6.4.1 presents the justification that any fixed point of the proposed iterative scheme satisfies the optimality conditions (6.9)–(6.16) of the PEV-CC problem. Finally, subsection 6.4.2 verifies the optimality of the achieved limit point.

Definition: Suppose that the updates of $\mathcal{CI}-\mathcal{PEVCC}$ algorithm at iteration k yield $X^*(k)$, then $X^*(k)$ is a fixed point of the $\mathcal{CI}-\mathcal{PEVCC}$ algorithm if

$$\forall \;\; k' \geq k \qquad X^*(k') = X^*(k).$$

Here X^* denotes the vector of stacked variables $(\mathbf{x}^\star_{v,s}, \mathbf{L}^\star_{v,s}, \lambda^\star_{v,s})$ for all agents $v = \{1, \ldots, V\}$ under all scenarios $s \in \mathcal{S}$.

Lemma 1: Let the tuning parameters follow the tuning criteria that is presented in Sect. 2.3.2. Then, the update structure $\mathcal{CI}-\mathcal{PEVCC}$ result in asymptotic consensus of the λ variables, i.e., $\lim_{k\to\infty} |\lambda_{v,s}(k) - \lambda_{w,s}(k)| = 0 \;\; \forall v, w \in \{1, \cdots, V\}, s \in \mathcal{S}$.

Reference [64] presents a formal proof that projected *consensus+innovations* update structures of the form presented in Sect. 2.3.2, (see (2.12)), achieve consensus under the stated assumptions on the tuning parameters (see Sect. 2.3.2).

6.4.1 Evaluation of PEV-CC's optimality conditions at the fixed point of $\mathcal{CI}-\mathcal{PEVCC}$ algorithm

Let X^* be a fixed point of the proposed $\mathcal{CI}-\mathcal{PEVCC}$ algorithm. Then, X^* fulfills all of the optimality conditions of the PEV-CC problem (6.9)–(6.16).

Justification: The justification is achieved by the series of individual claims developed below.

Claim 1: X^* fulfills the optimality conditions that correspond to the aggregation of PEVs load, i.e., (6.12).

Verification by contradiction: Let us assume, on the contrary, that the above claim does not hold, i.e., X^* does not fulfill (6.12) for all $s' \in \mathcal{S}$. Let us evaluate (6.17) for all $v \in \{1, \ldots, V\}$ under scenario s' at $X^\star$.

$$\lambda^\star_{v,s'} = \mathbb{P}\left[\lambda^\star_{v,s'} - \beta_k \left(\sum_{w \in \Omega_v} (\lambda^\star_{v,s'} - \lambda^\star_{w,s'})\right) - \alpha_k \left(\frac{\mathbf{L}^\star_{v,s'}}{V} - \mathbf{x}^\star_{v,s'}\right)\right]_{[\frac{c_2}{S}, \infty)} \tag{6.21}$$

Note, at the fixed point of the $\mathcal{CI} - \mathcal{PEVCC}$ algorithm the projection in (6.17) is redundant since X^* fulfills (6.17), hence, it lies within the feasible space $[\frac{c_2}{S}, \infty)$. Also, it follows by Lemma 1 that λ's are required to reach consensus at the fixed point, i.e., in particular, $\forall v \in \{1, \ldots, V\}$ and $s' \in \mathcal{S} \Rightarrow \lambda^\star_{v,s'} = \lambda^\star_{w,s'}, w \in \Omega_v$. Now let us refer to $\lambda^\star_{s'}$ as the achieved consensus value among all local copies of $\lambda^\star_{v,s'}$. This further implies local estimates of total load under scenario s' ($\mathbf{L}^\star_{v,s'}$) are also in agreement at the fixed point, denoted by $\mathbf{L}^\star_{s'}$. Now, lets define $\mathcal{H} \in \mathbb{R}^{(S\times T)\times(T\times S\times V)}$ as follows

$$\mathcal{H} = \frac{1}{V}[I \mid \cdots \mid I],$$

where $I \in \mathbb{R}^{(S\times T)\times(T\times S)}$ is the identity matrix. Multiplying (6.21) by $\mathcal{H}$ would yield

$$\lambda^\star_{s'} = \lambda^\star_{s'} - \alpha_k \frac{\mathcal{H}}{V}\left(\frac{\mathbf{L}^\star_{v,s'}}{V} - \mathbf{x}^\star_{v,s'}\right).$$

In the above, we used the fact that, since $\lambda^{\star}_{v,s'} = \lambda^{\star}_{s'}$, their average is also equal to $\lambda^{\star}_{s'}$. The above equation could be further simplified to

$$\lambda^{\star}_{s'} = \lambda^{\star}_{s'} - \frac{\alpha_k}{V}\left(\mathbf{L}^{\star}_{s'} - \sum_{v=1}^{V} \mathbf{x}^{\star}_{v,s'}\right).$$

Since we assumed that $X^{\star}$ does not fulfill (6.12) for some $s' \in \mathcal{S}$, the innovation term in the above equation is non-zero. Therefore the above equation does not hold. This clearly contradicts the fact that X^{*} is the fixed point of (6.17).

Claim 2: X^{*} satisfies the optimality conditions that correspond to the coupling between λ_s and $\mathbf{L}_s$, i.e., (6.9).

Verification by contradiction: Let us assume, on the contrary, that X^{*} does not fulfill (6.9) for some s, i.e., there exists s such that the value of (6.9) is non-zero when evaluated at X^{*}. Clearly this would lead to

$$\mathbf{L}^{\star}_{s} \neq \frac{S\lambda^{\star}_{s} - c_2}{2c_1},$$

thus contradicting with our original assumption that X^{*} is the fixed point of (6.18). Here, $\mathbf{L}^{\star}_{s}$ and $\lambda^{\star}_{s}$ are the achieved consensus values (see Claim 1 and Lemma 1).

Claim 3: $X^{\star}$ fulfills the optimality conditions associated with the energy constraints for each PEV under each scenario, i.e., (6.13).

Verification by contradiction: Let us assume on the contrary, that there exists a scenario s' under which the $\mathbf{x}^{\star}_{v,s'}$ does not fulfill (6.13). Now, note that, plugging in $\mathbf{x}^{\star}_{v,s'}$ in (6.19) would then yield a value different from $\mathbf{x}^{\star}_{v,s'}$, since the projection operator enforces the charging schedule updates to satisfy the energy constraint, i.e., $A \cdot \mathbf{x}_{v,s'} \leq b_{v,s'}$. This, in turn, contradicts the fact that X^{*} is a fixed point of (6.19).

A similar argument establishes that X^{*} satisfies (6.14)-(6.16).

Claim 4: $X^{\star}$ satisfies the optimality conditions (6.10) and (6.11).

Justification: Given our problem setup, the optimal values for Lagrange multipliers $\mu, \mu_+, \mu_-, \gamma$ are not unique. Also, since Lagrange multipliers only appear in (6.10) and (6.11), we can find various combinations of these multipliers that satisfy (6.10) and (6.11) while fulfilling complementary slackness conditions. In other words, for any $\lambda^\star_{v,s}$ there exists a set of Lagrange multipliers $\mu_{v,s}, \mu_{v,s+}, \mu_{v,s,-}, \gamma_v$ such that (6.10) and (6.11) are satisfied. Given that $\mathcal{CI} - \mathcal{PEVCC}$ consists of continuous transformations of the iterates, if $\mathcal{CI} - \mathcal{PEVCC}$ converges, the achieved limit point is necessarily a fixed point of the iterative mapping. Hence, this subsection justifies that any limit point of the $\mathcal{CI} - \mathcal{PEVCC}$ fulfills the first order optimality conditions, (6.9)–(6.16), of the PEV-CC problem. Moreover, the following subsection 6.4.2 discusses the optimality of limit points of our proposed $\mathcal{CI} - \mathcal{PEVCC}$ algorithm.

6.4.2 Optimality of the $\mathcal{CI} - \mathcal{PEVCC}$ algorithm's fixed point

Let the PEV-CC problem (6.1)-(6.5) have a feasible solution, and, further, assume that the proposed $\mathcal{CI} - \mathcal{PEVCC}$ algorithm converges to a point $X^\star$. Then X^* is the optimal solution of the PEV-CC problem (6.1)-(6.5).

Justification: Based on subsection 6.4.1, $X^\star$ satisfies the optimality conditions (6.9)–(6.16). Since the PEV-CC is a convex problem, the primal variables $(\mathbf{x}^\star_{v,s}, \mathbf{L}^\star_{v,s})$ in X^* constitutes an optimal solution to the PEV-CC problem (6.1)-(6.5).

All in all, subsection 6.4.1 and 6.4.2 guarantee that any fixed point of the proposed $\mathcal{CI} - \mathcal{PEVCC}$ constitutes an optimal solution to the PEV-CC problem. In other words, if the $\mathcal{CI} - \mathcal{PEVCC}$ reaches convergence, the limit point is necessarily an optimal solution of the PEV-CC problem.

6.5 Simulation Results

In this section, we provide a proof of concept by carrying out simulations.

6.5.1 Test System Set up

We consider a fleet of vehicles for the simulations and each PEV has the following characteristics: maximum charging power 3.5 kW, charging efficiency 0.9, minimum state of charge 0.2, and battery size of either 16kWh or 24kWh. Note, the average travel distance of the fleet is 35km. Individual driving pattern information is obtained from a transport simulation for Switzerland with the tool MATSim [65]. The deterministic driving behaviors obtained form MATsim software includes arrival time, departure time and energy consumption of each trip for each PEV. This input data translates to a deterministic reference sample based on which stochastic samples for modeling driving behavior of PEVs are generated (see [66] for more detail). The parameter $b_{v,s}$ is obtained from these patterns, hence, $b_{v,s}$ represents the driving pattern, e.g., trip specifications, arrival and departure times, of PEV v. Also, the load profile used in the simulation represents a typical winter load in the city of Zurich. Note that this original load profile is scaled so that the total PEV charging consumption load constitutes 10% of total demand. The optimization time horizon is one day, divided into 15 minutes time intervals, hence, $\mathbf{x}_{v,s} \in \mathbb{R}^{96\times 1}$. In this vector $\mathbf{x}^1_{v,s}$ represents the charging of PEV v under scenario s at the end of the first time interval (15 minutes). Moreover, Fig. 6.2 illustrates c_2, i.e., the cost function parameter, over the time horizon. Also, the communication graph is considered to be a line graph. In a line graph, each agent except the first and last agent, exchanges information with two neighboring agents (see Fig. 6.1). The tuning parameters are set to the values given in Table 6.2. The tuning parameters follow the below format:

$$\text{Tuning Parameter} = \frac{\nabla}{k^{\mathcal{O}}},$$

where k is the iteration counter and ∇, $\mathcal{O}$ are positive constants. The above format follows the tuning criteria that is introduced in Sect. 2.3.2. We use cold start for the simulations, i.e., all variables are set to zero at the start of the simulation. Note, for an actual implementation, reasonable initial settings for all of these variables could be the optimal values computed for the previous time step. The computer simulations are carried out using MATLAB on a PC with a Core i-7 processor (2.7 GHz) and 8 GB RAM.

Table 6.2: Tuning Parameter Values

Parameter	∇	$\mathcal{O}$
α	6.384	0.2457
β	0.500	0.001
η	0.75	0.3
δ	0.135	0.2

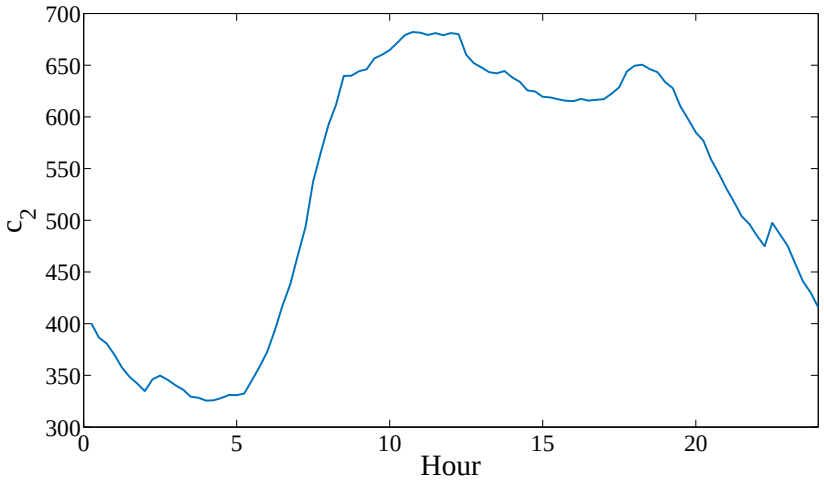

Figure 6.2: Cost function parameter c_2 over 24 hours horizon.

6.5.2 Convergence Measurements

Here we introduce two convergence measures to evaluate the performance of our $\mathcal{CI}-\mathcal{PEVCC}$ approach. The first measure is similar to the one introduced in chapter 3 and calculates

the relative distance of the objective function from the optimal value over the iterations,

$$rel = \frac{|f - f^*|}{f^*}, \tag{6.22}$$

where f^* is the optimal objective function value obtained from solving the centralized PEV-CC problem. The value of f^* is obtained from solving the centralized problem in the MATLAB environment using the optimization package Tomlab.

The second measure is based on the difference between consecutive $\mathbf{x}_{v,s}$s over the course of iterations, which is defined as

$$\mathrm{X}_v^{\mathrm{diff}}(k-1) = \max_{\mathrm{s}} \frac{|\mathbf{x}_{v,s}(k) - \mathbf{x}_{v,s}(k-1)|}{\overline{P}_v}. \tag{6.23}$$

Here, $\overline{P}_v$ is the maximum charging rate of PEV v. Note, this convergence measure could be implemented in a distributed fashion since it merely involves local information. To be more specific, if the absolute value of change in $\mathrm{X}_v^{\mathrm{diff}}$ for agent v stays less than a threshold after a predefined number of iterations, agent v stops updating its associated variables.

6.5.3 Case Study 1: Multi-Step Optimization

Here we first present simulation results for the $\mathcal{CI} - \mathcal{PEVCC}$ algorithm with deterministic modeling of the driving behaviors which is equivalent to having just one scenario. The $\mathcal{CI} - \mathcal{PEVCC}$'s resulting load profile for a fleet of 20 PEVs is illustrated in Fig. 6.3. Based on this figure, most of the charging load is scheduled during the low-load hours of the night which contributes to valley-filling. Moreover, charging partially takes place during the shoulder hours, i.e., the hours between the daily peaks. This indicates that in these hours demand is not flexible enough to be shifted completely to the valley hours. Note, the resulting load profile matches the c_2 trend over the time horizon.

Figs. 6.4 and 6.5 illustrate the two convergence measures rel and $\mathrm{X}_v^{\mathrm{diff}}$ over the course

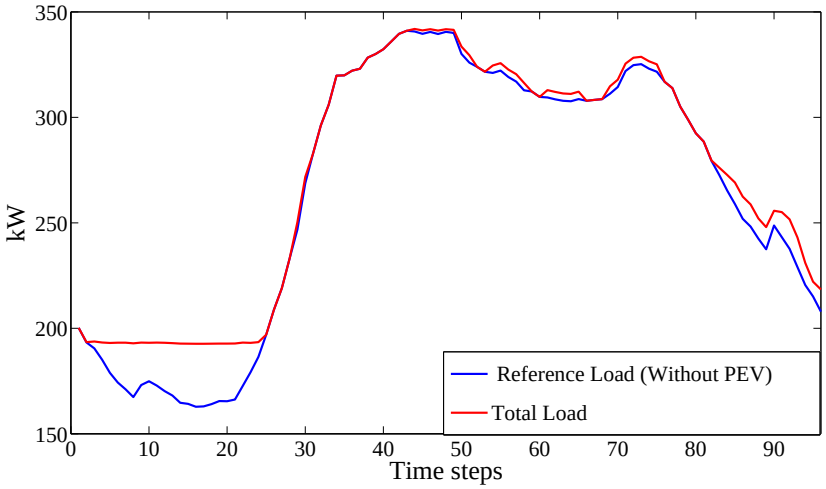

Figure 6.3: Total load profiles for the full 24 hours horizon (15 minutes time steps), $V = 20$.

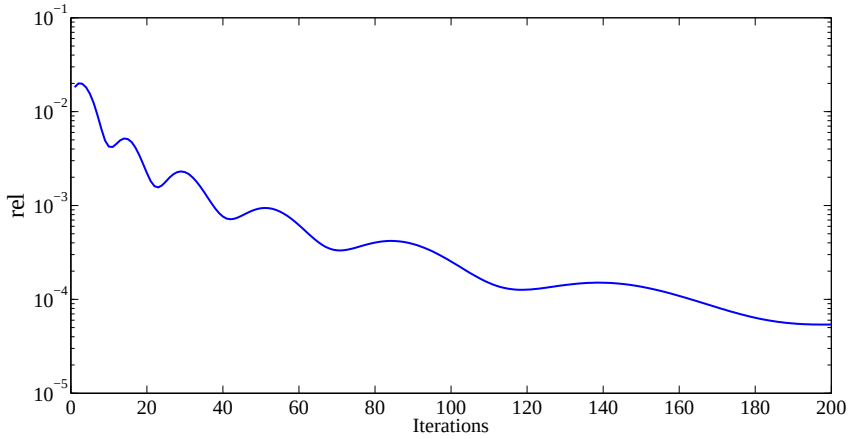

Figure 6.4: Relative distance from optimal objective function (rel), $V = 20$.

of the iterations with the value being 5.40e-005 and 0.0011 (maximum value among all vehicles) after 200 iterations, respectively. The oscillations could be prevented by reducing some of the tuning parameters, although this might result in a larger number of iterations until convergence.

Note, the fleet's daily total load stays the same during the course of the iterations. This is because each PEV's required daily energy is known and is in fact part of the constraint specification that needs to be provided. As $\mathcal{CI} - \mathcal{PEVCC}$ is defined such that it yields a feasible solution at every iteration, the overall energy is equal to the total required energy

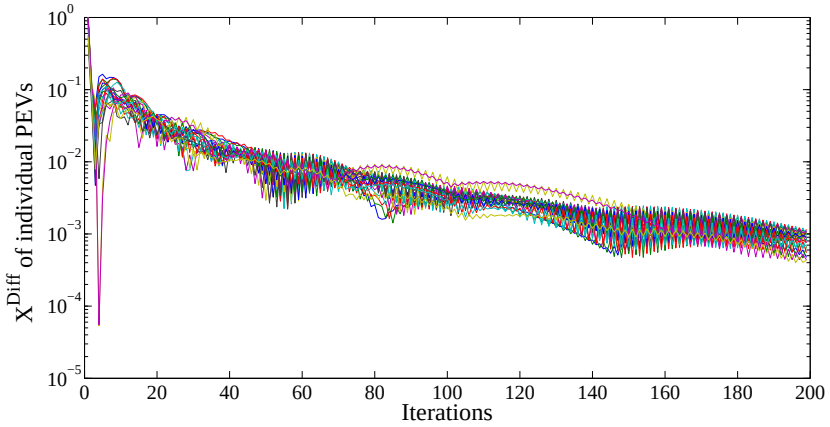

Figure 6.5: Difference between consecutive charging schedules (X^{diff}) for individual PEV, $V = 20$.

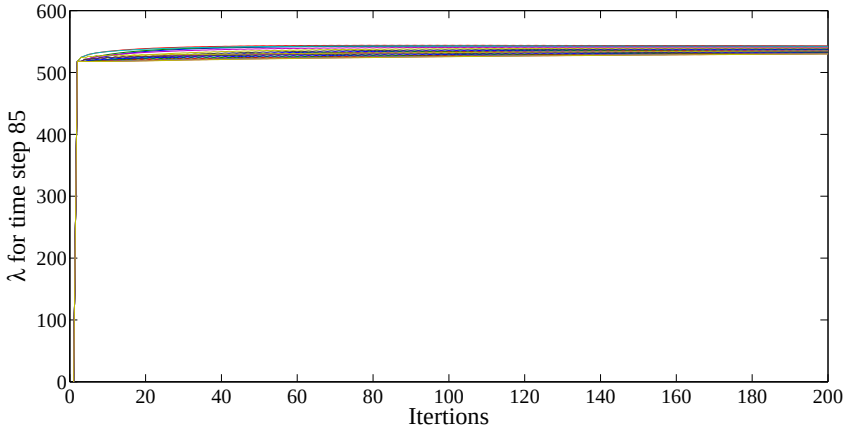

Figure 6.6: Evolution of the consensus variable for time step 85 during the iterations (λ_v^{85}), $V = 20$.

at all iterations. Finally, Fig. 6.6 depicts agents' values for the consensus on λ for a sample time (time step 85). Based on the figure, the λ_v's are reaching consensus as the algorithm converges towards the optimal solution. Similar behavior can be observed for the other time steps.

Each iteration of $\mathcal{CI} - \mathcal{PEVCC}$ is computationally inexpensive since it only requires the evaluation of algebraic functions, namely (6.17)-(6.20), which could be executed in parallel. It is important to mention once more that the depicted intermediate values constitute a feasible solution for the PEV-CC problem fulfilling the total load constraint but also the

individual constraints on the charging schedules and energy levels.

Furthermore, Figs. 6.7 and 6.8 present the $\mathcal{CI}-\mathcal{PEVCC}$'s resulting convergence measures *rel* and $\mathrm{X}^{\mathrm{diff}}$ over the iterations for a fleet of 100 PEVs. We used the tuning parameters that are given in in Table 6.2. This indicates that a set of tuning parameters could potentially function properly for different fleet sizes, hence, allowing for dynamic adjustment of the fleet size without having to readjust the parameters.

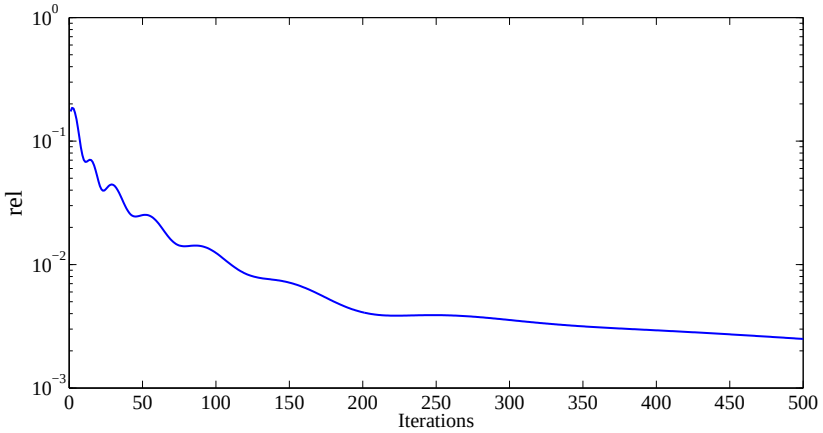

Figure 6.7: Relative distance from optimal objective function (*rel*), $V = 100$.

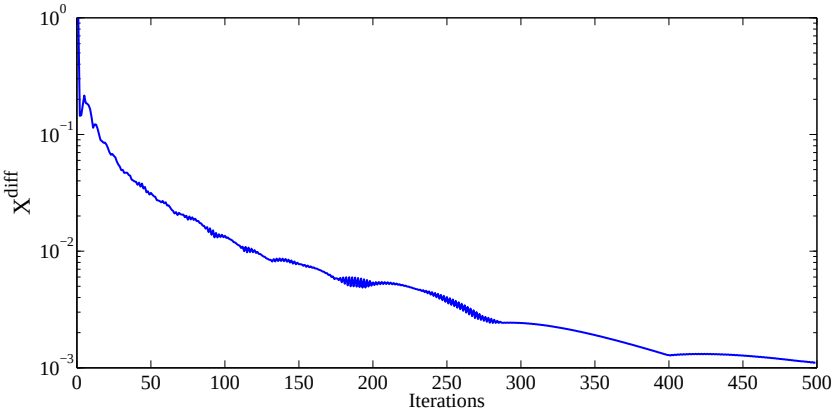

Figure 6.8: Difference between consecutive charging schedules ($\mathrm{X}^{\mathrm{diff}}$) maximum value for the fleet, $V = 100$.

As it was mentioned, the connectivity of the communication graph is the only requirement for the proper functioning, achieving the optimal solution of the original PEV-CC

problem, of our proposed algorithm. Figure 6.9 compares the *rel* for the two communication topologies, i.e, path (line) communication structure and fully connected communication graph. Based on this figure, fully connected communication graph leads to increased speed of information spread which further improves convergence speed of $\mathcal{CI} - \mathcal{PEVCC}$.

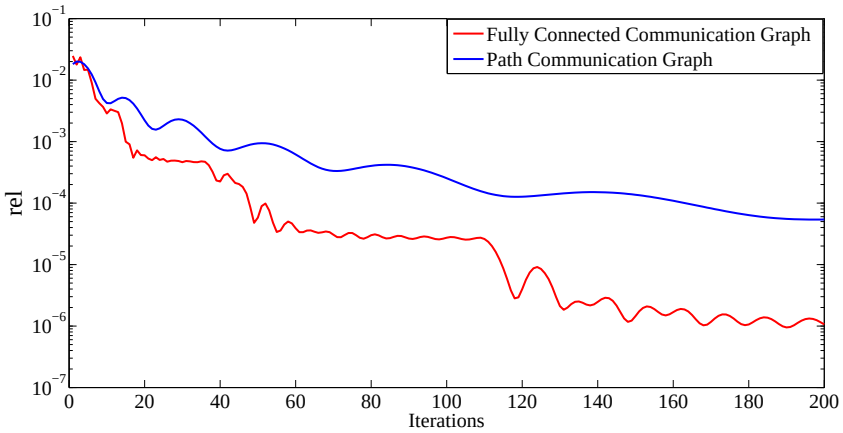

Figure 6.9: Relative distance from optimal objective function for two communication structures, i.e., path communication structure and fully connected communication graph, $V = 20$.

6.5.4 Case Study 2: Receding Horizon Multi-Step Optimization

Here, we analyze the performance of the receding horizon version of $\mathcal{CI} - \mathcal{PEVCC}$ using 5 scenarios to model different realizations of a fleet of 20 PEVs. Fig. 6.10 shows the resulting aggregated load at the first time step of the 24 hour horizon. Note, the load at the first step is therefore the same in all samples because (6.5) is enforced. Also, Figs. 6.11 and 6.12 depict the two convergence measures for this setup.

The average combined CPU time for all agents per iteration is 0.009 seconds. By assigning the computational load to distributed agents in real-world applications, the computations could be executed in parallel at each iteration.

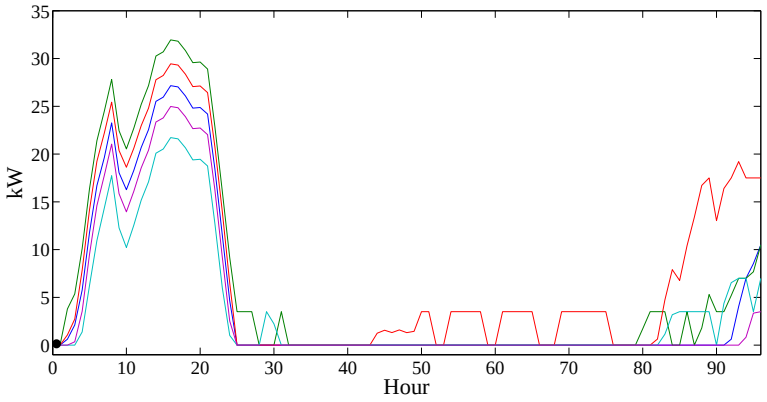

Figure 6.10: PEVs aggregated load under five scenarios for the first horizon, $V = 20$ and $S = 5$.

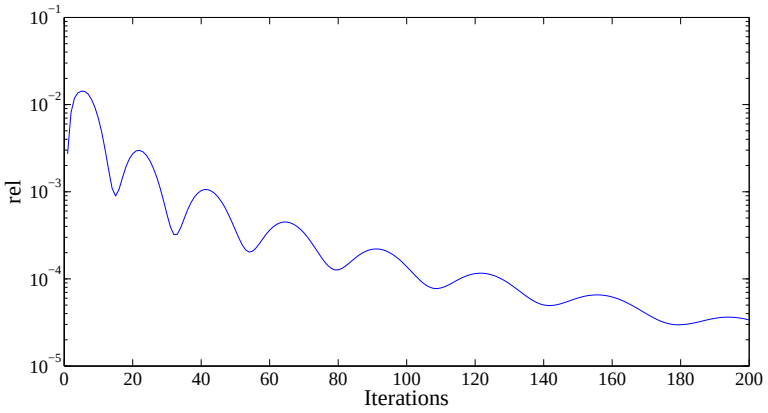

Figure 6.11: Relative distance from optimal objective function (rel_{obj}) for the first horizon, $V = 20$ and $S = 5$.

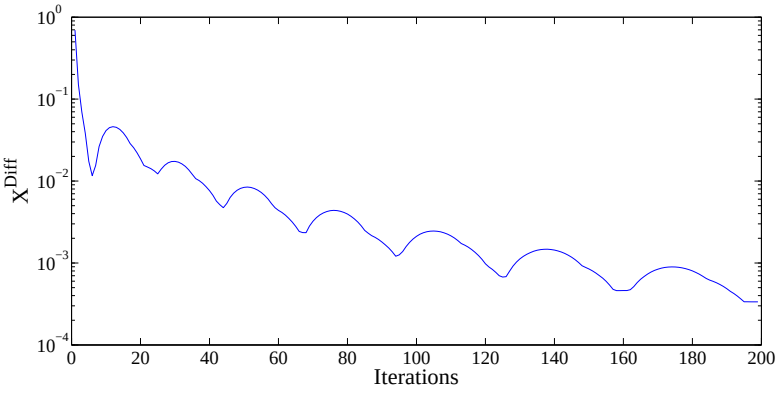

Figure 6.12: Difference between consecutive charging schedules (X^{diff}) maximum value for the first horizon of the fleet, $V = 20$ and $S = 5$.

6.6 Summary

In this chapter, we have proposed a fully distributed *consensus+innovations*-based approach to solve the PEVs' cooperative charging problem which searches for the charging schedules that minimize the cost to supply the demand while fulfilling each PEV's constraints. This algorithm is based on a receding horizon approach and allows for a fully distributed implementation down to the agent (PEV) level without the need for a central coordinator. As the main feature, the proposed algorithm yields a feasible solution at each iteration thereby enabling an implementation of an intermediate solution at the cost of a suboptimal solution. Moreover, our solution approach accounts for uncertain driving behavior of individual PEVs by considering various scenarios for PEVs' driving pattern. Each PEV is responsible for updating/evaluating simple functions over the course of the iterations while information exchange is limited to communicating Lagrange multipliers, which determines the value of consumption from each PEV's point of view, with neighboring agents. In particular, there is no need to share sensitive information such as driving patterns. Also, the communication graph could be defined arbitrarily as long as it is connected. Moreover, the proposed distributed algorithm could easily capture individual cost functions for the PEVs, e.g., battery degradation costs and drivers utility as a function of battery's SOC. The algorithm has been tested on a fleet of PEVs showing that our proposed model converges to the overall optimal solution. Finally, note that investigating the stability of our proposed receding horizon framework is out of the scope of this research, but it is an interesting future research direction.

Chapter 7

Conclusion and Future Work

The electric power grid is evolving to increased levels of distributed generation, distributed storage, and demand response leading to new challenges in operating the grid. At the same time, increased electronics and sensing technologies are being deployed that provide the means to overcome some of these challenges. The key is to design the monitoring and control structure in a way that is suitable to a distributed physical infrastructure and takes advantage of locally available information. In this thesis, we have presented distributed approaches to monitoring and control problems in the smart grid. The solutions presented exhibit a *consensus+innovations* type structure for solving a class of cooperative energy management problem in future smart grids in a distributed manner. Our proposed iterative scheme finds a distributed solution for first order optimality conditions of the underlaying optimization problem. At each iteration, the algorithm combines two terms: (1) the *consensus* term that mixes as a weighted sum the information received from (a few) other agents areas; and (2) the *innovation* term that incorporates the gradient information.

In this thesis, we have discussed applications of our proposed distributed approach for solving energy management problems in the transmission grid as well as the distribution network. In the transmission grid, we proposed distributed solution for optimal dispatch problems including optimal power flow, security constrained optimal power flow, and power

flow control. Our proposed approach to solve these optimal power dispatch problems is based on obtaining a solution to the first order optimality conditions of the corresponding optimization problem in a fully distributed fashion. Specifically, these conditions include the power balance equations as well as constraints which constitute a coupling of the Lagrange multipliers associated with the power flow equations and line constraints at neighboring entities and lines. Each entity evaluates the local equations using the current values for the variables and then uses linear combinations of the evaluated equations to update the local variables. The result is a computationally very inexpensive algorithm to solve the optimal power dispatch problems. Moreover, we have presented a more realistic version of our distributed algorithm by clustering the buses into areas and then allowing intra and inter-area communications. Intra-area communication refers to the information exchange between the buses in the same area which happens after each variable update iteration, while inter-area information exchange takes place between neighboring areas only every few iterations. The clustering also decreases the communication overhead, hence, handling the communication delay challenge. Furthermore, in our work, we propose different communication topologies for implementing our proposed distributed iterative algorithms. Commonly distributed iterative methods include exchange of information with only physically connected neighbors. Specifically, the algorithms in this thesis enable the possibility to incorporate additional communication through information exchange between system buses that are not physically connected, in order to enhance the convergence rate.

With regards to the distribution side of the future grid we have solved cooperative charging of plug-in electric vehicles (PEV)s. Specifically, we proposed a fully distributed approach to determine charging schedules for a fleet of PEVs such that the cost to supply demand is minimized while each PEVs constraints are fulfilled. This algorithm is based on a receding horizon approach and allows for a fully distributed implementation down to the agent (PEV) level without the need for a central coordinator. As the main feature,

the proposed algorithm yields a feasible solution at each iteration thereby enabling an implementation of an intermediate solution at the cost of a suboptimal solution. Each agent has to update/evaluate simple functions over the course of iterations while information exchange is restricted to communicating a Lagrange multiplier, i.e., a price signal, with neighboring agents. In particular, there is no need to share information about driving patterns or charging schedules.

There are multiple directions in which the work presented in this thesis could be extended. We can point to various extensions of our proposed solution for solving energy management problems at the transmission level of the future grid. The first goal would be to develop methods for solving the non-convex DC security constrained optimal power flow problem including power flow control devices in a distributed manner. The mathematical representation of the DC security constrained optimal power flow, with the added modeling of FACTS devices, is a nonlinear program (NLP). In this regards, [67] proposed a method to convert this NLP into a mixed-integer linear program (MILP) and then reformulated the obtained MILP as a two-stage linear program, which enforces the same sign for the voltage angle differences for the lines equipped with FACTS. Using the method presented in [67], our proposed distributed solution can be generalized to solve the security constrained optimal power flow including power flow control devices with guaranteed convergence performance. In addition, given the ever increasing investments in clean energy and incentives for leveraging flexibility of end users' consumption, accounting for intermittency of renewable generation resources and demand response flexibility in transmission level energy management problems, e.g., OPF and SCOPF, is essential. Therefore, the second goal would be to extend our proposed framework to find a distributed solution for optimal dispatch problems while taking into account operational uncertainties of renewable generation and demand response resources. Moreover, investigating the impacts of noise and communication error on the performance of our proposed algorithms is worth

to pursue. Also, given the communication topology's role in convergence of our proposed methods, deriving an analytical relation between convergence rate and connectivity of the communication graph is a possible future research direction. Along this line and to speed up the convergence of our proposed iterative schemes, the idea of adjusting tuning parameters for each agent (a single bus or a collection of buses) over iterations can be also explored. Furthermore, our distributed updates for OPF and SCOPF problems can be extended to account for transmission system's loss.

Finally, the idea of reshaping residential energy use by utilizing distributed energy resources recently has received tremendous attention, e.g., Tesla announced producing a stationary battery for home owners recently. Also, as the number of distributed controllable resources in the distribution grid are increasing, the potential advantages of coordinated control of these resources is the driving force behind collaboration of significant market players. For example, SolarCity, i.e., the nations largest residential solar installer, is partnering with Googles Nest to integrate smart thermostats with rooftop solar, and uses PVs excess of energy for pre-cooling and pre-heating. In this regard, distributed energy management methods are essentially the glue to tie distributed resources together. These resources may include distributed generations, e.g., solar photovoltaic, distributed storages, e.g., batteries, and distributed manageable loads, e.g., residential thermal loads. In fact, the intelligent control of the distributed resources, enhances the flexibility in the grid, hence, results in electricity cost reduction.

Therefore, an extremely valuable future direction for this research would be to apply our proposed distributed method to control distributed assets in an active distribution grid. An active distribution grid is composed of autonomous elements which should collaborate with each other in order to operate the entire distribution grid in a secure and economic manner. In this thesis, we have developed an extension of the algorithm to solve PEVs' coordination problem (see chapter 6) which could potentially serve as a starting point moving forward

to enable our solution to practically control stationary batteries, manageable thermal load, and distributed generations.

Appendix

14-bus Line Parameters

The system layout and line reactances for the 14-bus test system are shown in the following table. The reactance values are given in per-unit (p.u.). The parameters were obtained from MATPOWER [68].

Table 1: Line parameters for the 14-bus system.

Line	From	To	Resistance (R)	Reactance (X)	Shunt Susceptance (B)	Turns Ratio
1	1	2	0.01938	0.05917	0.0528	1.0
2	1	5	0.05403	0.22304	0.0492	1.0
3	2	3	0.04699	0.19797	0.0438	1.0
4	2	4	0.05811	0.17632	0.034	1.0
5	2	5	0.05695	0.17388	0.0346	1.0
6	3	4	0.06701	0.17103	0.0128	1.0
7	4	5	0.01335	0.04211	0.0	1.0
8	4	7	0.0	0.20912	0.0	0.978
9	4	9	0.0	0.55618	0.0	0.969
10	5	6	0.0	0.25202	0.0	0.932
11	6	11	0.09498	0.1989	0.0	1.0
12	6	12	0.12291	0.25581	0.0	1.0
13	6	13	0.06615	0.13027	0.0	1.0

Line	From	To	Resistance (R)	Reactance (X)	Shunt Susceptance (B)	Turns Ratio
14	7	8	0.0	0.17615	0.0	1.0
15	7	9	0.0	0.11001	0.0	1.0
16	9	10	0.03181	0.0845	0.0	1.0
17	9	14	0.12711	0.27038	0.0	1.0
18	10	11	0.08205	0.19207	0.0	1.0
19	12	13	0.22092	0.19988	0.0	0.970
20	13	14	0.17093	0.34802	0.0	0.978

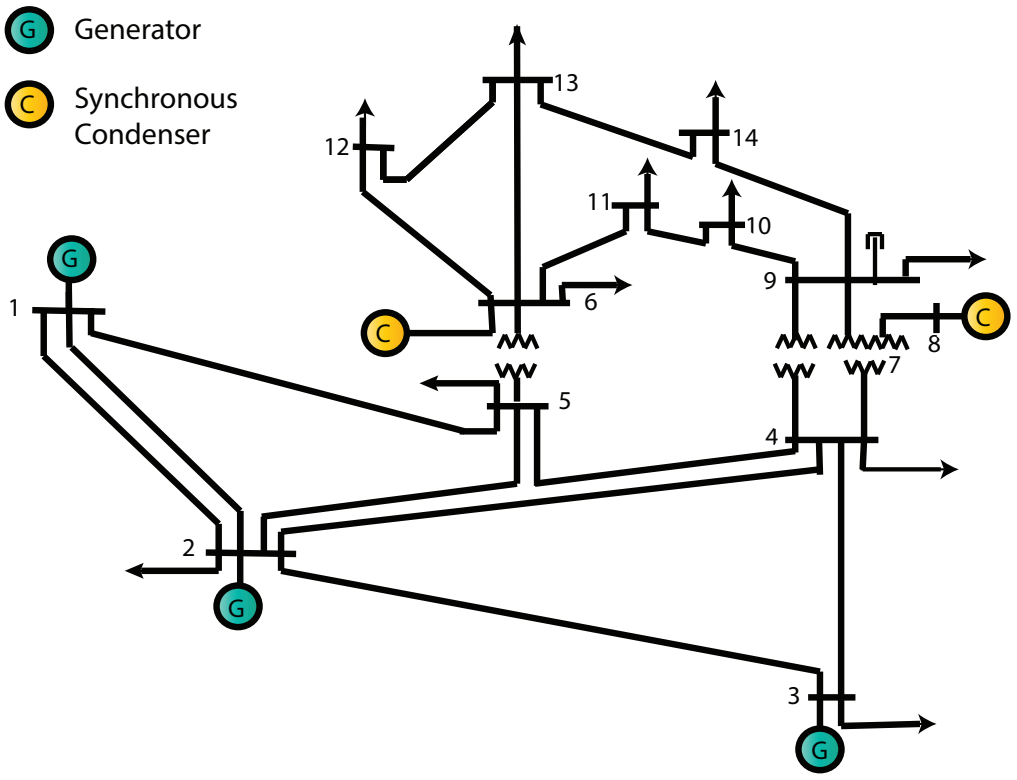

Figure 1: IEEE 14-bus System

57-bus Line Parameters

The values for the resistance, reactance, shunt susceptance, and transformer turns ratio for each branch in the IEEE 57-bus test system are given in p.u. in the below table [68].

Table 2: Line parameters for the 57-bus system.

Line	From	To	Resistance (R)	Reactance (X)	Shunt Susceptance (B)	Turns Ratio
1	1	2	0.0083	0.0280	0.1290	1.0
2	2	3	0.0298	0.0850	0.8180	1.0
3	3	4	0.0112	0.0366	0.0380	1.0
4	4	5	0.0625	0.1320	0.0258	1.0
5	5	6	0.0430	0.1480	0.0348	1.0
6	6	7	0.0200	0.1020	0.0276	1.0
7	7	8	0.0339	0.1730	0.0470	1.0
8	8	9	0.0099	0.0505	0.0548	1.0
9	9	10	0.0368	0.1679	0.0440	1.0
10	9	11	0.0258	0.0848	0.0218	1.0
11	9	12	0.0648	0.2950	0.0772	1.0
12	9	13	0.0481	0.1580	0.0406	1.0
13	13	14	0.0132	0.0434	0.0110	1.0
14	13	15	0.0269	0.0869	0.0230	1.0
15	1	15	0.0178	0.0910	0.0988	1.0
16	1	16	0.0454	0.2060	0.0546	1.0
17	1	17	0.0238	0.1080	0.0286	1.0
18	3	15	0.0162	0.0530	0.0544	1.0
19	4	18	0.0	0.5550	0.0	0.970
20	4	18	0.0	0.4300	0.0	0.978
21	5	6	0.0302	0.0641	0.0124	1.0
22	7	8	0.0139	0.0712	0.0194	1.0
23	10	12	0.0277	0.1262	0.0328	1.0
24	11	13	0.0223	0.0732	0.0188	1.0
25	12	13	0.0178	0.0580	0.0604	1.0

Line	From	To	Resistance (R)	Reactance (X)	Shunt Susceptance (B)	Turns Ratio
26	12	16	0.0180	0.0813	0.0216	1.0
27	12	17	0.0397	0.1790	0.0476	1.0
28	14	15	0.0171	0.0547	0.0148	1.0
29	18	19	0.4610	0.6850	0.0	1.0
30	19	20	0.2830	0.4340	0.0	1.0
31	21	20	0.0	0.7767	0.0	1.0430
32	21	22	0.0736	0.1170	0.0	1.0
33	22	23	0.0099	0.0152	0.0	1.0
34	23	24	0.1660	0.2560	0.0084	1.0
35	24	25	0.0	1.1820	0.0	1.0
36	24	25	0.0	1.2300	0.0	1.0
37	24	26	0.0	0.0473	0.0	1.0430
38	26	27	0.1650	0.2540	0.0	1.0
39	27	28	0.0618	0.0954	0.0	1.0
40	28	29	0.0418	0.0587	0.0	1.0
41	7	29	0.0	0.0648	0.0	0.9670
42	25	30	0.1350	0.2020	0.0	1.0
43	30	31	0.3260	0.4970	0.0	1.0
44	31	32	0.5070	0.7550	0.0	1.0
45	32	33	0.0392	0.0360	0.0	1.0
46	34	32	0.0	0.9530	0.0	0.9750
47	34	35	0.0520	0.0780	0.0032	1.0
48	35	36	0.0430	0.0537	0.0016	1.0
49	36	37	0.0290	0.0366	0.0	1.0
50	37	38	0.0651	0.1009	0.0020	1.0
51	37	39	0.0239	0.0379	0.0	1.0

Line	From	To	Resistance (R)	Reactance (X)	Shunt Susceptance (B)	Turns Ratio
52	36	40	0.0300	0.0466	0.0	1.0
53	22	38	0.0192	0.0295	0.0	1.0
54	11	41	0.0	0.7490	0.0	0.9550
55	41	42	0.2070	0.3520	0.0	1.0
56	41	43	0.0	0.4120	0.0	1.0
57	38	44	0.0289	0.0585	0.0020	1.0
58	15	45	0.0	0.1042	0.0	0.9550
59	14	46	0.0	0.0735	0.0	0.9000
60	46	47	0.0230	0.0680	0.0032	1.0
61	47	48	0.0182	0.2033	0.0	1.0
62	48	49	0.0834	0.1290	0.0048	1.0
63	49	50	0.0801	0.1280	0.0	1.0
64	50	51	0.1386	0.2200	0.0	1.0
65	10	51	0.0	0.0712	0.0	0.9300
66	13	49	0.0	0.1910	0.0	0.8950
67	29	52	0.1442	0.1870	0.0	1.0
68	52	53	0.0762	0.0984	0.0	1.0
69	53	54	0.1878	0.2320	0.0	1.0
70	54	55	0.1732	0.2265	0.0	1.0
71	11	43	0.0	0.1530	0.0	0.9580
72	44	45	0.0624	0.1242	0.0040	1.0
73	40	56	0.0	1.1950	0.0	0.9580
74	56	41	0.5530	0.5490	0.0	1.0
75	56	42	0.2125	0.3540	0.0	1.0
76	39	57	0.0	1.3550	0.0	0.9800
77	57	56	0.1740	0.2600	0.0	1.0

Line	From	To	Resistance (R)	Reactance (X)	Shunt Susceptance (B)	Turns Ratio
78	38	49	0.1150	0.1770	0.0030	1.0
79	38	48	0.0312	0.0482	0.0	1.0
80	9	55	0.0	0.1205	0.0	0.9400

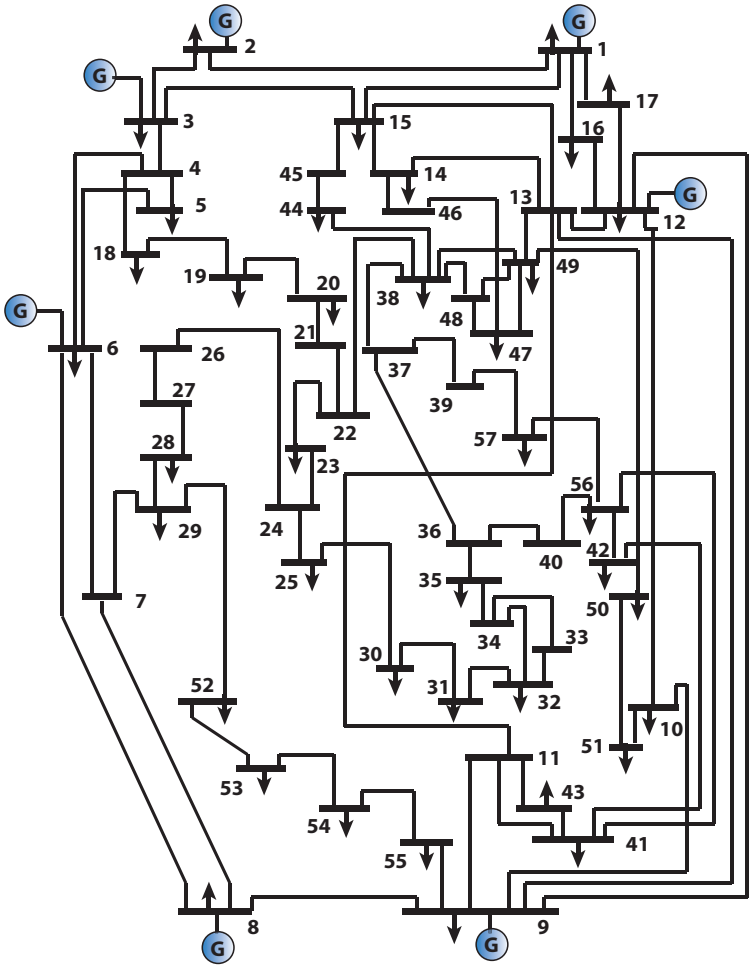

Figure 2: IEEE 57-bus System

118-bus Line Parameters

The values for the resistance, reactance, and shunt susceptance for each branch in the IEEE 118-bus test system are given below in p.u. These values were taken from MATPOWER [68].

Table 3: Line parameters for the 118-bus system

From	To	Resistance (R)	Reactance (X)	Shunt Susceptance (B)
1	2	0.0303	0.0999	0.0254
1	3	0.0129	0.0424	0.01082
4	5	0.00176	0.00798	0.0021
3	5	0.0241	0.108	0.0284
5	6	0.0119	0.054	0.01426
6	7	0.00459	0.0208	0.0055
8	9	0.00244	0.0305	1.162
8	5	0	0.0267	0
9	10	0.00258	0.0322	1.23
4	11	0.0209	0.0688	0.01748
5	11	0.0203	0.0682	0.01738
11	12	0.00595	0.0196	0.00502
2	12	0.0187	0.0616	0.01572
3	12	0.0484	0.16	0.0406
7	12	0.00862	0.034	0.00874
11	13	0.02225	0.0731	0.01876
12	14	0.0215	0.0707	0.01816
13	15	0.0744	0.2444	0.06268
14	15	0.0595	0.195	0.0502
12	16	0.0212	0.0834	0.0214
15	17	0.0132	0.0437	0.0444
16	17	0.0454	0.1801	0.0466
17	18	0.0123	0.0505	0.01298

From	To	Resistance (R)	Reactance (X)	Shunt Susceptance (B)
18	19	0.01119	0.0493	0.01142
19	20	0.0252	0.117	0.0298
15	19	0.012	0.0394	0.0101
20	21	0.0183	0.0849	0.0216
21	22	0.0209	0.097	0.0246
22	23	0.0342	0.159	0.0404
23	24	0.0135	0.0492	0.0498
23	25	0.0156	0.08	0.0864
26	25	0	0.0382	0
25	27	0.0318	0.163	0.1764
27	28	0.01913	0.0855	0.0216
28	29	0.0237	0.0943	0.0238
30	17	0	0.0388	0
8	30	0.00431	0.0504	0.514
26	30	0.00799	0.086	0.908
17	31	0.0474	0.1563	0.0399
29	31	0.0108	0.0331	0.0083
35	36	0.00224	0.0102	0.00268
35	37	0.011	0.0497	0.01318
33	37	0.0415	0.142	0.0366
34	36	0.00871	0.0268	0.00568
34	37	0.00256	0.0094	0.00984
38	37	0	0.0375	0
37	39	0.0321	0.106	0.027
37	40	0.0593	0.168	0.042
30	38	0.00464	0.054	0.422
39	40	0.0184	0.0605	0.01552
40	41	0.0145	0.0487	0.01222

From	To	Resistance (R)	Reactance (X)	Shunt Susceptance (B)
40	42	0.0555	0.183	0.0466
41	42	0.041	0.135	0.0344
43	44	0.0608	0.2454	0.06068
34	43	0.0413	0.1681	0.04226
44	45	0.0224	0.0901	0.0224
45	46	0.04	0.1356	0.0332
46	47	0.038	0.127	0.0316
46	48	0.0601	0.189	0.0472
47	49	0.0191	0.0625	0.01604
42	49	0.0715	0.323	0.086
42	49	0.0715	0.323	0.086
45	49	0.0684	0.186	0.0444
48	49	0.0179	0.0505	0.01258
49	50	0.0267	0.0752	0.01874
49	51	0.0486	0.137	0.0342
51	52	0.0203	0.0588	0.01396
52	53	0.0405	0.1635	0.04058
53	54	0.0263	0.122	0.031
49	54	0.073	0.289	0.0738
49	54	0.0869	0.291	0.073
54	55	0.0169	0.0707	0.0202
54	56	0.00275	0.00955	0.00732
55	56	0.00488	0.0151	0.00374
56	57	0.0343	0.0966	0.0242
50	57	0.0474	0.134	0.0332
56	58	0.0343	0.0966	0.0242
51	58	0.0255	0.0719	0.01788
54	59	0.0503	0.2293	0.0598

From	To	Resistance (R)	Reactance (X)	Shunt Susceptance (B)
56	59	0.0825	0.251	0.0569
23	32	0.0317	0.1153	0.1173
31	32	0.0298	0.0985	0.0251
27	32	0.0229	0.0755	0.01926
15	33	0.038	0.1244	0.03194
19	34	0.0752	0.247	0.0632
60	62	0.0123	0.0561	0.01468
61	62	0.00824	0.0376	0.0098
63	59	0	0.0386	0
63	64	0.00172	0.02	0.216
64	61	0	0.0268	0
38	65	0.00901	0.0986	1.046
64	65	0.00269	0.0302	0.38
49	66	0.018	0.0919	0.0248
49	66	0.018	0.0919	0.0248
62	66	0.0482	0.218	0.0578
62	67	0.0258	0.117	0.031
65	66	0	0.037	0
66	67	0.0224	0.1015	0.02682
65	68	0.00138	0.016	0.638
47	69	0.0844	0.2778	0.07092
49	69	0.0985	0.324	0.0828
68	69	0	0.037	0
69	70	0.03	0.127	0.122
24	70	0.00221	0.4115	0.10198
70	71	0.00882	0.0355	0.00878
24	72	0.0488	0.196	0.0488
71	72	0.0446	0.18	0.04444

From	To	Resistance (R)	Reactance (X)	Shunt Susceptance (B)
71	73	0.00866	0.0454	0.01178
70	74	0.0401	0.1323	0.03368
70	75	0.0428	0.141	0.036
69	75	0.0405	0.122	0.124
74	75	0.0123	0.0406	0.01034
76	77	0.0444	0.148	0.0368
69	77	0.0309	0.101	0.1038
75	77	0.0601	0.1999	0.04978
77	78	0.00376	0.0124	0.01264
78	79	0.00546	0.0244	0.00648
77	80	0.017	0.0485	0.0472
77	80	0.0294	0.105	0.0228
79	80	0.0156	0.0704	0.0187
68	81	0.00175	0.0202	0.808
81	80	0	0.037	0
77	82	0.0298	0.0853	0.08174
82	83	0.0112	0.03665	0.03796
83	84	0.0625	0.132	0.0258
83	85	0.043	0.148	0.0348
84	85	0.0302	0.0641	0.01234
85	86	0.035	0.123	0.0276
56	59	0.0803	0.239	0.0536
55	59	0.04739	0.2158	0.05646
59	60	0.0317	0.145	0.0376
59	61	0.0328	0.15	0.0388
60	61	0.00264	0.0135	0.01456
89	90	0.0238	0.0997	0.106
90	91	0.0254	0.0836	0.0214

From	To	Resistance (R)	Reactance (X)	Shunt Susceptance (B)
89	92	0.0099	0.0505	0.0548
89	92	0.0393	0.1581	0.0414
91	92	0.0387	0.1272	0.03268
92	93	0.0258	0.0848	0.0218
92	94	0.0481	0.158	0.0406
93	94	0.0223	0.0732	0.01876
94	95	0.0132	0.0434	0.0111
80	96	0.0356	0.182	0.0494
82	96	0.0162	0.053	0.0544
94	96	0.0269	0.0869	0.023
80	97	0.0183	0.0934	0.0254
80	98	0.0238	0.108	0.0286
80	99	0.0454	0.206	0.0546
92	100	0.0648	0.295	0.0472
94	100	0.0178	0.058	0.0604
95	96	0.0171	0.0547	0.01474
96	97	0.0173	0.0885	0.024
98	100	0.0397	0.179	0.0476
99	100	0.018	0.0813	0.0216
100	101	0.0277	0.1262	0.0328
92	102	0.0123	0.0559	0.01464
101	102	0.0246	0.112	0.0294
100	103	0.016	0.0525	0.0536
100	104	0.0451	0.204	0.0541
103	104	0.0466	0.1584	0.0407
103	105	0.0535	0.1625	0.0408
100	106	0.0605	0.229	0.062

From	To	Resistance (R)	Reactance (X)	Shunt Susceptance (B)
104	105	0.00994	0.0378	0.00986
105	106	0.014	0.0547	0.01434
105	107	0.053	0.183	0.0472
105	108	0.0261	0.0703	0.01844
106	107	0.053	0.183	0.0472
108	109	0.0105	0.0288	0.0076
103	110	0.03906	0.1813	0.0461
109	110	0.0278	0.0762	0.0202
110	111	0.022	0.0755	0.02
110	112	0.0247	0.064	0.062
17	113	0.00913	0.0301	0.00768
32	113	0.0615	0.203	0.0518
32	114	0.0135	0.0612	0.01628
27	115	0.0164	0.0741	0.01972
86	87	0.02828	0.2074	0.0445
85	88	0.02	0.102	0.0276
85	89	0.0239	0.173	0.047
88	89	0.0139	0.0712	0.01934
89	90	0.0518	0.188	0.0528
114	115	0.0023	0.0104	0.00276
68	116	0.00034	0.00405	0.164
12	117	0.0329	0.14	0.0358
75	118	0.0145	0.0481	0.01198
76	118	0.0164	0.0544	0.01356

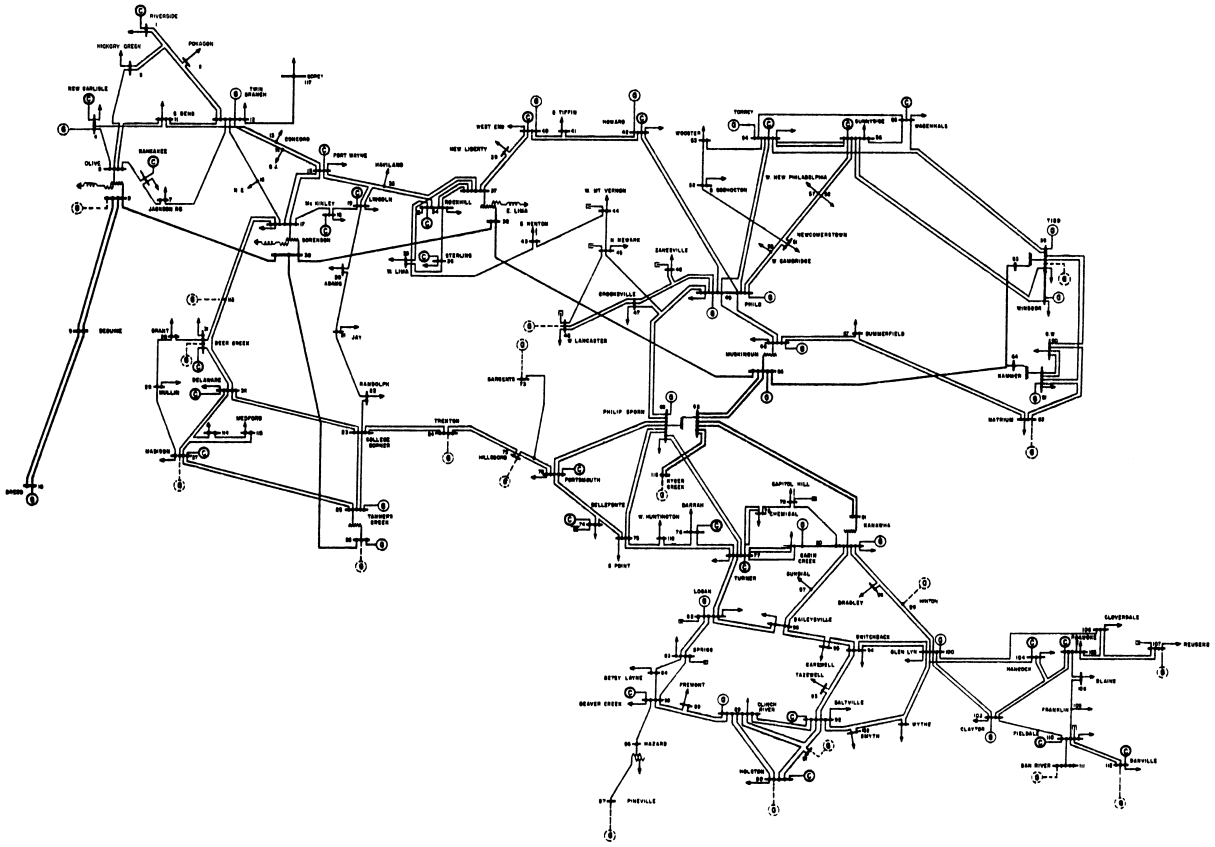

Figure 3: IEEE 118-bus System

Bibliography

[1] S. Kar, J. M. Moura, and K. Ramanan, "Distributed parameter estimation in sensor networks: Nonlinear observation models and imperfect communication," *IEEE Transactions on Information Theory*, vol. 58, no. 6, pp. 3575–3605, 2012.

[2] G. Hug, S. Kar, and C. Wu, "Consensus+ innovations approach for distributed multiagent coordination in a microgrid," *IEEE Transactions on Smart Grid*, vol. 6, no. 4, pp. 1893–1903, 2015.

[3] E. Castillo, R. Minguez, A. Conejo, and R. Garcia-Bertrand, *Decomposition techniques in mathematical programming*. Springer, 2006.

[4] D. Hur, J. Park, and B. Kim, "Evaluation of convergence rate in the auxiliary problem principle for distributed optimal power flow," *IEE Procedings - Generation, Transmission and Distribution*, vol. 149, no. 5, pp. 525–532, 2002.

[5] F. J. Nogales, F. J. Prieto, and A. J. Conejo, "A decomposition methodology applied to the multi-area optimal power flow problem," *Annals of Operations Research*, vol. 120, pp. 99–116, Apr. 2003.

[6] G. Hug-Glanzmann and G. Andersson, "Decentralized optimal power flow control for overlapping areas in power systems," *IEEE Transactions on Power Systems*, vol. 24, no. 1, pp. 327–336, 2009.

[7] X. Ma and N. Elia, "A sufficient saddle point characterization for the lagrangian associated with general OPF problems," in *53rd Annual Conference on Decision and Control (CDC)*, pp. 1119 – 1124, 2014.

[8] B. Kim and R. Baldick, "A comparison of distributed optimal power flow algorithms," *IEEE Transactions on Power Systems*, vol. 15, no. 2, pp. 599–604, 2000.

[9] A. Conejo and J. Aguado, "Multi-area coordinated decentralized DC optimal power flow," *IEEE Transactions on Power Systems*, vol. 13, no. 4, pp. 1272–1278, 1998.

[10] A. G. Bakirtzis and P. N. Biskas, "A decentralized solution to the DC-OPF of interconnected power systems," *IEEE Transactions on Power Systems*, vol. 18, no. 3, pp. 1007–1013, 2003.

[11] M. Kraning, E. Chu, J. Lavaei, and S. Boyd, "Dynamic network energy management via proximal message passing," *Foundations and Trends in Optimization*, vol. 1, no. 2, pp. 1–54, 2013.

[12] T. Erseghe, "Distributed optimal power flow using ADMM," *IEEE Transactions on*

Power Systems, vol. 29, no. 5, pp. 2370–2380, 2014.

[13] Z. Zhang and M. Y. Chow, "Convergence analysis of the incremental cost consensus algorithm under different communication network topologies in a smart grid," *IEEE Transactions on Power Systems*, vol. 27, pp. 1761 –1768, Nov. 2012.

[14] G. Binetti, A. Davoudi, D. Naso, B. Turchiano, and F. L. Lewis, "A distributed auction-based algorithm for the nonconvex economic dispatch problem," *IEEE Transactions on Industrial Informatics*, vol. 10, no. 2, pp. 1124–1132, 2014.

[15] S. Kar and G. Hug, "Distributed robust economic dispatch in power systems: A consensus + innovations approach," in *IEEE Power and Energy Society General Meeting*, July 2012.

[16] S. Yang, S. Tan, and J.-X. Xu, "Consensus based approach for economic dispatch problem in a smart grid," *IEEE Transactions on Power Systems*, vol. 28, no. 4, pp. 4416–4426, 2013.

[17] G. Binetti, A. Davoudi, F. L. Lewis, D. Naso, and B. Turchiano, "Distributed consensus-based economic dispatch with transmission losses," *IEEE Transactions on Power Systems*, vol. 29, no. 4, pp. 1711–1720, 2014.

[18] F. Dörfler, J. W. Simpson-Porco, and F. Bullo, "Plug-and-play control and optimization in microgrids," in *53rd IEEE Conference on Decision and Control*, pp. 211–216, IEEE, 2014.

[19] N. Li, L. Chen, C. Zhao, and S. H. Low, "Connecting automatic generation control and economic dispatch from an optimization view," in *American Control Conference*, pp. 735–740, 2014.

[20] M. Andreasson, D. V. Dimarogonas, K. H. Johansson, and H. Sandberg, "Distributed vs. centralized power systems frequency control," in *2013 12th European Control Conference, ECC 2013; Zurich; Switzerland; 17 July 2013 through 19 July 2013*, pp. 3524–3529, 2013.

[21] T. Kato, *Perturbation theory for linear operators*, vol. 132. Springer Science & Business Media, 1976.

[22] R. Christie, "Power systems test case archive," *Electrical Engineering dept., University of Washington*, 2000.

[23] A. B.-D. JD Taft, "Grid architecture," tech. rep., Pacific Northwest National Laboratory, 2015.

[24] S. B. Michael Milligan, Brendan Kirby, "Combining balancing areas variability:impacts on wind integration in the western interconnection," tech. rep., National Renewable Energy Laboratory, 2010.

[25] E. K. Richard P. ONeill, Thomas Dautel, "Recent iso software enhancements and future software and modeling plans," tech. rep., Federal Energy Regulatory Commission, 2011.

[26] D. Phan and J. Kalagnanam, "Distributed methods for solving the security-constrained optimal power flow problem," in *Innovative Smart Grid Technologies*

(ISGT), pp. 1–7, 2012.

[27] Y. Li and J. D. Mccalley, "Decomposed scopf for improving efficiency," *IEEE Transaction on Power System*, vol. 24, no. 1, pp. 494–495, 2009.

[28] J. Mohammadi, G. Hug, and S. Kar, "A benders decomposition approach to corrective security constrained OPF with power flow control devices," in *Power and Energy Society General Meeting (PES)*, pp. 1–5, 2013.

[29] J. M. Alves, C. L. Borges, and A. L. Oliveira Filho, "Distributed security constrained optimal power flow integrated to a dsm based energy management system for real time power systems security control," in *High Performance Computing for Computational Science-VECPAR 2006*, pp. 131–144, Springer, 2007.

[30] P. Biskas and A. Bakirtzis, "Decentralised security constrained dc-opf of interconnected power systems," *IEE Proceedings-Generation, Transmission and Distribution*, vol. 151, no. 6, pp. 747–754, 2004.

[31] J. H. Kim, J. K. Park, B. Kim, J. B. Park, and D. Hur, "A method of inclusion of security constraints with distributed optimal power flow," *International journal of electrical power & energy systems*, vol. 23, no. 3, pp. 189–194, 2001.

[32] L. Liu, A. Khodaei, W. Yin, and Z. Han, "A distribute parallel approach for big data scale optimal power flow with security constraints," in *International Conference on Smart Grid Communications (SmartGridComm)*, pp. 774–778, 2013.

[33] S. Chakrabarti, M. Kraning, E. Chu, R. Baldick, and S. Boyd, "Security constrained optimal power flow via proximal message passing," in *Power Systems Conference (PSC)*, pp. 1–8, 2014.

[34] R. A. Horn and C. R. Johnson, *Matrix analysis*. Cambridge university press, 2012.

[35] C. Grigg, P. Wong, P. Albrecht, R. Allan, M. Bhavaraju, R. Billinton, Q. Chen, C. Fong, S. Haddad, S. Kuruganty, W. Li, R. Mukerji, D. Patton, N. Rau, D. Reppen, A. Schneider, M. Shahidehpour, and C. Singh, "The IEEE reliability test system-1996. a report prepared by the reliability test system task force of the application of probability methods subcommittee," *IEEE Transactions on Power Systems*, vol. 14, no. 3, pp. 1010–1020, 1999.

[36] D. Divan and H. Johal, "Distributed FACTS a new concept for realizing grid power flow control," *IEEE Transactions on Power Electronics*, vol. 22, no. 6, pp. 2253–2260, 2007.

[37] U. Hager, S. Lehnhoff, C. Rehtanz, and H. Wedde, "Multi-agent system for coordinated control of facts devices," in *15th International Conference on Intelligent System Applications to Power Systems*, pp. 1–6, 2009.

[38] S. C. Müller, U. Häger, and C. Rehtanz, "A multiagent system for adaptive power flow control in electrical transmission systems," *IEEE Transactions on Industrial Informatics*, vol. 10, no. 4, pp. 2290–2299, 2014.

[39] X.-P. Zhang, C. Rehtanz, and B. Pal, "Multi-agent systems for coordinated control of FACTS-devices," in *Flexible AC Transmission Systems: Modelling and Control*,

pp. 321–337, Springer, 2012.

[40] D. Panasetsky and N. Voropai, "A distributed control of facts devices against line overloading," in *International Conference on Power System Technology (POWERCON)*, pp. 1–6, 2010.

[41] G. Hug-Glanzmann and G. Andersson, "Coordinated control of facts devices in power systems for security enhancement," in *Bulk Power System Dynamics and Control-VII. Revitalizing Operational Reliability, 2007 iREP Symposium*, pp. 1–10, IEEE, 2007.

[42] A. N. Venkat, I. A. Hiskens, J. B. Rawlings, and S. J. Wright, "Distributed mpc strategies with application to power system automatic generation control," *IEEE transactions on control systems technology*, vol. 16, no. 6, pp. 1192–1206, 2008.

[43] S. Magnússon, P. C. Weeraddana, and C. Fischione, "A distributed approach for the optimal power-flow problem based on admm and sequential convex approximations," *IEEE Transactions on Control of Network Systems*, vol. 2, no. 3, pp. 238–253, 2015.

[44] R. A. Verzijlbergh, M. O. W. Grond, Z. Lukszo, J. G. Slootweg, and M. D. Ilic, "Network impacts and cost savings of controlled EV charging," *IEEE Transactions on Smart Grid*, vol. 3, no. 3, pp. 1203–1212, 2012.

[45] R. J. Bessa, M. A. Matos, F. J. Soares, and J. A. Peças Lopes, "Optimized bidding of a EV aggregation agent in the electricity market," *IEEE Transactions on Smart Grid*, vol. 3, no. 1, pp. 443–452, 2012.

[46] S. I. Vagropoulos and A. G. Bakirtzis, "Optimal bidding strategy for electric vehicle aggregators in electricity markets," *IEEE Transactions on Power Systems*, vol. 28, no. 4, pp. 4031–4041, 2013.

[47] M. González Vayá and G. Andersson, "Optimal bidding strategy of a plug-in electric vehicle aggregator in day-ahead electricity markets under uncertainty," *IEEE Transactions on Power Systems*, vol. 30, no. 5, pp. 2375 – 2385, 2015.

[48] M. H. Amini and M. P. Moghaddam, "Probabilistic modelling of electric vehicles' parking lots charging demand," in *21st Iranian Conference on Electrical Engineering (ICEE)*, 2013.

[49] J. Hu, S. You, M. Lind, and J. Ostergaard, "Coordinated charging of electric vehicles for congestion prevention in the distribution grid," *IEEE Transactions on Smart Grid*, vol. 5, no. 2, pp. 703–711, 2014.

[50] N. Rotering and M. Ilic, "Optimal charge control of plug-in hybrid electric vehicles in deregulated electricity markets," *IEEE Transactions on Power Systems*, vol. 26, no. 3, pp. 1021–1029, 2011.

[51] M. H. Amini and A. Islam, "Allocation of electric vehicles' parking lots in distribution network," in *Innovative Smart Grid Technologies Conference (ISGT)*, 2014.

[52] Z. Ma, D. S. Callaway, and I. A. Hiskens, "Decentralized charging control of large populations of plug-in electric vehicles," *IEEE Transactions on Control Systems Technology*, vol. 21, no. 1, pp. 67–78, 2013.

[53] L. Gan, U. Topcu, and S. Low, "Optimal decentralized protocol for electric vehicle

charging," *IEEE Transactions on Power Systems*, vol. 28, no. 2, pp. 940–951, 2013.

[54] F. Parise, M. Colombino, S. Grammatico, and J. Lygeros, "Mean field constrained charging policy for large populations of plug-in electric vehicles," in *53rd Annual Conference on Decision and Control (CDC)*, pp. 5101–5106, 2014.

[55] J. Rivera, P. Wolfrum, S. Hirche, C. Goebel, and H. A. Jacobsen, "Alternating direction method of multipliers for decentralized electric vehicle charging control," in *52nd Annual Conference on Decision and Control (CDC)*, pp. 6960–6965, 2013.

[56] M. González Vayá, G. Andersson, and S. Boyd, "Decentralized control of plug-in electric vehicles under driving uncertainty," in *IEEE PES Innovative Smart Grid Technologies Conferece*, (Istanbul, Turkey), 2014.

[57] N. Rahbari-Asr and M.-Y. Chow, "Cooperative distributed demand management for community charging of PHEV/PEVs based on KKT conditions and consensus networks," *IEEE Transactions on Industrial Informatics*, vol. 10, no. 3, pp. 1907–1916, 2014.

[58] Z. Ma, S. Zou, L. Ran, X. Shi, and I. A. Hiskens, "Efficient decentralized coordination of large-scale plug-in electric vehicle charging," *Automatica*, vol. 69, pp. 35–47, 2016.

[59] Y. Xu, "Optimal distributed charging rate control of plug-in electric vehicles for demand management," *IEEE Transactions on Power Systems*, vol. 30, no. 3, pp. 1536–1545, 2015.

[60] J. Mattingley, Y. Wang, and S. Boyd, "Code generation for receding horizon control," in *IEEE International Symposium on Computer-Aided Control System Design (CACSD)*, pp. 985–992, 2010.

[61] Y. Wang and S. Boyd, "Fast model predictive control using online optimization," *IEEE Transactions on Control Systems Technology*, vol. 18, no. 2, pp. 267–278, 2010.

[62] P. Braun, L. Grüne, C. M. Kellett, S. R. Weller, and K. Worthmann, "A distributed optimization algorithm for the predictive control of smart grids," *IEEE Transactions on Automatic Control*, 2015.

[63] S. Boyd and L. Vandenberghe, *Convex optimization*. Cambridge university press, 2004.

[64] A. K. Sahu, S. Kar, J. Moura, and H. V. Poor, "Distributed constrained recursive nonlinear least-squares estimation: Algorithms and asymptotics," *[online] http://arxiv.org/pdf/1602.00382v1.pdf*.

[65] M. Balmer, K. Axhausen, and K. Nagel, "Agent-based demand-modeling framework for large-scale microsimulations," *Journal of the Transportation Research Board*, vol. 1985, pp. 125–134, 2006.

[66] M. González Vayá and G. Andersson, "Centralized and decentralized approaches to smart charging of plug-in vehicles," in *Power and Energy Society General Meeting*, 2012.

[67] M. Sahraei-Ardakani and K. W. Hedman, "A fast lp approach for enhanced utilization of variable impedance based facts devices," *IEEE Transactions on Power Systems*,

vol. 31, no. 3, pp. 2204–2213, 2016.

[68] R. D. Zimmerman, C. E. Murillo-Sánchez, and R. J. Thomas, "Matpower: Steady-state operations, planning, and analysis tools for power systems research and education," *IEEE Transactions on power systems*, vol. 26, no. 1, pp. 12–19, 2011.